#2 Oceanog. Lab Meteorol. Res. Inst.
Collected Reprints

COLLECTED REPRINTS

VOLUME 2

OCEANOGRAPHICAL LABORATORY,
METEOROLOGICAL RESEARCH INSTITUTE
MABASHI, SUGINAMI,
TOKYO, JAPAN.

April 1955

Contents

24) NAKANO, M., S. UNOKI, M. HANZAWA, R. MARUMO and J. FUKUOKA: Oceanographic features of a submarine eruption that destroyed the Kaiyo-maru No. 5.
Jour. Mar. Res. **13** (1), 1954.

25) NAN'NITI, T.: A current meter using a phototube (III)—Experiment on a tidal current—
Papers Met. Geophys. **5** (1), Apr. 1954.

26) ABE, T.: A study on the foaming of sea water (8th report)—On the mechanism of the decay of foam layer of sea water (Part 3)—
Jour. Oceanogr. Soc. Japan. **10** (1), May 1954.

27) NAN'NITI, T.: A new plastic water sampler.
Papers Met. Geophys. **5** (1), Apr. 1954.

28) NAN'NITI, T.: Relations between the turbidity factor and the transparency, the extinction, the absorption, the scattering coefficients.
Papers Met. Geophys. **5** (1), Apr. 1954.

29) DAIDOJI, S., S. UNOKI and K. KAJIURA. Waves at Hachijo Island caused by Typhoon Tess and Alice in 1953.
Jour. Meteor. Res. **6** (7), Sept. 1954.

30) ABE, T.: A study on the foaming of sea water (9th report)—On the distribution of the size of bubbles in foam layer of sea water—
Oceanogr. Report, Central Met. Obs., **3** (4), Dec. 1954.

31) ABE, T.: A study on the foaming of sea water.—On the mechanism of the decay of bubbles and their size distribution in foam layer of sea water—
Papers Met. Geophys. **5** (3~4), Jan. 1955.

32) NAN'NITI, T.: On the structure of ocean currents (1)—Test manufacture of a new current meter and some experiments on the sea—
Papers Met, Geophys. **5** (3~4), Jan. 1955.

33) ABE, T.: On the mechanism of the decay of bubbles and their size distribution in foam layer of sea water.
Rec. Oceanogr. Works in Japan. **2** (1), Mar. 1955.

34) UNOKI, S. and M. NAKANO: A note on forecasting ocean waves caused by typhoons.
Rec. Oceanogr. Works in Japan. **2** (1), Mar. 1955.

Digitized by the Internet Archive
in 2025

https://archive.org/details/collected-reprints-oceanographical-laboratory_1955-04_2

OCEANOGRAPHIC FEATURES OF A SUBMARINE ERUPTION THAT DESTROYED THE KAIYO-MARU NO. 5[1]

By

MASITO NAKANO

Meteorological Research Institute and Tokyo University

SANAE UNOKI, MASAO HANZAWA, RYUZO MARUMO AND JIRO FUKUOKA

Central Meteorological Observatory of Japan

ABSTRACT

When Myojinsho Reef erupted in September 1952, tsunami waves were recorded several times by a self-registering wave gauge installed on the southwestern coast of Hachijo Island about 130 km from that Reef. The largest one of these tsunamis appeared on 24 September, and it is presumed that this wave caused the destruction of the KAIYO-MARU No. 5. Results of investigation of these recorded tsunami waves and other phenomena are reported.

INTRODUCTION

Since September 1952, a station for the observation of sea waves has been maintained by the Central Meteorological Observatory of Japan in the vicinity of Port Yayene on the southwestern coast of Hachijo Island (Fig. 1). The station, equipped with a self-registering wave gauge, was established with the aim of investigating the relations between wind waves or swells and atmospheric disturbances such as cyclones or typhoons. In mid-September, Myojinsho Reef erupted, and tsunamis caused thereby were recorded several times by this wave gauge. In the present paper, the results of investigations of these tsunamis are reported, together with other pertinent observations.

RESULTS OF WAVE GAUGE OBSERVATIONS

The wave gauge is of the pressure recorder type and was reconstructed from a statoscope of the type in ordinary use for recording microbarographic oscillations. The pressure change, corresponding to the rise and fall of the sea level, is automatically traced on a roll of paper at a speed of about 33 cm/hr. The device is capable of making a continuous record of waves for about 12 hours. The reducing scale

[1] A surveying ship (211 tons) of the Hydrographic Office, Maritime Safety Agency of Japan.

Reprint from SEARS FOUND. JOURN. MAR. RES.

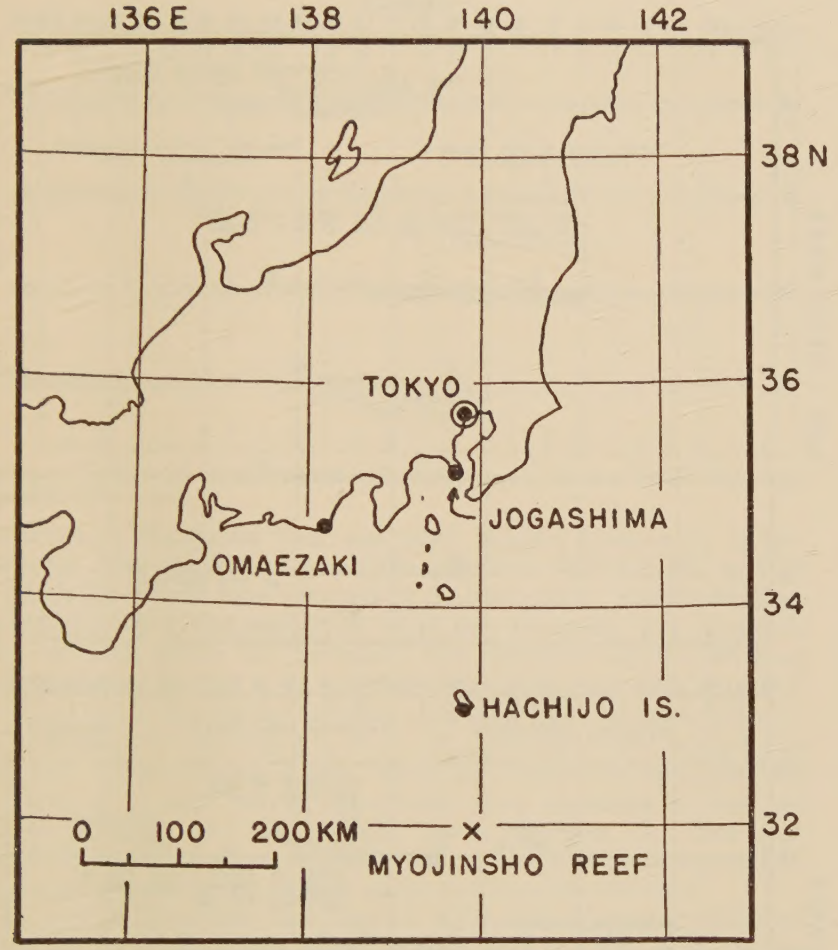

Figure 1. Geographical locations of Myojinsho Reef and Hachijo Island.

of the instrument is about 1/70 for ordinary wind waves or swells but is somewhat less for the tsunamis in question, which have a period of about 1 min or so. A slow-leak device is attached to the instrument to eliminate waves of longer periods, such as tides.

Fig. 2 shows in tabular form the periods[2] in which the observations were taken during the interval of 16–30 September 1952 as well as

[2] In the present paper, the time of observation is always referred to the meridian of 135° E (Japanese Standard Time).

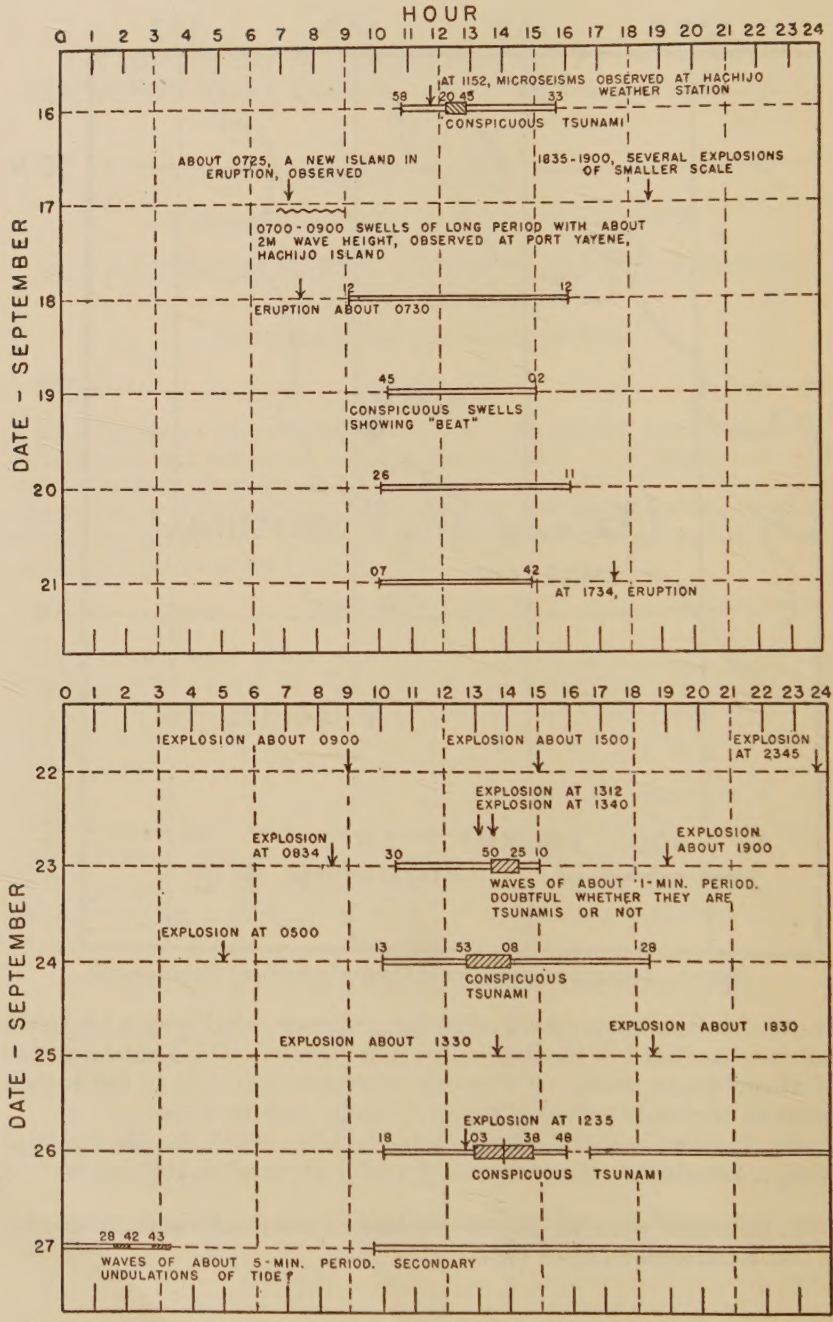
HOUR
0 1 2 3 4 5 6 7 8 9 10 11 12 13 14 15 16 17 18 19 20 21 22 23 24
DATE - SEPTEMBER
16
17
18
19
20
21
AT 1152, MICROSEISMS OBSERVED AT HACHIJO WEATHER STATION
58 20 45 33
CONSPICUOUS TSUNAMI
ABOUT 0725, A NEW ISLAND IN ERUPTION, OBSERVED
1835-1900, SEVERAL EXPLOSIONS OF SMALLER SCALE
0700-0900 SWELLS OF LONG PERIOD WITH ABOUT 2M WAVE HEIGHT, OBSERVED AT PORT YAYENE, HACHIJO ISLAND
12 12
ERUPTION ABOUT 0730
45 02
CONSPICUOUS SWELLS SHOWING "BEAT"
26 11
07 42
AT 1734, ERUPTION
0 1 2 3 4 5 6 7 8 9 10 11 12 13 14 15 16 17 18 19 20 21 22 23 24
DATE - SEPTEMBER
22
23
24
25
26
27
EXPLOSION ABOUT 0900
EXPLOSION ABOUT 1500
EXPLOSION AT 2345
EXPLOSION AT 1312
EXPLOSION AT 1340
EXPLOSION AT 0834
30 50 25 10
EXPLOSION ABOUT 1900
WAVES OF ABOUT 1-MIN. PERIOD. DOUBTFUL WHETHER THEY ARE TSUNAMIS OR NOT
EXPLOSION AT 0500
13 53 08 28
CONSPICUOUS TSUNAMI
EXPLOSION ABOUT 1330
EXPLOSION ABOUT 1830
EXPLOSION AT 1235
18 03 38 48
CONSPICUOUS TSUNAMI
28 42 43
WAVES OF ABOUT 5-MIN. PERIOD. SECONDARY UNDULATIONS OF TIDE?

Figure 2. Results of sea wave observations at Hachijo Island with a self-registering wave gauge.

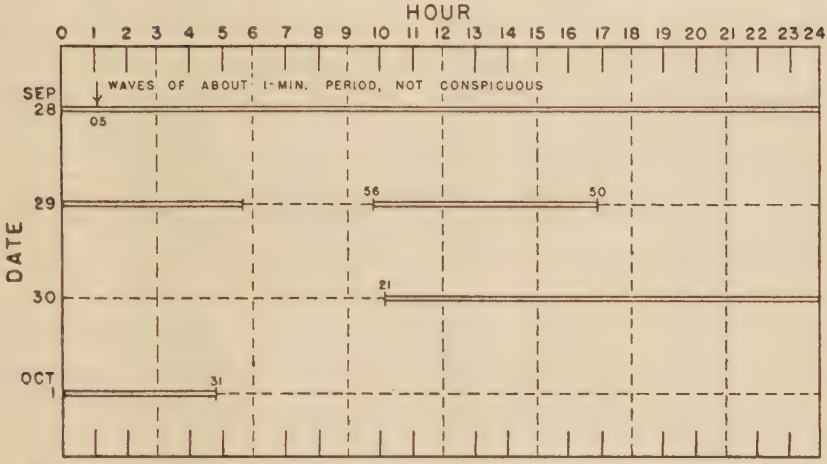

Figure 2 (*Continued*). Results of sea wave observations at Hachijo Island with a self-registering wave guage.

eruptions of Myojinsho Reef and other unusual phenomena in this interval. The thick horizontal line segments indicate the periods in which the records were obtained by the wave gauge, and the hatched portions indicate the periods in which the tsunamis were recorded. The numerals above the horizontal line segments indicate the time (in minutes). In Fig. 2 we see that conspicuous tsunamis appeared on 16, 24 and 26 September and that something like a tsunami occurred on 23 September (see Fig. 3A, B, C, D; a normal record is shown in Fig. 3E). Since records of wind waves and swells were superimposed on those of tsunami waves, the records were smoothed so that the curves represent only the tsunami waves (see Fig. 4). The time marks shown in the above records are those obtained by interpolation. Hence possible errors in time of about $\pm$ 3 min are involved.

(A) On 16 September (see Figs. 3A, 4A), although no one witnessed eruptions, microseisms (or better, seismic surface waves) of maximum amplitude 5 μ and of period 4.1 sec were recorded at 11^h52^m on a portable seismometer installed at the Hachijojima Weather Station. According to seismologists, these microseisms were probably due to an eruption of Myojinsho Reef. If we assume that the velocity of propagation of these microseismic waves is several kilometers per second and that it is the same as that of ordinary seismic waves (surface waves), we may consider that the eruption occurred at about 11^h52^m. Since the tsunami began to occur at Hachijo Island at 12^h20^m, the time taken by the tsunami wave to travel from Myojinsho Reef to the observing station was $12^h20^m - 11^h52^m = 28$ min. The maximum wave height of this tsunami was 56 cm.

(B) On 24 September (see Figs. 3B, 4B), a more conspicuous tsunami was recorded. The eruption which caused it was probably the one

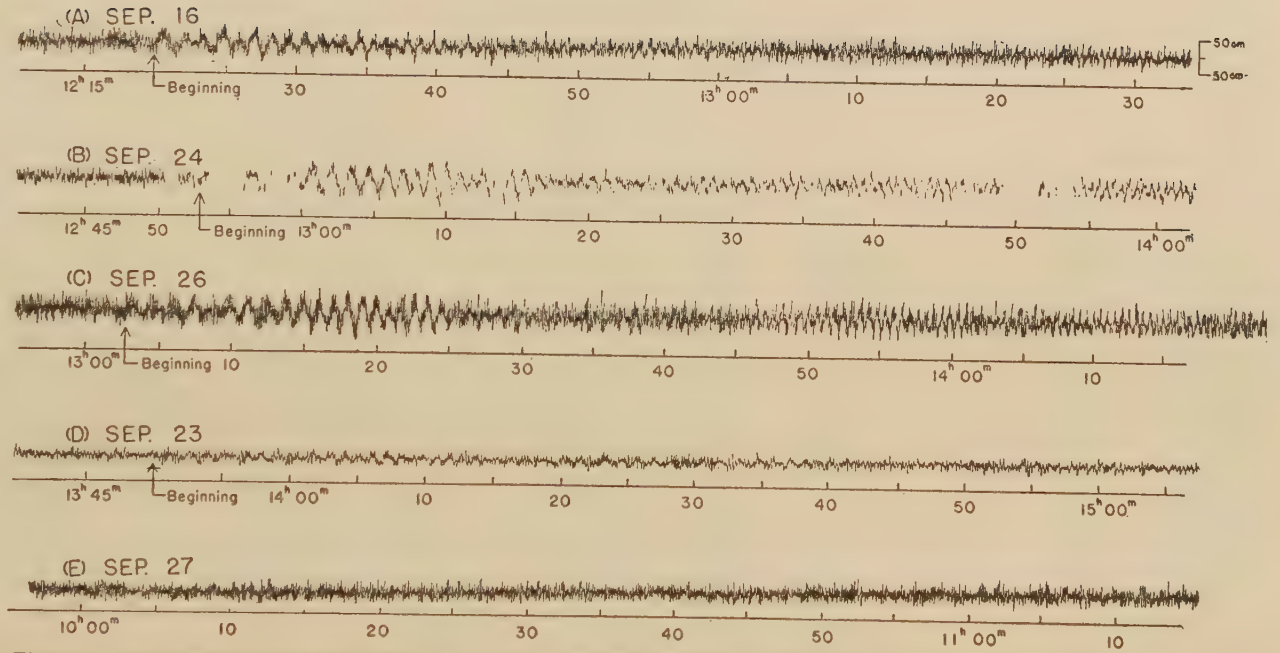

Figure 3. Wave records at Hachijo Island. A, B and C represent tsunamis caused by the eruption of a submarine volcano at Myojinsho Reef. D shows a probable tsunami wave and E a normal record.

which also caused the disaster to the KAIYO-MARU No. 5. Since there were no survivors, no first-hand account of the eruption is reported. The tsunami began at 12^h53^m and the maximum wave height was 92 cm.

(C) On 26 September (see Figs. 3C, 4C), another conspicuous tsunami occurred; its maximum wave height was 71 cm and the time of its first movement was 13^h03^m. In this instance a ship of the Maritime Safety Agency, sent to investigate the fate of the KAIYO-MARU No. 5,

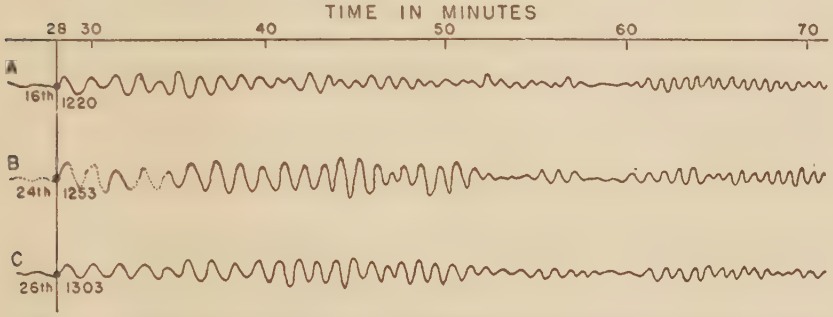

Figure 4. Wave records A, B and C of the tsunamis, obtained by smoothing the actual wave records A, B and C of Fig. 3 to eliminate wind waves and swells.

ascertained that an eruption occurred at Myojinsho Reef at 12^h35^m. The time taken by the tsunami wave to travel from Myojinsho Reef to the observing station on Hachijo Island was $13^h03^m - 12^h35^m = 28$ min, the same value obtained for the one on 16 September.

On 23 September (see Fig. 3D), two eruptions of Myojinsho Reef at 13^h12^m and 13^h40^m were witnessed by members of the Tokyo College of Fisheries on board the SHINYO-MARU. Referring to Fig. 3D, undulations, apparently tsunami waves, began to occur at 13^h50^m. However, when this record is compared with those in Figs. 3A, B and C, we see that the record for 23 September differs from those for 16, 24 and 26 September in wave period as well as in wave height; that is, although at first sight the said undulations for 23 September appear to have been tsunami waves,they might have been the peculiar type of wave which appears when a typhoon or cyclone approaches, or they might have been what Munk (1949) calls "surf beats." Moreover, as regards the determination of the time of beginning of the said undulation, 13^h50^m, it is less clearly defined. Therefore we shall not consider here the observations obtained on this date.

TRAVEL TIME OF TSUNAMI WAVES AND MAGNITUDE OF ERUPTION

In computing the travel time of a tsunami, that is, the time taken by the tsunami wave to travel from Myojinsho Reef to the observing station, we must decide whether it is a shallow, intermediate, or deep wave and whether it propagates with phase or group velocity. Since the depth of water is 200–1400 m and the wave period 30–100 sec, and considering the relative depth (ratio of water depth to wave length), we see that the wave cannot be treated either as a deep or shallow wave (long wave); therefore it must be treated as an intermediate wave (elliptical particle orbits). If we denote the period by τ, the wave length by λ, and the depth of water by d, we have for such waves, according to the Airy theory,

$$\text{phase velocity} \qquad C = \left\{\frac{g\lambda}{2\pi}\tanh\left(\frac{2\pi d}{\lambda}\right)\right\}^{\frac{1}{2}}, \tag{1}$$

$$\text{group velocity} \qquad C_g = \frac{C}{2}\left\{1 + \frac{\frac{4\pi d}{\lambda}}{\sinh\left(\frac{4\pi d}{\lambda}\right)}\right\}, \tag{2}$$

where g is the acceleration due to gravity and $\lambda = C\tau$.

It is found that, within the range of magnitude of the quantities and the distance here considered, computations by equations (1) and (2) yield the following result; the phase velocity C and the group velocity C_g of the intermediate wave differ little from those of the deep water wave.

In Figs. 3A, B and C or Figs. 4A, B and C, we see that the period of the wave which first reached the observing station is about 95 sec. If we consider that this wave proceeded with group velocity, and if we compute the travel time t by the formula

$$t = \int \frac{ds}{C_g} = \sum \frac{\Delta s}{C_g}, \tag{3}$$

we have $t = 32.1$ min. Again, if we consider that this wave travelled with phase velocity, we have $t = 28.5$ min. As stated previously, the actual travel time of the wave was about 28 min as determined for 16 and 26 September. But, as noted earlier, this value has a possible error of about ± 3 min. Consequently it is difficult to reach a definite conclusion as to whether the wave travelled with phase velocity or with group velocity. To ascertain the exact dif-

ference of travel-time within the range of wave period, water depth and distance of travel under consideration, more accurate time-marking would have been necessary.

We are also concerned with the time of occurrence of the volcanic eruption which presumably caused the destruction of the KAIYO-MARU No. 5 on 24 September.[3] If the waves shown in Figs. 3B or 4B (IX/24) are compared with those of Figs. 3A or 4A (IX/16) and 3C or 4C (IX/26), we see that the value of initial wave-period as well as the modes of variation of wave-period and wave-height are very similar. Hence it may be supposed that the travel time was about 28 min. in all cases. Accordingly, the eruption in question presumably occurred at about 24th $12^h53^m - 28^m = 24\text{th } 12^h25^m \pm 6^m$. According to the result of a SOFAR hydrophone observation made by the U. S. Navy, it is estimated that the said eruption on 24 September occurred at about 12^h20^m, which is in good agreement with our result.[4]

Regarding the magnitude of the eruption, Unoki and Nakano (1953, 1953a) have made a detailed theoretical investigation which has shown that the present tsunami is a typical "Cauchy-Poisson wave" generated by a local disturbance over a limited extent of the sea surface. Assuming that the wave was generated by an initial impulse and that the radius of the disturbing source (the area to which the initial impulse was applied) was circular, it was found that the initial radius was about 2.2 km for A, B and C and that the magnitude of the initial impulse was 7.0×10^6, 11.6×10^6, and 8.9×10^6 dyne. sec/cm^2 for A, B, and C respectively.[5] Again, if the initial disturbance was assumed to be an initial elevation, then the radius of the disturbing source was about 2.2 km for A, B, and C, as above, and the magnitude of the initial elevation was 6.3 m, 10.3 m and 8.0 m for A, B, and C respectively.

[3] From navigation and communication, it is presumed that the KAIYO-MARU No. 5 had not yet reached Myojinsho Reef at 10^h on 24 September and that her destruction must have occurred between 10^h and 13^h on that same day.

[4] This information was kindly furnished by Dr. R. S. Dietz of the U. S. Navy Electronics Laboratory, San Diego, Calif.

[5] In the first paper (Unoki and Nakano, 1953), one-dimensional treatment was given to the problem and the effect of friction was neglected, while in the second paper (Unoki and Nakano, 1953a) a two-dimensional treatment was given, with consideration of the frictional factor. Hence the values of the computed quantities for the initial impulse, etc., are not the same in both studies. Naturally the latter values are considered to be closer to reality, and the numerical values of the computed quantities quoted here are those obtained in the second paper.

Moreover, it was found that, in the tsunami of 24 September, the action of the initial impulse exerted much more effect than did the initial elevation. Furthermore, it was known that the energy of the eruption was about 3.0×10^{19}, 7.9×10^{19} and 4.8×10^{19} ergs for A, B, and C respectively. Thus, it is seen that the eruption on the 24th was quite violent.

THE TIME OF DESTRUCTION OF THE KAIYO-MARU No. 5 AS INFERRED FROM DEBRIS

The time of the destruction of the KAIYO-MARU No. 5 may also be inferred from the distribution of the wreckage and debris that remained afloat. From these observations, it was determined that the KAIYO-MARU No. 5 was destroyed during the afternoon of 24 September 1952, a fact which seems to confirm the result deduced from the record of the self-registering wave gauge on Hachijo Island.

In Fig. 5 the abscissa[6] denotes the distance from Myojinsho Reef and the ordinate denotes time; the points correspond to the time and location where debris was found, and it is apparent that these points lie almost within an area limited by two straight lines. If we draw a straight line to represent as nearly as possible the distribution of these points and intersect this straight line with the axis of ordinate, we find that the time when drifting began (equivalent to the time of eruption or disaster) falls between 0^h and 12^h on the 24th. But if we consider Fig. 5 carefully, we notice that some flotsam, such as that indicated by (5), (7), (8) and (10), was driven relatively farther as compared with that indicated by (4), (6), etc. Since the starting time from Myojinsho Reef of all objects is considered to be the same, it is necessary to make a correction for the effect of leeway. According to Yasui (1940), the effect of leeway is expressed by the formula

$$U = k \sqrt{\frac{A}{B}} \cdot W , \tag{4}$$

where U denotes the drifting velocity of a vessel due to the effect of wind, W the velocity of wind, A and B the cross-sectional areas of the vessel above and below the sea surface, respectively, taken in a plane perpendicular to the direction of drift, and k a certain constant. If U and W are measured in cm/sec, the value of k is 0.03. The value of the ratio A/B will differ for different flotsam, but in the present

[6] Here it is assumed that the KAIYO-MARU No. 5 was destroyed in close proximity to Myojinsho Reef.

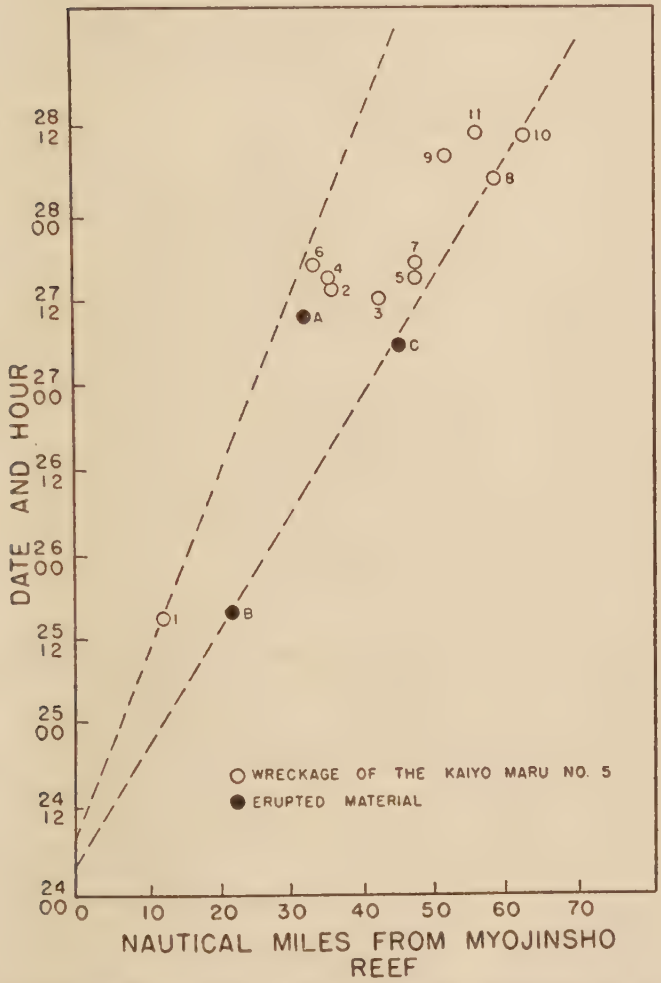

Figure 5. Drifting distance of erupted materials and wreckage from the KAIYO-MARU No. 5 relative to time of drifting. 1. Wooden box, soy keg, angular timber, log, pieces of cork, and numerous timbers. 2. Surveying buoy. 3. Surveying log. 4. Wood from a sampan stern, and a piece of cork. 5. Rack of a sampan, life buoy, and a piece of wood from a vegetable container. 6. Fragment of a life buoy. 7. Fragment of bulwark. 8. Crossbar of bed from operator's room. 9. Four kegs. 10. Part of environs of boat. 11. Part of compass bridge deck. A. Piece of comparatively new wood. B. Volcanic ashes and solidified substances. C. Sulphur and pumice. (Note: Flotsam "A" was picked up by a fishing boat, and it is uncertain whether or not this is part of the KAIYO-MARU No. 5 wreckage.)

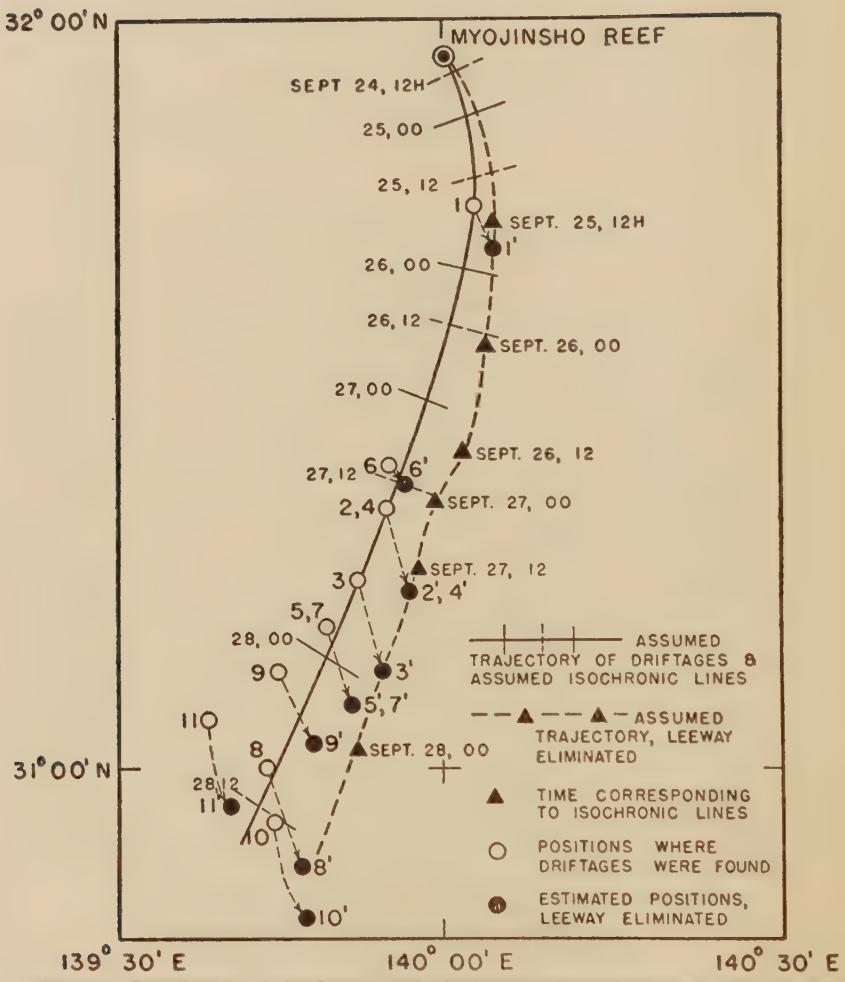

Figure 6. Distribution of the flotsam with the leeway effect eliminated. The numbers applied to the flotsam are in accord with the data of the Hydrographic Office, Maritime Safety Agency of Japan.

case we take, as an approximation, A/B as a constant and equal to $\frac{1}{2}$ for all the flotsam concerned.

By means of weather charts published by the Central Meteorological Observatory of Japan, the wind velocity and direction over the area considered were estimated; and by using equation (4), the effect of leeway was eliminated. In Fig. 6, the small white circles represent the positions where the items of flotsam were actually picked up.

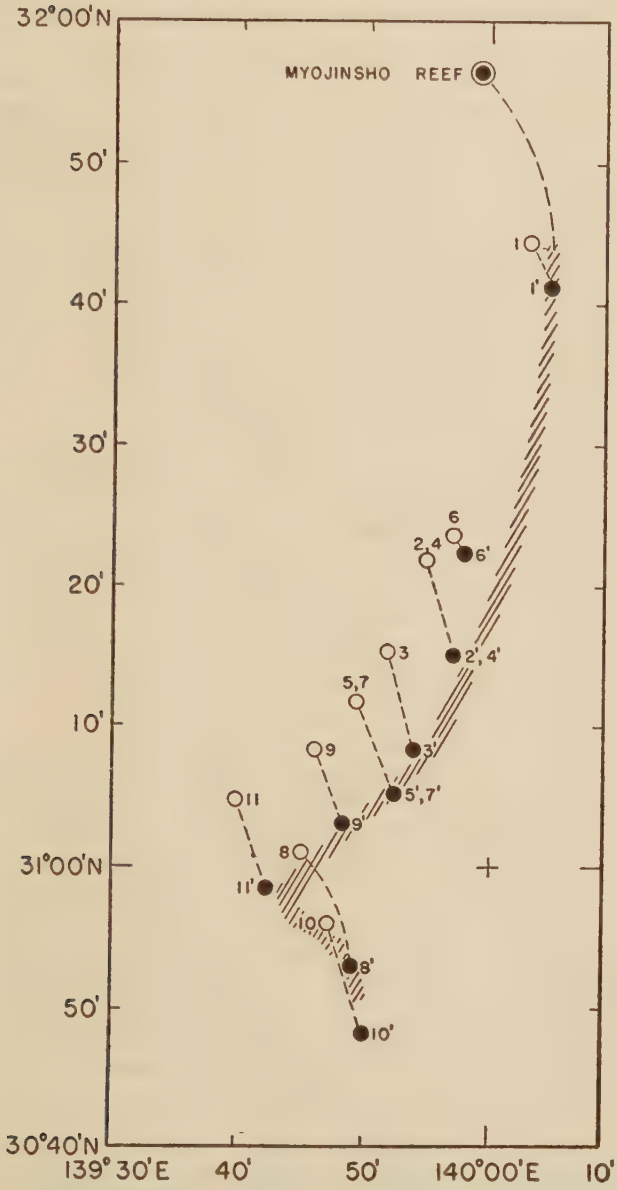

Figure 7. Chart of streamlines of the ocean current, drawn from the estimated positions of flotsam with the effect of leeway eliminated.

If the effect of leeway were nonexistent and if the flotsam had been carried by the general current alone, wreckage would have been found at the positions indicated by the black circles in Fig. 6.

Fig. 7 shows the streamlines of the ocean current in the area concerned; these were drawn from the estimated positions of flotsam after the effect of leeway had been eliminated. Unfortunately the direction of the current is somewhat obscure near 139° 50' E and 31° 00' N because of the fact that there was at that time a stationary front in this vicinity. Since some of the flotsam was situated on the northern side and some on the southern side of the front, some errors were unavoidably introduced when the effect of leeway was calculated.

With the effect of leeway eliminated, Fig. 8[7] is drawn to show the "travel-time curve" of Fig. 5 with corrected values; the values of time and distance correspond to the black circles in Fig. 6. In Fig. 8 we see that the items of flotsam are distributed more or less regularly along a straight line. If we read the value of time at the point where this straight line intersects the time axis, then the starting time of the driftages from Myojinsho Reef occurred during the afternoon of the 24th (about 18^h, we venture to say).

Since there are probably some errors in our estimated values of wind direction and velocity over the sea (the values adopted for k and A/B in the formula $U = k\sqrt{A/B}\,.W$) and of the positions where the flotsam was found, we cannot draw a more detailed conclusion than this from the travel-time curve method used above.

Again we note that the above discussion is based on the assumption that the flotsam came from close proximity to Myojinsho Reef. If the KAIYO-MARU No. 5 met with disaster at some point far apart from Myojinsho Reef, then a major correction would have to be made in our calculations and conclusions. However, at present there is nothing which seems to contradict our assumption. At any rate, the above result of driftage investigation is not inconsistent with the result inferred from the record of the self-registering wave gauge on Hachijo Island. Moreover, if we calculate the velocity of the ocean current from the travel-time curve in Fig. 8, we have approximately 0.7 knot, which is in fairly good accord with the result of observations taken hitherto in this vicinity (Hydrographic Office of Japan, 1948; see also Hanzawa, 1953).

[7] As noted earlier, it is not certain that flotsam "A" in Fig. 5 is a part of the wreckage of the KAIYO-MARU No. 5. Again, it is not certain that the erupted materials "B" and "C" in Fig. 5 were ejected from Myojinsho Reef at the time of the eruption which destroyed the KAIYO-MARU No. 5. Hence, in Fig. 8, A, B and C are omitted.

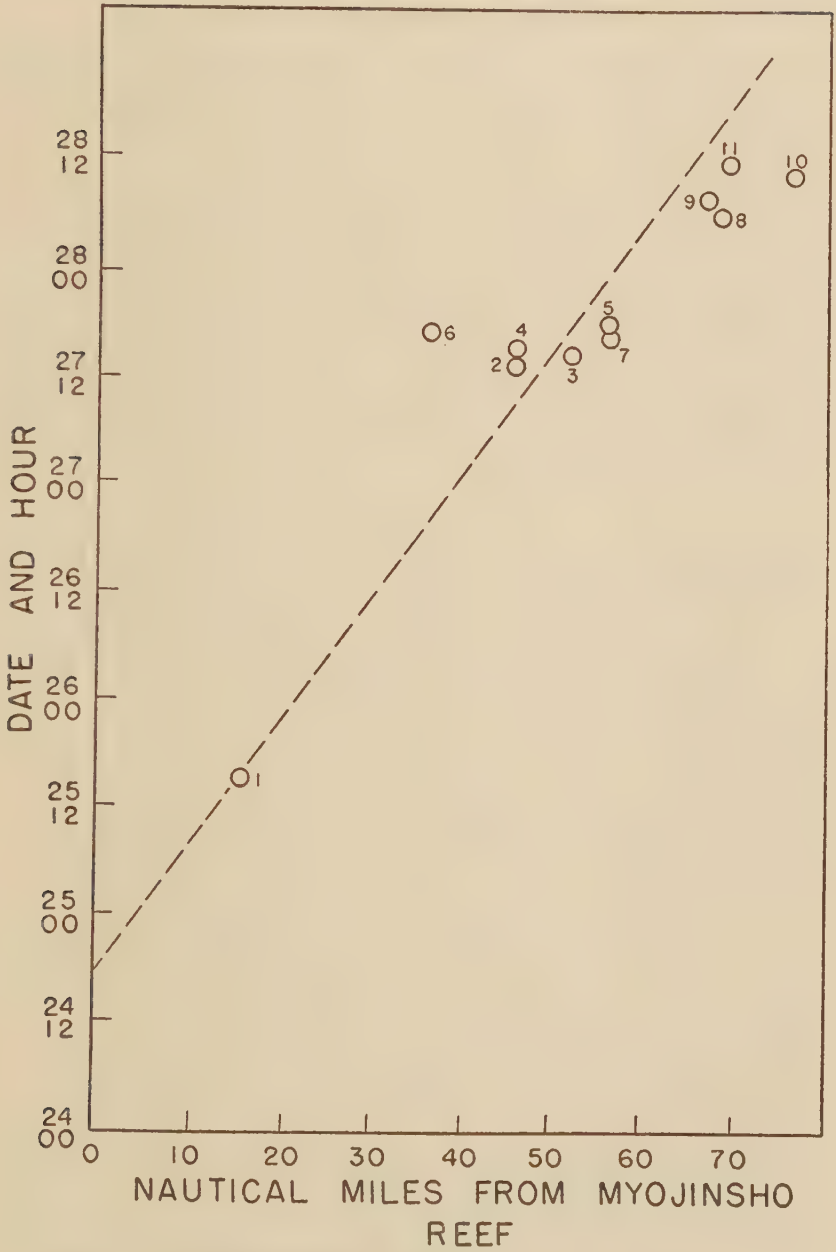

Figure 8. Drifting distance relative to time, corrected for the effect of leeway.

ACKNOWLEDGMENT

In conclusion, we wish to express our thanks to members of Hachijojima Weather Station who obtained wave records for us, to the observers and crew of the CHIKUBU-MARU, at whose personal risk data in the danger zone were obtained, to Dr. K. Suda, director of the Hydrographic Office, Maritime Safety Agency of Japan, who kindly gave additional data concerning the disaster of the KAIYO-MARU No. 5, and to Dr. K. Wadati, director of the Central Meteorological Observatory of Japan, for his encouragement and advice. Similar thanks for helpful information and suggestions are due Dr. Y. Kawabata of the Central Meteorological Observatory of Japan, Dr. C. Tsuboi of Tokyo University, and Dr. R. S. Dietz of the U. S. Navy Electronics Laboratory, San Diego, California. And the authors pray heartily for the heavenly bliss of the investigators and crew on board the KAIYO-MARU No. 5 whose precious lives were lost in the southern sea of Japan in the interest of science.

REFERENCES

CENTRAL METEOROLOGICAL OBSERVATORY OF JAPAN, OCEANOGRAPHICAL SECTION
1952. Report of investigations on the disaster of the KAIYO-MARU No. 5 (a surveying ship of the Hydrographic Office, Maritime Safety Agency of Japan) in relation to oceanography (in Japanese). Prepared by Masito Nakano, then Chief of the Oceanographical Section. Oceanogr. Rep. Central Meteorol. Observ. Japan, *2* (4): 295–304.

HACHIJOJIMA WEATHER STATION
1952. Prompt report on the eruption of Myojinsho Reef in September 1952 (in Japanese).

HANZAWA, M.
1953. On the eddy diffusion of pumices ejected from Myojin Reef in the southern Sea of Japan. Rec. Oceanogr. Works Japan, N. S. *1* (1): 18–22.

HYDROGRAPHIC OFFICE OF JAPAN
1948. The results of oceanographical observations taken in the western part of the North Pacific Ocean during 1923–1929 (in Japanese). Kaisho-Jiho, No. 3: 1–15.
1952. The report presented by the Investigation Committee for the Cause of the KAIYO-MARU No. 5 Disaster (in Japanese).

LAMB, H.
1932. Hydrodynamics. 6th ed., Arts 238–240, pp. 384–394.

MUNK, W. H.
1949. Surf beats. Trans. Amer. geophys. Un., *30* (6): 849–854.

NAKANO, M.
1949. On the secondary undulations of tides caused by cyclonic storms (1st paper). Oceanogr. Mag., *1* (1): 13–32.

UNOKI, SANAE AND MASITO NAKANO.
1953. On the Cauchy-Poisson waves caused by the eruption of a submarine volcano (1st paper). Oceanogr. Mag., *4* (4): 119–141.

1953a. On the Cauchy-Poisson waves caused by the eruption of a submarine volcano (2nd paper). Oceanogr. Mag., *5* (1): 1–13.

YASUI, Z.

1940. On the effect of leeway upon a vessel (in Japanese). Umi to Sora (Sea and Sky), *20* (7): 177–181.

APPENDIX

Although these data and observations have no direct bearing on the disaster of the KAIYO-MARU No. 5, we have added them here for the record.

The CHIKUBU-MARU, a weather ship of the Central Meteorological Observatory of Japan, was navigating in waters near Myojinsho Reef from 15^h to 19^h on 21 September 1952 on her passage from Torishima to Tokyo, at which time her crew witnessed an eruption at Myojinsho Reef about $17^h\ 35^m$. Their observations on that occasion are noted herewith. Fig. 9 shows the positions of their stations, the numeral in brackets denoting the time of observation.

(1) APPEARANCE OF THE ERUPTION

15^h20^m; odour of sulphur noted about 22 nautical miles SSE from Myojinsho Reef.

15^h50^m; intense odour of sulphur noted about 17 nautical miles SSE from the Reef.

16^h10^m; column of white smoke trailing westward was seen on the horizon NNW from the ship, about 13 nautical miles from the Reef.

16^h22^m; from the sea surface at the foot of the column of white smoke, a column of black smoke shot upward to a height of about 200 m; this dispersed and turned white subsequently.

16^h30^m; on the sea surface, west of the ship, a stream of yellowish green sulphide spread SSW in the shape of a belt from the direction of Myojinsho Reef.

17^h35^m; column of deep black smoke belched upward from the steam and white smoke, and several seconds later a column of fire appeared.

17^h38^m; this same column of black smoke attained a height of more than 5000 m, and a large quantity of incandescent lava fell into the sea. The surface of the sea swelled up, and the diameter of this swollen portion increased to about 740 m almost instantly.

17^h40^m; volcanic ashes fell from the sky on the deck of the ship, which was then about 5000 m SE from the point of eruption; when these ashes struck the observers' cheeks, the men felt pain, and in the interest of safety, the ship retreated northeastward at full speed.

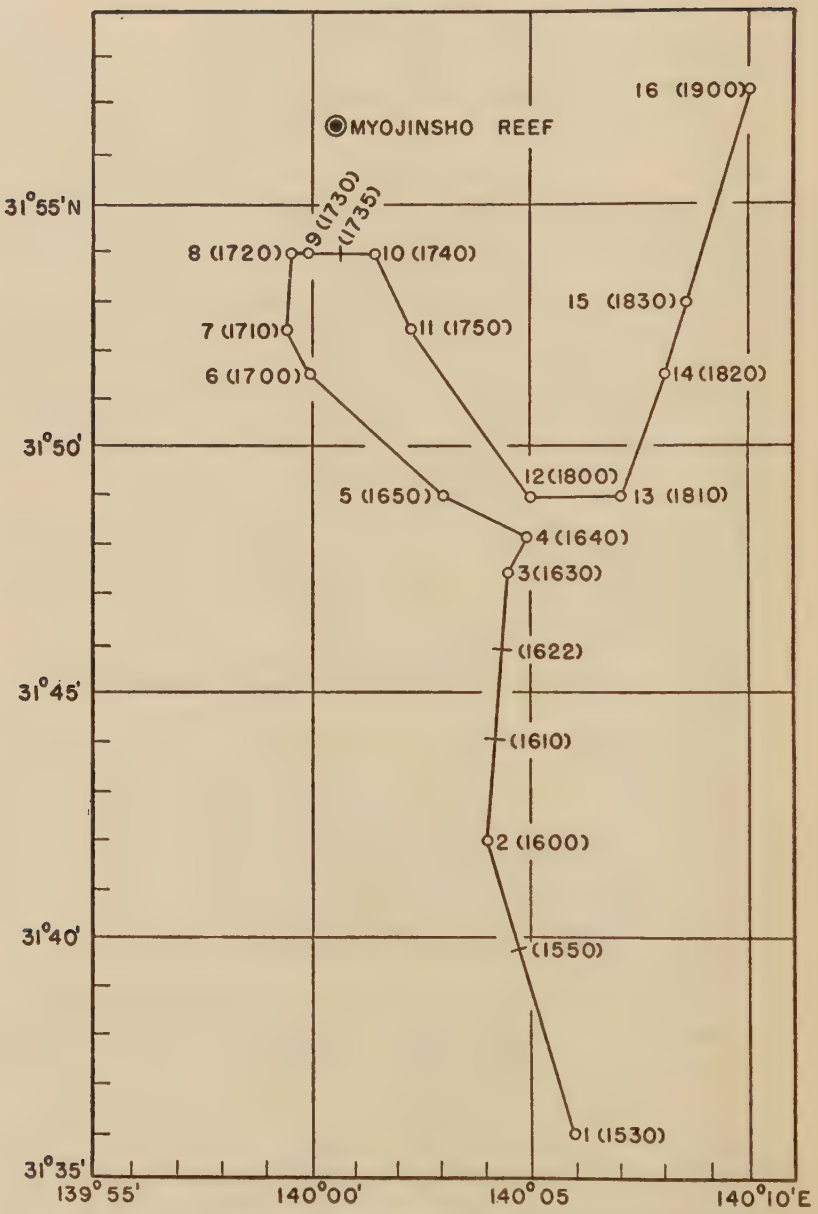

Figure 9. Observation stations occupied by the CHIKUBU-MARU.

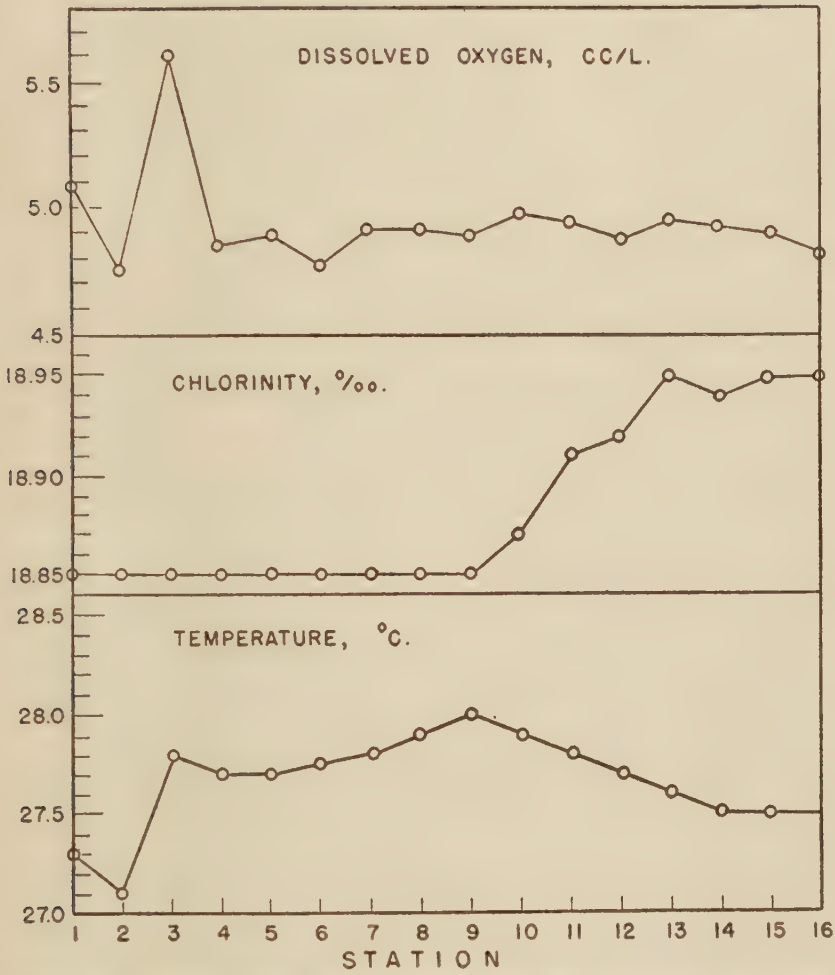

Figure 10. Dissolved oxygen, chlorinity and temperature of the surface water at each station occupied by the CHIKUBU-MARU.

(2) WATER TEMPERATURE, CHLORINITY AND DISSOLVED OXYGEN

Fig. 10 shows the temperature, chlorinity, and dissolved oxygen values of the surface water at each station. The water temperature at stations 6–11, close to Myojinsho Reef, was 27.8°, which is somewhat higher than the temperatures at more distant stations. Apparently this higher temperature was partly due to the heating of the water by various substances ejected from Myojinsho Reef which were carried southward by currents.

The chlorinity values for stations 1–9 are somewhat less than those for stations 13–16. The cause of this discrepancy is not clear at present, but a part of it may be explained qualitatively; possibly water of low salinity spurted from Myojinsho Reef together with other substances, flowed southward with the ocean current, and, by mixing, diluted the surface sea water.[8]

As for the distribution of the dissolved oxygen, no particular tendency is noted.

(3) Floating Mineral Substances and Plankton

Floating mineral substances and plankton organisms from each 100 cc sample of surface-water were examined by the following method. The catch in each water sample was concentrated into 2 cc with a centrifuge, and 0.5 cc of this sample was then examined through a microscope. Brown volcanic dust, presumably small fragments of pumices, were abundant in all samples; a small quantity of pyroxene crystals was also included. Heavier volcanic dusts probably sank rapidly. The quantity of floating mineral substances was greatest at stations 6–11, close to Myojinsho Reef, and least at eastern stations 12–16.

Furthermore, the quantity of plankton organisms was small, amounting to approximately 40 individuals per litre even in samples that were comparatively rich in population. The intercellular substances of organisms such as *Rhizosolenia calcar-avis*, *Coscinodiscus* sp., *Trichodesmium thiebauti* and *Pyrocystis pseudonoctiluca*, had disappeared completely. The scarcity of plankton in the surface water near Myojinsho Reef may have been caused by the injurious action of the eruptive efflux and the subsequent sinking of plankton to lower layers. However, the data are too scanty for definite conclusions.

[8] According to data from observers aboard the Tokyo College of Fisheries boat Shinyo-maru on 23 September, surface chlorinity of the sea adjacent southward of Myojinsho Reef was especially low; H. Niino, a member of the party, suggests that this may have been due to mixing of low salinity water which issued from Myojinsho Reef during its eruption with adjacent water.

Reprinted from the *Papers in Meteorology and Geophysics* Vol. V No. 1, 1954
Published by the Meteorological Research Institute

A Current Meter Using a Phototube (Ⅲ)

—Experiment on a Tidal Current—

by

T. Nan'niti

Published by the Meteorological Research Institute,

Mabashi, Suginami, Tokyo, Japan

April, 1954

551.460.18.3:551.465

A Current Meter Using a Phototube (Ⅲ)

—Experiment on a Tidal Current—

by

T. Nan'niti

Meteorological Research Institute

(Received March 8, 1954)

Abstract

The author observed a tidal current using his current meter [1] and two others of different kinds simultaneously. He explained that the observed velocity fluctuation with the period of 1.5 hours was caused by the instantaneous penetration of the waters broken from the disturbance, and the time variation of velocity was due to the effect of vertical eddy viscosity and the change of the surface slope with time. Further. he analysed the shorter period disturbance and found that its eddy diffusion coefficient K∼269 c.g.s, its mean length of edddy l∼124 cm.

1. Materials

The experiment was performed in Uraga Strait on board the research ship "Asasiwo Maru" on September 15, 1953, using three kinds of current meters simultaneously, that is, an Ekman-Merz, the author's and a T.S.* recording current meters. The location of the station was 35°15.5′N, 139°44.7′E. The observation was carried out from 12h till 17h40m. Meteorological and other data are tabulated in Table 1.

Table 1. Oceanographical observation taken in Uraga Strait.

Station 35°15.5 N, 139°44.7′E.	Date September 15, 1953. Mag. Var. 5°W
Tide (at Mera) H.W. 8h35m, 19h10m; L.W. 1h45m, 13h10m	Lunar Age 6.8 days
Probable Value at the Station H.W. 8h45m, 19h35m; L.W. 2h10m, 13h33m.	
Marine-meteorological Observation	
Time 13h00m, Air Temperature 27.8°C, Weather Fine, Wind SSW 2,	
Clouds 6 Ci, 1 Ac, 0 Cu, Sea SSW 2, Swell None, Visibility 6.	

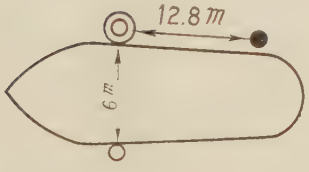

○ Author's current meter
● T.S. current meter
◎ Ekman-Merz current meter

Fig. 1. Positions of the three current meters in the simultaneous observation.

The relative positions of the current meters in the experiment are shown in Fig. 1.

The results obtained by the current meters are shown in Fig. 2. As shown in the figure, the observation was done at a layer of 10 meters, from 12h20m till 15h10m continuously, but after that, the observation was done at several layers

* The current meter of this type was made by Mr. M. Iwamiya, the Turumi Seiki Company. It records directions at intervals of 10 minutes on a chart and speeds, too.

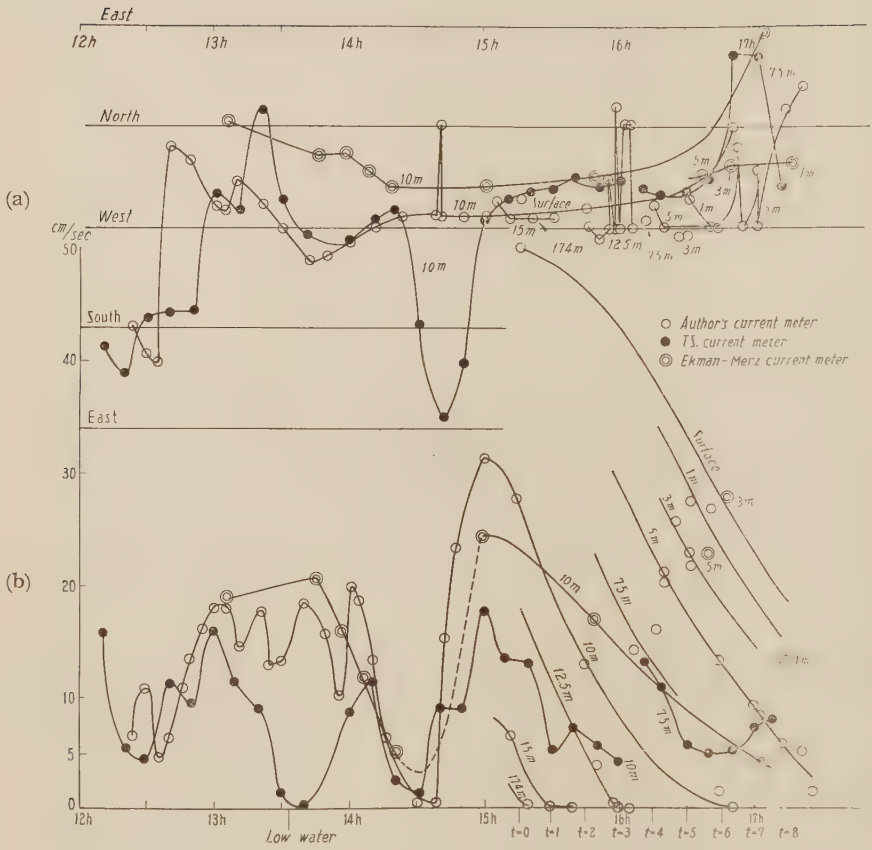

Fig. 2. Observed tidal current at a short distance from the coast of Cape Kan'non Saki in Uraga Strait. (a) directions (b) speeds

of different depths, moving rapidly the author's current meter up and down. Such rapid observations of current profiles are possible only by the current meter of this type. In these observations, of course, the determinations of standard levels of directions [1] were made, and we could not find any differences of levels of directions at these layers, and so the water might be homogeneous from top to bottom in regard to its optical character, within this observation at least.

And the 10 m layer was also observed by the T.S. current meter simultaneously from 12h10m till 16h and after that, the 7.5m layer was observed, and many observations were made by the Ekman-Merz current meter at some layers.

The station was at a short distance from the coast of the cape of Kan'non Saki as shown in Fig. 3 and, might have dimensions up to 250m or more. Directions of the main tidal currents in Uraga Strait will be NNW and SSE, and maximum currents near the station are shown in Fig. 3 (c). But the station was very near to the coast, so complications would arise because of the configuration of the form line of the coast and the bottom topography.

At ebb tide, from 8h45m till 13h33m, the current direction changed suddenly from SSE to NNW, and again turned to W (See Figs. 2 and 5).

(a) (b) (c)

Fig. 3. Charts published by the Hydrographic Office showing the station.

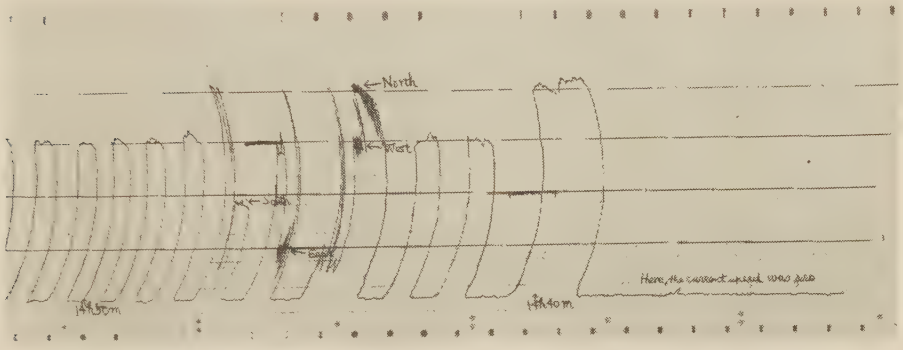

Fig. 4. A record of the current obtained at a 10m layer showing an abrupt change of velocity.

At 13h10m~40m and 14h20 m~15h00m, the tendencies of the change of the currents observed by the author's and the T.S. current meters are quite different from each other. So there must be some disturbances on a very small scale of a few meters to the current, such as eddies, turbulent flow, etc.

At 14h38m, that is, 65 minutes after the low water, the current speed was almost zero. At that time, six ships, each about 50 tons, passed by the port side to NW or NNW. Then the current began to run, and its direction changed to N for about one or two minutes tuning to the ship's path, and again turned back to W (Fig. 4). After that, at about 16h, an abrupt change occurred at a 12.5m layer for one to three minutes and also at 17h, it occurred at 5m layer. These changes always occurred in weak currents.

As mentioned in the above, observations were done at many layers after this, and the results are plotted in Fig. 2. From the figure we can say that the current directions were almost 270°~290° from the surface to the bottom. From about 16h40m~50m, the current direction turned to N. It was the middle time of flood tide at 16h34m.

As shown in Fig. 3, the strait is the intermediate transitional position for the type of tidal waves between progressive and standing waves. So the maximum current to NW in the strait would occur at some different time from mean water (16h34m) between low and high water. At 12h, 1.5 hours before the low water, the current ran to SSE. After that owing to the effect of the coastal line, the compensation current or the interrupted current ran to W. Next, at flood tide, the main current in the strait would run to NW or NNW. It can be suspected in Fig. 3 that the current at this station would be governed by the form line of the coast and the bottom topography.

Next, we have the current diagram in Fig. 5 observed by the author's and the T.S. current meters. Their relative positions were shown in Fig. 1. Also using the Fig. 5, we have the trajectories of water particles as shown in Fig. 6. At 12h30m the relative position of water particles had a distance of 12.8m due to their observing points, but after that particles diffused. And as the current direction changed, the direction of the ship's keel line might also change because we dropped only one anchor. But for the observation time the current direction were almost NW or NNW, so the trajectories in Fig. 6 might be almost correct.

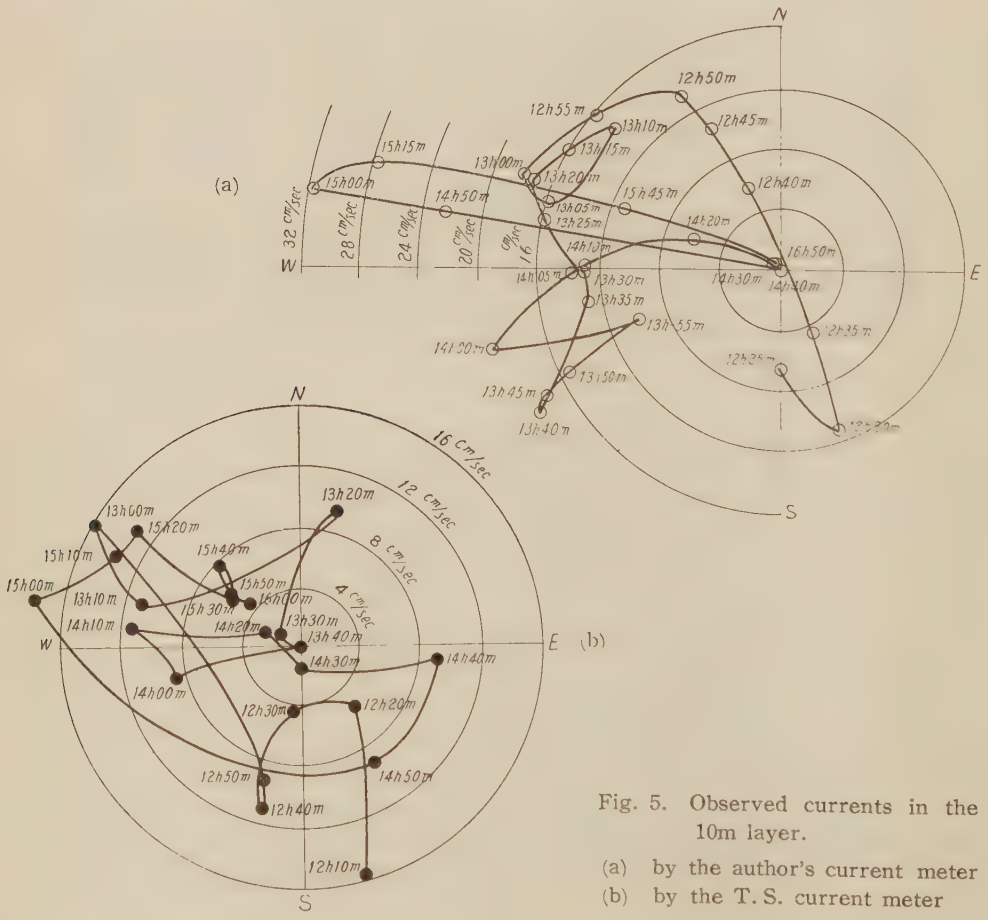

Fig. 5. Observed currents in the 10m layer.

(a) by the author's current meter
(b) by the T. S. current meter

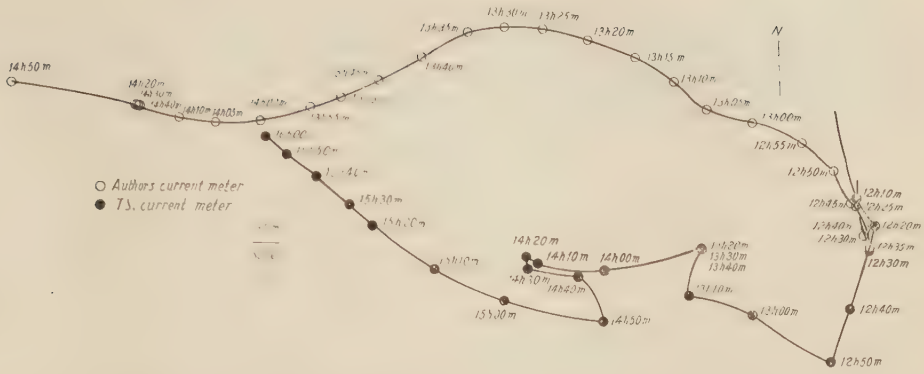

Fig. 6. Trajectories of water particles in the 10m layer observed by the author's and the T.S. current meters.

At any rate, the water moved southwards, then went back to NW or WNW, and next went to N or NE.

Thus the distance between them is not negligible in such a station, that is, at a station near the coast, the complications might arise due to the configuration of the coast and the bottom topography. By these facts, a representative domain in such an observation becomes very small, perhaps it will be only several meters.

2. Discussion of Materials

1) The long period fluctuations.

As seen from Fig. 2, we suppose that the current speed would decrease monotonously from the top to the bottom. Extrapolating the speeds at each layer, we have the current speed profile in Fig. 7. In the figure, the current profile at 15h15m shows that the bottom layer about one meter high scarcely moved and there is a point of inflexion above it.

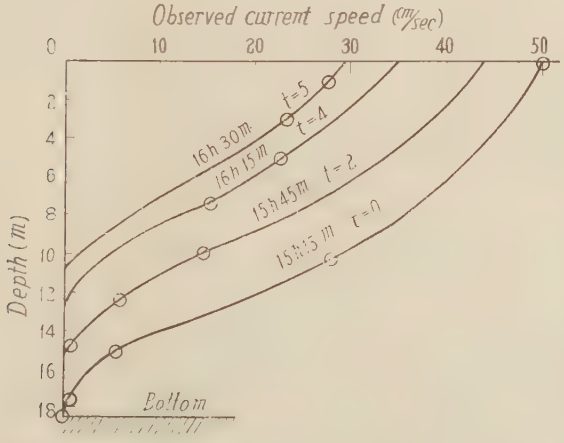

Fig. 7. The observed current profiles at some stages.

As seen from Figs. 2 and 7 the current velocity changed abruptly between 14h40m and 16h50m. Such fluctuation is not perhaps of tidal origin, but due to the intrusion of the vortex produced at Uraga Strait by the orographic effect [2], since the period of the fluctuation is about 1.5h, shorter than the tidal currents and further the current profile at each time shows the remarkable decrease with the depth, in contrast to the the tidal currents, which are generally almost of the same velocity near the bottom.

Thus the present observation gives an interesting example of the current

fluctuation caused by the irregular vortex. As a simple model, we assume the decrease of the velocity to be only due to the eddy viscosity and the bottom friction and neglect the effect of the change of the surface slope and the coastal boundary, then the equation of motion becomes simply

$$\frac{\partial u}{\partial t}=\frac{\partial (K\cdot\partial u/\partial z)}{\partial z}. \tag{1}$$

Further we put K=const and take the boundary conditions as

$$\begin{cases} K\dfrac{\partial u}{\partial z}=0 & (\text{at } z=0, \text{ surface}^*) \\ \dfrac{\partial u}{\partial z}=ku & (\text{at } z=h, \text{ or bottom}), \end{cases} \tag{2}$$

and the initial conditions as

$$u=f(z) \qquad (\text{at } t=0), \tag{3}$$

then the solution is also simply given by

$$u=2\sum_{s=1}^{\infty}e^{-K\mu_s^2 t}\cdot\frac{\mu_s^2+k^2}{h(\mu_s^2+k^2)-k}\cos\mu_s z\cdot\int_0^h f(\lambda)\cos\mu_s\lambda\, d\lambda, \tag{4}$$

where μ_s is the successive root of the relation

$$\mu\frac{\sin\mu h}{\cos\mu h}=-k.$$

We can take the initial velocity from the observed curve at 15h15m (Fig. 7) as

$$\begin{aligned} f(z)&=A\cos(\pi z/2h_0) && (0<z<h_0) \\ f(z)&=0 && (h_0<z<h), \end{aligned} \tag{5}$$

then

$$\int_0^{\lambda}f(\lambda)\cos\mu_s\lambda\, d\lambda=\frac{2Ah_0}{\pi}\cdot\frac{\cos\mu_s h_0}{1-4h_0^2\mu_s^2/\pi^2}. \tag{6}$$

In practical computations we take the extreme conditions of $k=0$ and $k=\infty$ and the solution becomes in each case

$$k=0, \quad u=\frac{2Ah_0}{\pi h}\left[1+2\sum_{m=1}^{\infty}e^{-K\left(\frac{m\pi}{h}\right)^2 t}\frac{\cos(m\pi h_0/h)\cos(m\pi z/h)}{1-4m^2h_0^2/h^2}\right] \tag{7}$$

$$k=\infty, \quad u=\frac{4Ah_0}{\pi h}\sum_{m=1}^{\infty}e^{-K\left(\frac{2m-1}{2h}\cdot\pi\right)^2 t}\cdot\frac{\cos\dfrac{2m-1}{2h}\pi h_0\cos\dfrac{2m-1}{2h}\pi z}{1-(2m-1)^2h_0^2/h^2} \tag{8}$$

We can estimate K to be about 10^2 c.g.s. from the discussion below and also we can put A=50 cm/sec, h_0=16 m from the curve at 15h15m (Fig. 7). In Fig. 8 we show the computed current profiles from the equations (7) and (8) by taking K=77.5 and 155 (c.g.s.) respectively for simplicity of numerical computations. In each case the agreement between the observed and the computed results is not so good, especially in regard to the small velocity below the depth about 10m at the later stage in the observation. The cause of the disagreement is to be sought in the variation of K with the depth and in the difference of charactors between the

*The wind force was Beaufort class 2.

upper and the bottom water masses. But since the initial velocity is small near the bottom, the first effect can not be considered to be important, and as for the second effect we have no knowledge about the structure of the water masses in the present stage. Therefore we should take into account the effect of the surface slope hitherto neglected. When we put

$$-g\frac{\partial \zeta}{\partial x}=\gamma, \tag{9}$$

then the additive term due to this effect becomes

$$k=0,\quad u_1=\int_0^t \gamma(\tau)\,d\tau, \tag{10}$$

$$k=\infty,\quad u_1=\frac{4}{\pi}\sum_{m=1}^{\infty}\frac{(-1)^{m-1}}{2m-1}\int_0^t \gamma(\tau)\,e^{K\left(\frac{2m-1}{2h}\pi\right)^2(\tau-t)}\,d\tau\cdot\cos\frac{2m-1}{2h}\pi z. \tag{11}$$

As seen from these solutions the strong back flow is necessary near the bottom in the model $k=0$ when we determine the values of $\gamma(t)$ or u_1 in order to make the observed curves consistent with the theoretical ones. However, when the change of $\gamma(t)$ with time is assumed to be given roughly by the differences of the observed current velocities and the computed ones in the model $k=0$ without the term u_1, then we have the curve of $-u_1$ as shown in Fig. 9(a). This can be expressed roughly by the function $u_1=U(1-e^{-\alpha t})$ for $U=25$ cm/sec, $\alpha=1.6/45$ (1/min).

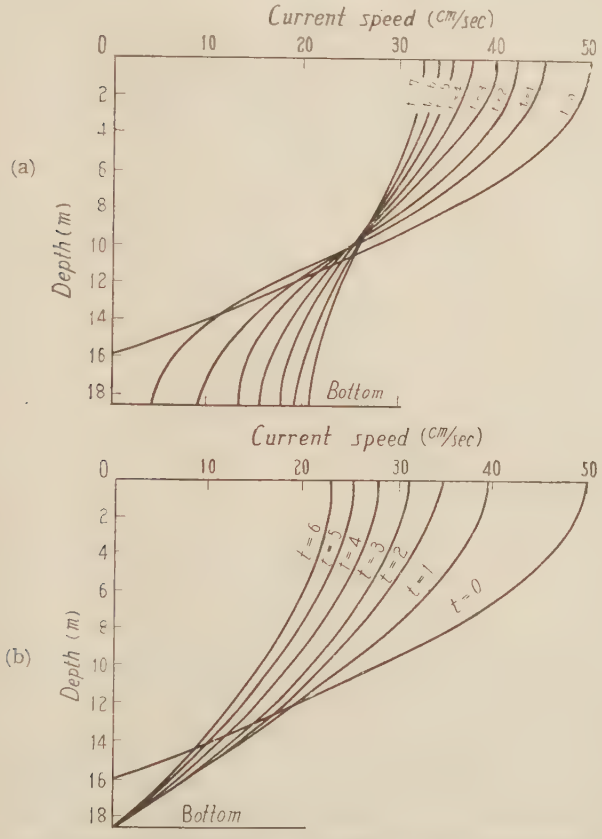

Fig. 8. Theoretical current profiles at the successive stages. $t=1$ means 15 min.
(a) for the case of no bottom friction, $k=0$ when $K=$ ~~150~~ 195 cm²/sec.
(b) for the case of no bottom current, $k=\infty$ when $K=$ ~~77.5~~ 155 cm²/sec.

For such velocity change the values of $\gamma(t)$ are given by $-\alpha U e^{-\alpha t}$. By taking $U=10$ cm/sec and the same numerical constants for K and α, we compute the equation of u_1 of the model $k=\infty$ as shown in Fig. 9(b).

Thus by taking into account the slope term $\gamma(t)$, we show the current profiles in Fig. 10 for the case of no bottom current ($k=\infty$), which indicate better agreement with the observation. The disagreement in speed at 1 and 3 meters layers might be caused by the above assumption that the speed would decrease monotonously.

Therefore, on the whole, we

can conclude that the observed velocity fluctuation is caused by the instantaneous penetration of the waters broken from the disturbance and the change of velocity with time is explained by the effect of vertical eddy viscosity and the change of the surface slope with time. Further as seen from the functional form of $\gamma(t)$ and the direction of current which flowed to the coast, the surface elevation seems to increase with time reaching the equilibrium height after about one hour. This disturbance is not due to the proper oscillation of Tokyo Bay or Uraga Strait, nor to the tidal oscillation, as in the case reported in Ref. [2]. The velocity decrease with depth is so large in the present case as follows. $u=62.1\log_{10} z/2.9$ (u cm/sec, z in meter being measured upwards). The back flow caused the point of inflexion of velocity profile.

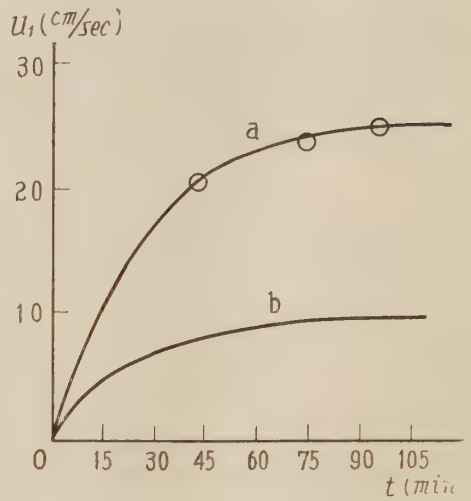

Fig. 9. The estimated velocity of back flow, $u_1=U(1-e^{-\alpha t})$ when $K=155\,\mathrm{cm^2/sec}$
(a) for the case of no bottom friction $k=0$ $U=25$ cm/sec, $\alpha=1.6/45$ (1/min)
(b) for the case of no bottom current, $k=\infty$, taking $U=10$ cm/sec, $\alpha=1.6/45$ (1/min)

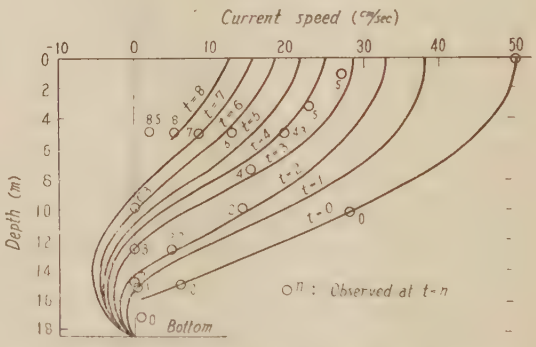

Fig. 10. Theoretical current profiles computed by taking into account of the change of the surface slope for no bottom current. $k=\infty$, $K=155\,\mathrm{cm^2/sec}$.

2) The short period fluctuations.

Next, the shorter period velocity fluctuations in Fig. 11 are analysed. From the figure, we have Fig. 12 instead of Fig. 2 as we traced the fluctuation of water currents more minutely, at regular intervals of one minute. In the figure, we analysed fluctuations between 13h00m and 13h26m. In Fig. 13, the auto-correlations of the speed $R(t)$ are shown, where the curve (a) means those computed from the data of one minute interval and the curve (b) those from the data of 0.5 minutes interval, which indicate a pseudo-periodicity in contrast with the usual correlation curve of turbulent flow. This means that the present short period fluctuations include not only the turbulence but also the periodic disturbance with the period of about 3 minutes. Such periodicity becomes more remarkable when we take the velocity deviations from the mean velocity decreasing with time, the line as shown in Fig. 12. In other words, the present data give an example where the disturbing force gives energy to the region of the special wave length in the spectrum of turbulence [3]. Further in the present example the function $R(t)$ almost vanishes at about $t=1$ minute and from the theory of Dr. Y. Ogura [4] the functional form of $R(t)$ will change with the relations among the length of time under analysis, the scale of turbulence and the sensitivities

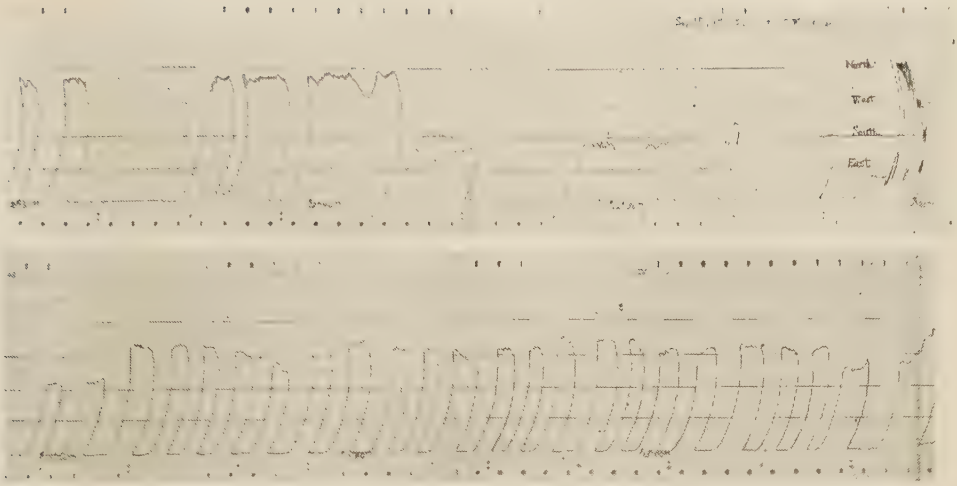

Fig. 11. A record of the current obtained at the 10m layer showing the short period fluctuations.

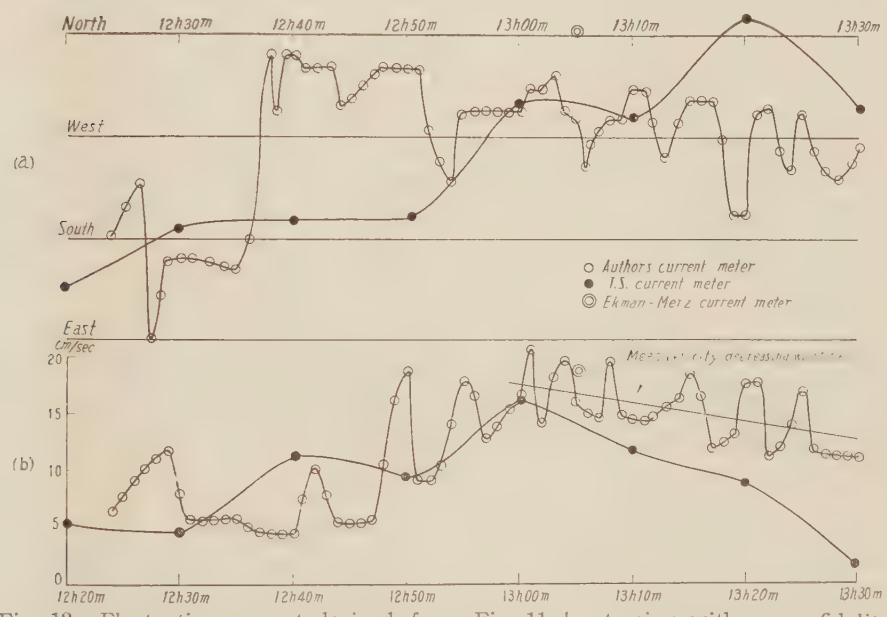

Fig. 12. Fluctuating current derived from Fig. 11 by tracing with more fidelity than in Fig. 2. (a) directions (b) speeds

of the instrument. Especially since the overlapping time interval t^* is 1 minute and the passage time of maximum turbulon t_0 seems to be less than 1 minute in the present case, $R(t)$ should be modified in the range between $t=0$ and $t=1$ minute. And the significant points of 5% for the numbers of 20 and 27 readings are 0.350 and 0.305, respectively [5]. However, the periodicity is not affected so greatly by such process, though various quantities such as period and decrement must be different from the true correlation function.

Further when we assume that only the irregular fluctuations contribute to the

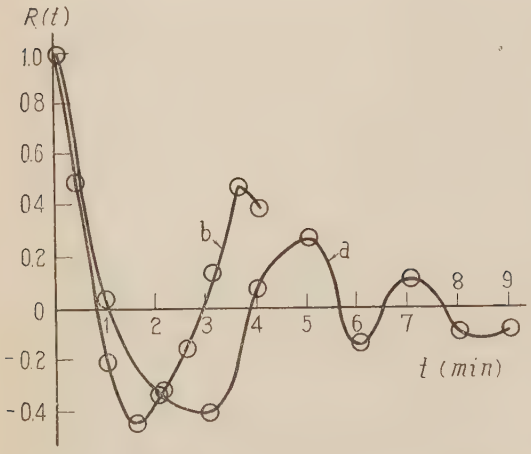

Fig. 13. Auto-correlation curves at the 10 cm layer.

turbulent diffusion of momentum, then the eddy diffusion coefficient K and the mean length of eddy l is given by

$$l \sim U\int_0^{t_0} R(t)\,dt, \qquad K \sim l(\overline{u'^2})^{1/2}.$$

Since the negative values of $R(t)$ is not expected from the usual model of correlation function, we should neglect the computed values of $R(t)$ beyond the range of $t=1$ minute as meaningless. If we assume $t_0 = t/\{1-R(t)\}^{3/2}$, we get t_0 as 65~85 sec. Then we have $t^*/t_0 = 1 \sim 0.5$. Then by the above theory [4], we must take $R^*(t)$ instead of $R(t)$. Considering $R^*(t)=0.5$, $t=30$ sec, $t^*=30$ or 60 sec, we estimate $t_0=20$ sec or less by Fig. 8 of Ref. [4]. Putting $U \sim 15.5$ cm/sec, $\overline{u'^2} \sim 4.73$, $t_0 \sim 20$ sec, we have $l \sim 124$ cm, $K \sim 269$ c.g.s. So we have $L^{4/3} = 1.9 \times 10^5$. Furthermore, the representative scale of phenomena L defined by $L=UT$ is 9.3×10^3. These values are confirmable for the formula $K=0.01\ L^{4/3}$ in Fig. 1 of Ref. [6], p.65.

In the previous subsection the decrease of the observed mean velocity with time can be explained for $K=155$ and this is probably due to the fact that only the irregular fluctuations contribute to the decrease of mean currents when we observe them at about 15 minutes interval. The periodic disturbance as seen in Figs. 12 and 13 superposed on the irregular fluctuations seems to be more effective to the horizontal diffusion, but more observations are necessary to make a definite conclusion.

Acknowledgements ——The author expresses his hearty thanks to the members of the Oceanographical Section, Central Meteorological Observatory of their help during the observation, and also to Dr. T. Ichiye and Dr. Y. Ogura for their kind advices concerning mathematical treatment.

References

[1] Nan'niti, T. 1953: A Current Meter Using a Phototube (I). Pap. Met. Geophys. **3**, p. 286.

[2] Ichiye, T. and Moriyasu, S. 1952: On the Tidal Current in the Mihara Seto. Oceanogr. Rep. Tokyo, **2**, p. 77.

[3] Ichiye, T. 1951: Theory of Oceanic Turbulence. Oceanogr. Mag. Tokyo, **3**, p. 83.

[4] Ogura, Y. 1952: Relations between the Length of Time under Analysis and the Statistical Quantities of the Atmospheric Turbulence. Journ. Met. Soc. Japan, **30**, p. 103.

[5] Anderson, T. W. 1948: On the Theory of Testing Serial Correlation. Skand. Aktuarietidskrift **31**, p. 88.

[6] Inoue, E. 1952: On the Structure of Wind near the Ground. Bull. Nat. Inst. Agricul. Sci., Tokyo, Series A, No. 2.

海水の泡沫性の研究（第8報）
海水泡沫層の崩壊機構について（その3）

阿部友三郎

日本海洋学会誌 第10巻 第1号別刷 （昭和29年5月）

海水の泡沫性の研究　第八報

海水泡沫層の崩壊機構について　(その 3)

阿部友三郎
(気象研究所海洋研究室)

A Study on the Foaming of Sea Water (8th report)

—On the Mechanism of the Decay of Foam Layer of Sea Water (Part 3)—

By

TOMOSABURO ABE

(Oceanographical Laboratory, Meteorological Research Institute)

Abstract: On the standpoint of energy, the author discussed the phenomenon of the decay of foam layer of sea water and obtained the following results.

In the process of the decay of foam layer, he has considered the same quantity "A" as the activation energy in chemical changes. "A" increases with increasing concentration, up to a certain maximum, and then decreases with further increase of concentration.

§1. 緒　言

先に，筆者は海水泡沫層の崩壊が一次化学反応の形式で行われること，又この際，求まる崩壊定数等を用いて泡沫層内の泡沫粒の寿命等につき，多少論じた。

今回は，エネルギー論の観点から，この崩壊現象を既に十分研究されている化学反応論の類推で考察してみた。

化学反応においては，普通の所謂不活性分子に，何等かの方法で，ある程度のエネルギー量(勿論反応により異る)が与えられると，初めてこの分子は活性化されて反応を起すと考えられている。このエネルギー量を活性化エネルギー，又は賦活エネルギー Activation energy と呼んでいる。さて，これまで考察したことによつて，泡沫層内での泡沫粒子の崩壊する現象も一種の化学反応の形式で行われると考えられたのであるから，この崩壊の際に，前述の活性化エネルギーの如きものを形式上考えられ相である。そこで，斯様な energy を考えてみることにした，又，崩壊の際，層の持つている energy が如何様に消耗されて行くかを調べる下準備も行つてみた。

以下に，結果の大略を述べる。

§2. 所謂活性化エネルギー

今，ある分子反応を考えてみる。その反応速度恒数を k' として，Arrhenius の式を書けば，周知の通り次の如くなる。

$$\frac{dI_nk'}{dT}=\frac{A'}{RT^2} \qquad \cdots\cdots(1)$$

ここに，T は絶対温度，R は気体恒数，A' は活性化エネルギーである。即ち少なくとも A' 丈のエネルギーを，普通の不活性分子が貰うと，始めて活性化されて反応が起るのである。併し自然に起る化学反応は，常に出来る丈，活性化エネルギーが少なくてすむ如き形式或は道筋を通つて進むものであるから，与えられたエネルギーの内 A' 量だけが反応に使われる。次に (1) 式を積分するのであるが，Arrhenius の仮定した如く A' は温度に関しては一定であるとする。併し斯様に考えることは近代量子統計力学理論上では，問題があるが，A'=Const. と考えて積分した結果は十分良く実測に合うので，一応 A'=Const. と考えることにする。

(1) 式を積分すれば

$$\int dI_nk'=\frac{A'}{R}\int\frac{dT}{T^2}$$

或は

$$I_nk'=I_nC-\frac{A'}{RT} \qquad \cdots\cdots(2)$$

ここに，C は恒数であり，反応に特有なものである。

(2) を更に変形すれば

$$k'=Ce^{-\frac{A'}{RT}} \qquad \cdots\cdots(3)$$

(2) から明かな如く，A' を求めるには，種々な T につき，k' を実測して，$\frac{1}{T}$ に対して $\log k'$ をプロットすれば，両者は直線関係にある筈である。この直線の勾配 α を求めれば，$\tan\alpha=\frac{A'}{R}$ であるから，A' は次の如く求まる。

$$A'=R\tan\alpha$$

全く同様な方法を，これまで発表した泡沫層の実験試料につき，行つてみた。

第6報で発表した実験値の一部を再録すれば，Table 1 の如くである。

Table 1

Concentration / Sea water temp.	Decay Const. (k)					
	19.26‰ Cl	18.46	16.04	14.42	12.82	9.63
29°C	0.143	0.170	0.166	0.137	0.145	0.200
21	0.124	0.128	0.099	0.131	0.109	0.214
14	0.071	0.071	0.084	0.094	—	—
5	0.071	0.047	0.058	0.049	—	0.097
"A"	$146\times10K$	$208\times10K$	$150\times10K$	$148\times10K$	—	$100\times10K$

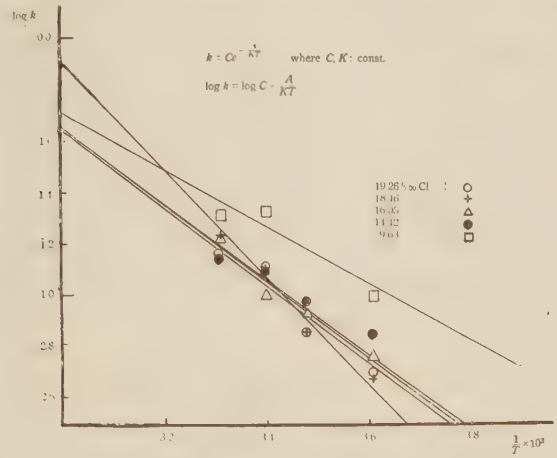

Fig. 1. Relation between the decay const. (k) and temp. (T) of sea water, where T is absolute temp.

さて，19.26‰ Cl 以下 5 種類の濃度につき，$\log k$ と $\frac{1}{T}$ とをプロットすれば，Fig. 1 の如くなり，夫々の濃度の場合につき，両者は略直線関係にあることがわかる。但し，ここに k は海水泡沫層の崩壊恒数である。これから，$\tan\alpha$ を求め，前述のA' 及び R に相当するものを夫々 "A" 及び K とすれば，形式上 "A" は Table 1 に示す如く求まる。但し恒数 K の物理的意味等についての精しい吟味は後報で取扱うことにして，今は触れない。

面白いことには，Table 1 から明かな如く，Cl 濃度が増すのにつれて，"A" が次第に増すが，ある濃度以上になると，再び減少する傾向のあることである。このことは Fig. 2 を見ると更に明瞭である。即ち，Cl 濃度の増加と共に，"A" は増加するが一定の極大値に到ると，再び "A" は減少する傾向にある。つまり，"A" は泡沫層内の泡粒

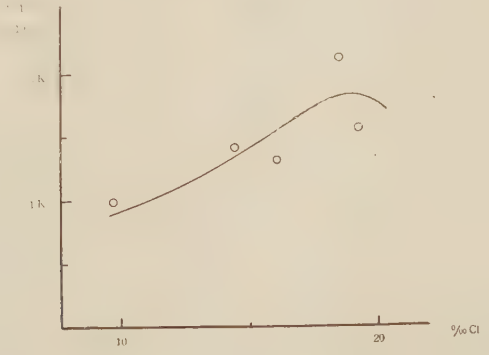

Fig. 2. Change of "A" with the chlorinity of sea water.

を活性化して，崩壊し易くするに必要なエネルギーと考えられるのであるから，Cl 濃度が増すにつれて，次第に崩壊が起り難くなるが，ある濃度以上になると再び崩壊が起り易くなることを示している。この傾向は，先に発表した（第5報）海水及び無機電解質水溶液の泡沫層では，之等の濃度が増加すると共に，泡高は次第に増して行くが，ある濃度にて極大値となり，其後は濃度が増すと反つて減少する如き特性のあることと，対比して考えると興味深い。以上は僅小な資料からの結果であるが，大略の事実は示すものと思う。更にこの点に関し，種々の水温等につき数多くの実験を行うことが望ましい。

さて，化学反応における反応分子に相当するものは，勿論，この崩壊の際は泡沫粒子であるが，これは次に示す如く，この変化中での平均の大きさの泡粒を仮想すればよいであろう。

即ち，
$$\frac{1}{2\tau}\cdot\frac{1}{\theta_2-\theta_1}\int_0^{2\tau}\int_{\theta_1}^{\theta_2}\bar{r}(t,\theta)\,dt.d\theta$$

ここに，$\bar{r}(t,\theta)$ は泡沫の平均半径（第 6,7 報参照），τ は半減期である。

§3. $\bar{D}^2$ の時間的変化

泡沫層の有するエネルギー変化を調べるための準備として，本報では表面エネルギーを求めるための第一歩として，泡沫層の全表面積の変化を調べてみた。勿論，全表面積とは，或時刻における泡沫粒の表面積の合計，即ち $\int_0^\infty nD^2\cdot f(D)\cdot dD$ のことである.

ここに $\bar{D}$ は泡粒の平均直径（t の函数，前報では実験式を第一近似として t の一次函数として取扱つた），n は個数，$f(D)$ は頻度分布函数である。$\bar{D}$ 及び $\bar{D}^2$ を 14.42 ‰ Cl の海水につき，実験値より計算すれば Table 2 に示す通りである。これ等の値を t につきプロットすれば，Fig. 3 の如くなる。図から，如何に泡沫層の全表面積

Table 2.

Temp. / Time	21°C		14		5	
	$\bar{D}$	$\bar{D}^2$	$\bar{D}$	$\bar{D}^2$	$\bar{D}$	$\bar{D}^2$
2 sec.	3.98mm	15.8	5.23	27.4	4.52	20.4
4	4.25	18.1	4.80	23.0	5.46	29.8
6	4.37	19.1	4.30	18.5	4.83	23.3
8	3.16	9.9	3.67	13.5	3.63	13.2
10	1.64	2.7	4.02	16.2	4.62	21.3
12	—	—	3.35	11.2	4.42	19.5
14	—	—	2.45	6.0	4.06	16.5
16	—	—	—	—	3.39	11.5
Half life (τ)	5.3		7.5		12.6	
$-\frac{dD^2}{dt}$ mean. $\left(\frac{mm^2}{sec.}\right)$ $(0\sim2\tau)$	2.60		2.65		1.62	

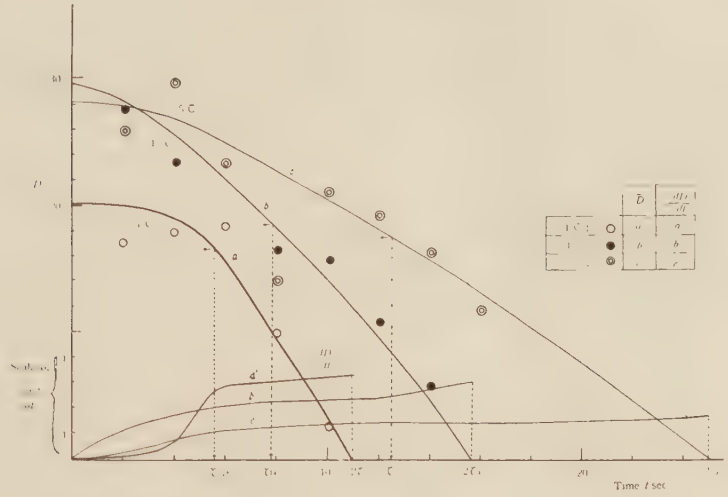

Fig. 3. Changes of D^2 with the time t. sea water 14.42‰ Cl.

が時間と共に減少して行くかがわかる。この減小を見ると，各温度について一般的に云えることは，初めの間は比較的僅かな減小しか起つていないが，ある程度時間がたつと，急速になり，づんづん減小して終に泡粒は消え去つて了うのである。つまり，全表面積は初期では，極めてゆるやかな減小であるが，後急速な減小に変ると云う二様の道程を通るのである。これを多少，量的に示すため $-\frac{d\bar{D}^2}{dt}\left(\frac{\text{mm}^2}{\text{sec.}}\right)$ の変化を求めれば，Table 3 の如くなる。これを平滑化した曲線を Fig. 3 の下端に示して置いた。

Table 3. Value of $-\frac{dD^2}{dt}$. sea water Cl. 14.42‰

Temp. \ Time	2 sec.	4	6	8	10	12	14	16
21°C	0.16	0.54	2.98	3.12	3.30	—	—	—
14	1.17	1.70	2.10	2.30	2.32	2.65	2.80	—
5	0.13	0.80	1.10	1.20	1.28	1.62	1.60	1.40

次に D^2 の割合が，時間と共に如何に変化するかを考察してみる。

Table 4.

Temp.	Time	0 sec.	2	4	6	8	10	12	14	16
21°C	$\bar{D}^2$	20.3	20.0	19.2	15.6	9.4	3.4	0	—	—
	Frequency	100.0%	98.5	94.5	76.8	46.3	16.7	—	—	—
14°C	$\bar{D}^2$	29.5	28.2	25.5	22.1	18.5	14.0	9.6	4.6	0
	Frequency	100.0	95.5	86.4	74.5	62.6	47.4	32.5	15.6	—
5°C	$\bar{D}^2$	28.1	27.7	26.8	25.1	22.8	20.5	18.2	15.9	13.1
	Frequency	100.0	98.5	95.4	89.3	81.0	73.0	64.7	56.5	46.6

今，$t=0$ のこの値を 100% として，各時刻における割合を計算すれば，Table 4 の通りである。勿論，$t=0$ の実験値はないので Fig. 3 の曲線を外挿して求めた。斯様にして得られた値を図上にプロットしたのが Fig. 4-a である。この図から，$\bar{D}^2$ 時間と

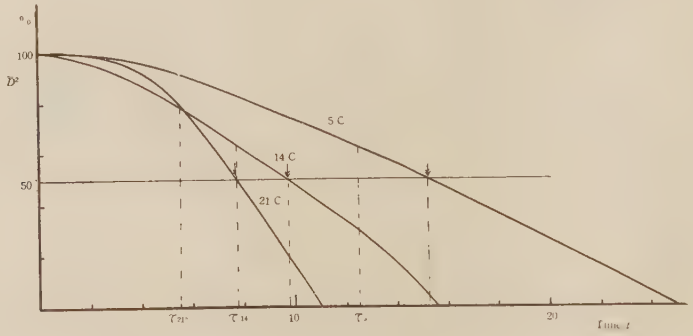

Fig. 4-a. Changes of $\bar{D}^2$ with the time t.

共に如何に減小して行くかがわかる。一般的に云えることは，3 種の水温の場合につき，$\bar{D}^2$ は同様な形式で減小して行くが，水温の高い程，急速に消耗して行く傾向にある。更に精しく，この辺の傾向を見るため次の操作を行つてみた。即ち，全表面積が初めの値の

Table 5.

Temp.	τ	$T_{0.5}$	(τ/5: unit)	$T_{0.5}-\tau$	$\frac{T_{0.5}-\tau}{\tau}$
21°C	5.55 sec.	7.75 sec.	6.95	2.20 sec.	0.396
14	7.8	9.70	6.20	1.90	0.244
5	12.5	15.2	6.05	2.70	0.216

半分になる時間を $T_{0.5}$ として，これを求めてみると，Table 5 の如くである。即ち，$T_{0.5}$ の値は水温 21°C では約 8 秒かかるのに，水温が低くなり 5°C ではその約 2 倍の

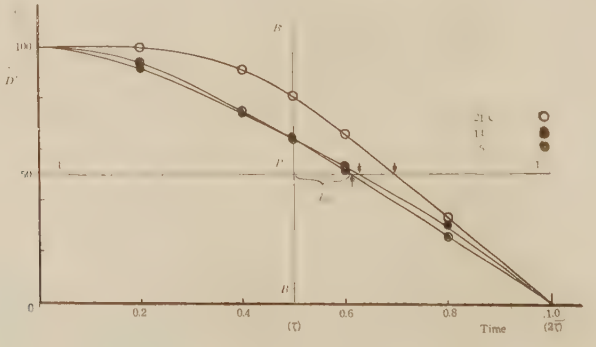

Fig. 4-b. Changes of $\bar{D}^2$ with the time t.

15 秒強かかることがわかる。以上を更に一般的に論ずるため，各場合に特有な半減期 τ を時間の単位にとる。今は便宜上，$\tau/5$ を単位とした。斯様にして Fig. 4-a を書き改めてみると Fig. 4-b の如くなる。ここで，D^2 の 50% の線，即ち AA'，τ の線即ち BB' を引き，それ等の交点を P とする，又 AA' と交わる各曲線との交点を L_θ とすれば，L_θ は，τ 即ち泡高が半減してから，L_θ 時間たつと初めて泡沫層の全表面積が半減することを表わしている。云い換えれば，外観上，泡沫層が半分になつても，まだ層の全表面積は半分にはなつておらず，これから L_θ 時間遅れて初めて半分になるのである。次に BB' 線と各曲線との交点を作つてみると，これ等が外観上，泡沫層が半減したとき，層の持つている全表面積の割合を示している。以上の値を図から求めて Table 6 とした。この

Table 6.

θ	L_θ	D^2 % at τ	τ
5°C	0.11	63	12.5 sec.
14	0.13	64	7.8
21	0.20	80	5.5

Table で L_θ をみると，5°C では時間 0.11 ($\tau/5$: unit) であるのが，21°C では更に長くなり 0.20 となつている。又，τ 即ち泡高が半分になつたとき，5°C では層の全表面積は半分ではなく 63% も残つており，21°C では更に多くて 80% も残つていることがわかる。

§4. 結　語

以上を要約すれば，

海水泡沫層の崩壊をエネルギー論的立場から多少考察して次の結果を得た。

1　分子間に起る化学反応の際考えられる活性化エネルギーの如きものをこの崩壊の際にも考えることができる。この際の所謂，活性化エネルギーは水温と共に増大して，ある極大値に到り，以後は反つて減小して行く傾向がある（§2.）.

2）次に，泡沫層のエネルギー変化を考える便宜上，先づ予備的計算として，層の持つ全表面積が如何に時間的に減小して行くかを調べた（§3.）.

終りに臨み，本研究に御興味を持たれ，色々と御討議して頂いた海洋研究室長中野猿人先生並びにこの崩壊を化学反応の類推で行う様御教示して頂いた当所地球化学研究室長三宅泰雄先生に深く御礼申上げます。又計測用写真の引伸等のわづらわしい仕事を快くとられた金沢五寿雄技官に深謝する。

参　考　文　献

1) 阿部友三郎：中央気象台海洋報告 3 巻 1 号 昭和 28 年
2) 〃　：日本海洋学会誌 9 巻 2号 昭和 28 年
3) 千谷利三：化学反応 上巻 岩波書店 昭和 20 年
4) Y. Miyake and T. Abe: Journ. Mar. Res. Vol. 7, No. 2, 1948.
5) C. N. Hinshelwood: The Kinetics of chemical change, Oxford Univ. Press. 1940.
6) S. Arrhenius: Z. Phys. Chem., Vol. 4, 226, 1889.

溶在酸素量の日変化（第1報）

杉浦吉雄
（気象研究所）

On the diurnal variation of dissolved oxygen (I)

By

Y. SUGIURA

Abstract: In eutropic lakes or coastal waters, a marked diurnal variation of oxygen content is found. There are two types of variations. In one of them, a minimum occurs mostly at about 6 h and a maximum at about 17 h. This type of variation is often seen in stable and homogeneous water masses. In the other type, minimum and maximum occur at different hours from the former. In this case, the influence of diffusion and advection or convection upon the diurnal variation of oxygen content must be considered. In this paper, the former case was chiefly treated. In this case, the amplitude of the diurnal variation depends upon the intensity of radiation, the duration of insolation, water temperature, number and size of phytoplanktons and etc.

Indeed, the amplitude is larger on a clear day than on a cloudy day and it is also larger in summer than in winter. It was obtained by the calculation that the diurnal variation should have a minimum and a maximum respectively at a certain time distance before and after the noon. By using the data of the diurnal variations of dissolved oxygen, the amount of the oxygen production or consumption during a whole day was computed.

Assuming a certain size and number of phytoplanktons, these values agreed well with those observed.

1. まえがき

溶在酸素量の日変化に関する研究は，基礎的問題であるにも拘らず，今日まであまり取上げられていない。すなわち，三宅，倉茂両氏の研究以外に，特筆すべきものはない。三宅氏[1]は，三崎水道に於ける日変化を，二水塊の混合によつて説明した。倉茂氏[2]は，日射量その他の気象条件と溶在酸素量の関係を，定性的に論じた。著者は，理論的考察を行い，毎時の溶在酸素量を与える式を導いた。その式は，次のような考察に基いて定められた。

海洋や湖沼に溶在する酸素は，水中の植物による炭素の固定に伴つて生成する一方，生物の呼吸や有機および無機物の酸化のために消費される。また，拡散や移流あるいは対流によつても変化する。

Reprinted from the *Papers in Meteorology and Geophysics* Vol. V No. 1, 1954
Published by the Meteorological Research Institute

A New Plastic Water Sampler

by

T. Nan'niti

and M. Iwamiya

Relations between the Turbidity Factor and the Transparency, the Extinction, the Absorption, the Scattering Coefficients

by

T. Nan'niti

Published by the Meteorological Research Institute,
Mabashi, Suginami, Tokyo, Japan
April, 1954

Reprinted from "papers in Meteorology and Geophysics" VOL. V No. 1.

SHORTER CONTRIBUTIONS

551.460.18

A New Plastic Water Sampler

by

T. Nan'niti

Meteorological Research Institute

and M. Iwamiya

Turumi Seiki Company

(Received March 23, 1954)

The authors made a new plastic water sampler as shown in Fig. 1. The cylindrical tube of the sampler is fitted with a stem mercury-in-glass thermometer, or a reversing thermometer if we want, in its inner side; and it has two nylon ropes, each 20 meters long, one of which is graduated in meters.

The instrument is lowered to the required depth head forward. Then the tube is at the upper end and the sampler is in the open position. It is allowed to remain there for about 3 or 5 minutes to permit the thermometer to reach the temperature of its surroundings, and as it is reversed by turning through 180 degrees by the other rope, the tube is slided down to the lower end of the sampler, and encloses a sample, to the amount of about 500 cc.

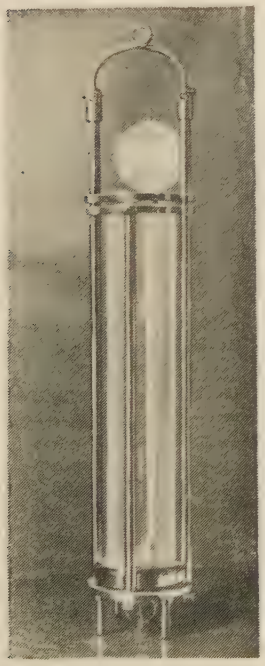

Fig. 1. The new plastic sampler fitted with a stem thermometer.

Then we can measure the water temperature by reading the thermometer through the tube, and the specific gravity by a hydrometer. And the water is sampled from a drain tube of rubber at the lower end of the instrument.

The heat conductivities of the new plastic sampler and the Kitahara's (a Petterson-Nansen type) were measured

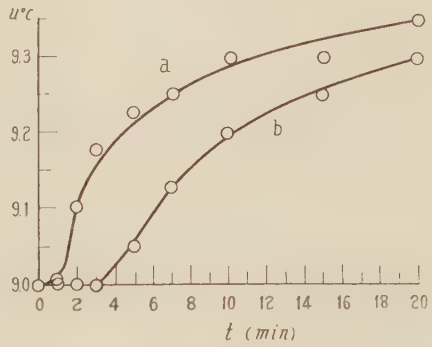

Fig. 2. Temperature-Time curves when the instruments were exposed to air of 11.5°C after they were dipped in water of 9.0°C for 5 minutes.
(a) for the case of the Kitahara's
(b) for the case of the new sampler

as shown in Fig. 2. By the equation

$$k=\frac{1}{(\pi^2/4l^2+2.4048/a^2)\,(t_2-t_1)}\log_e\frac{u_a-u_1}{u_a-u_2},\quad [1]$$

we have $k=0.032$ cm²/min for the new sampler and $k=0.053$ cm²/min for the Kitahara's.

Furthermore, water is obtained uncontaminated by the plastic instrument. In conclusion, the new sampler is a very useful one for shallow water observations.

Reference

[1] Nan'ni'i, T. 1950: A Lazy Thermometer, Oceanogr. Mag. **2**, p. 59.

551.463

Relations between the Turbidity Factor and the Transparency, the Extinction, the Absorption, the Scattering Coefficients

by

T. Nan'niti

Meteorological Research Institute

(Received April 9, 1954)

Introducing the factor "turbidity factor" T, which denotes the ratio of the total extinction coefficient $k(\lambda)$ to that for molecular scattering coefficient $s(\lambda)$ alone [1], we have

$$(1)\qquad T(\lambda)=\frac{k(\lambda)}{s(\lambda)}=\frac{f(\lambda)+s(\lambda)+a(\lambda)+r(\lambda)}{s(\lambda)},$$

where $f(\lambda)$, $s(\lambda)$, $a(\lambda)$ and $r(\lambda)$ are the absorption and the scattering coefficients of pure water and the absorption coefficient of dissolved substances, "Yellow substances", the scattering coefficient of suspended particles "Seston", respectively [2].

For example, putting $f(\lambda)=0.019$, $s(\lambda)=0.00223$ when $\lambda=5200$Å [2],

$$(2)\qquad T_{5200\text{Å}}=9.520+R_{5200\text{A}}/0.00223=448.43\,k_{520\text{JA}},$$

where $R(\lambda)=a(\lambda)+r(\lambda)$. In pure water, $T_{5200\text{Å}}=9.520$, $k_{5200\text{Å}}=0.02123$.

Or we have

$$\frac{1}{T(\lambda)}=\frac{s(\lambda)}{k(\lambda)}=\frac{\alpha(\lambda)-r(\lambda)}{k(\lambda)},$$

where $\alpha(\lambda)=s(\lambda)+r(\lambda)$ [2].

Then

$$(3)\qquad \frac{\alpha(\lambda)}{k(\lambda)}=\frac{1}{T(\lambda)}+\frac{r(\lambda)}{k(\lambda)}.$$

From the equation (7)*,

$$\frac{\alpha(\lambda)}{k(\lambda)}=\frac{(\rho(\lambda)/\pi)\{1-\rho_0(\lambda)\}^2-C(\lambda)\rho_0(\lambda)e^{2h(\lambda)k(\lambda)}}{(3/16\pi)\{1-\rho_0(\lambda)\}^2\{1+C(\lambda)e^{2h(\lambda)k(\lambda)}\}}. \tag{4}$$

So from the equations (3) and (4)

$$\frac{1}{T(\lambda)}+\frac{r(\lambda)}{k(\lambda)}=\frac{(\rho(\lambda)/\pi)\{1-\rho_0(\lambda)\}^2-C(\lambda)\rho_0(\lambda)e^{2h(\lambda)k(\lambda)}}{(3/16\pi)\{1-\rho_0(\lambda)\}^2\{1+C(\lambda)e^{2h(\lambda)k(\lambda)}\}}. \tag{5}$$

If $C(\lambda)$, $\rho(\lambda)$, $\rho_0(\lambda)$ are constants in any conditions but functions of wave length of light,

$$\frac{1}{T(\lambda)}+\frac{r(\lambda)}{k(\lambda)}=\frac{K_1(\lambda)-K_2(\lambda)e^{2h(\lambda)k(\lambda)}}{K_3(\lambda)+K_4(\lambda)e^{2h(\lambda)k(\lambda)}}. \tag{6}$$

Form the equations (2) and (6)

$$\frac{K_1(\lambda)}{T(\lambda)}-\frac{K_2(\lambda)}{K_3(\lambda)+e^{2h(\lambda)k(\lambda)}}=K_4(\lambda). \tag{7}$$

For instance, if we take $R\sim0.002(450\,k-9.52)$, $T\sim450\,k$, $\rho/\pi=0.15$, $\rho_0=0.05$, $C=1/100$, we have approximately

$$hk\sim2.5 \text{ or } hT\sim1120.$$

Of course, we can get the same result from the equation*. If we defined $T(\lambda)=k(\lambda)/\{s(\lambda)+f(\lambda)\}$, $T_{5200\text{Å}}=1+R_{5200\text{Å}}/0.021=47.6\,k_{5200\text{Å}}$.

Acknowledgement——The author wishes to express his hearty thanks to Dr. Y. Takenouti and Mr. K. Kajiura for their kind advices.

References

[1] Sutton, O.G., 1953: Micrometeorology. Mc. Graw-Hill Book Company Inc. London.
[2] Nan'niti, T., 1953: A Theory on the Transparency of Sea Water. Pap. Met. Geophys. **3**, p. 195.

* Eqution (7) in the provious paper [2].

Tess 台風と Alice 台風による八丈島の波浪

大道寺重雄・宇野木早苗・梶浦欣二郎

研 究 時 報 第 6 巻 第 7 号 別 刷 (1954年9月)

Tess 台風と Alice 台風による八丈島の波浪

大道寺重雄*・宇野木早苗**・梶浦欣二郎***

Waves at Hachijo Island Caused by Typhoon Tess and Alice in 1953

S. Daidoji, S. Unoki and K. Kajiura

551.465

The characteristics of waves generated by a typhoon are very difficult to forecast, because it moves rapidly and, moreover, the variation of wind velocity and direction is very large within the area of a typhoon.

In autumn, 1953, wave observations were carried out in two cases when typhoons were approaching Japan Island. The first case is when the path of a typhoon is in the western side of Hachijo Island and the second case is when the path is in the eastern side. In these two cases, the circumstances of wave attack against this Island were quite different, that is, in the first case only, a long wave with the period of about two minutes and about three meters in height were accompanied by wind waves, and this long wave may be some kind of oscillation generated by the mass transport resulted from very high wind waves and strong southerly wind.

Refraction effect is found to be slightly large compared with the theoretical estimate, and this may be attributed to the variability of a wave direction but the detailed discussion is not yet possible.

1. 緒 言

台風に伴う波浪によって，我が国の沿岸施設や船舶は年々大きな被害を受けているが，どの程度の週期と波高をもった波が襲来したのかという正確な資料は皆無といっても良い状態であった。沿岸のうねりと台風との関係は，富崎については奥山熊一[1]，八丈島については樺沢実[2]の研究が行われているが，これらは毎日 10 時1回の目視観測を整理したもので，資料が不充分なために台風による波浪の動的な実態をつかむことはなお困難であった。

1953 年9月下旬の Tess 台風（第13号）と同年 10 月中旬の Alice 台風（第 18 号）による波浪が，中央気象台によって八丈島に設置された自記波浪計に記録され，同時に若干の目視観測が行われた。これらの連続資料は台風による波について興味ある問題を提起したので，調査した結果を報告する。なお八丈島における自記波浪観測は 1952 年 9 月より現在まで実施されているの

* 鳥島気象観測所
** 気象研究所海洋研究室
***東京大学地球物理学教室

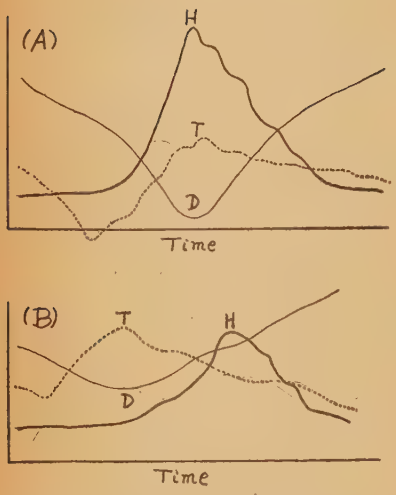

Fig. 4. Time sequence of the wave caused by cyclones at Jogashima Is. (A) or (B) corresponds to the case when a cyclone passes close to Jogashima Is. or the case when it passes far apart from the Island respectively.

であると考えられる。しかし，その詳細は今後の研究にまたねばならぬし，又このような点は波浪予報上大いに留意すべきと思われる。

次に台風による波浪が八丈島に影響し始めた時刻は，Tess 台風では9月23日の始めで，Alice 台風では10月18日の始めであって，その時の台風の位置は第1図の⊙で示されている。興味のあるのは何れも 20 °N 付近であって，八丈島の南方約 1500 km の所である。しかし，最初に現われる波は，はるか南方（20° N 以南）に台風があるときそこから発生した波が到達したと考えるより，寧ろ台風の前面一帯に吹走している北東風によって発生した波であると考える方が妥当かも知れない。

更に，台風による波浪の影響がなくなる時刻を調べると，Tess 台風の場合は波高最大時すなわち台風最接近時より丁度2日後に波がおさまっている。一方 Alice 台風の場合には，台風最接近時より4日間もの間，2～3 mのかなり高い波が引き続いて残っている。それに応じて週期も，Tess 台風の場合は急速に減少しているが，Alice 台風の場合には大きい週期が持続している。これは，Tess 台風は本州に上陸したため新しい波が生成されず，とり残された波がだんだん衰えながら八丈島に到達するのであるが，Alice 台風の場合には台風は八丈島から離れた後も相かわらず東方洋上にあるため，次々に生成された波が到達するためと考えられる。

3. 予報値との比較

波の予報に関して，significant wave に基礎をおいたものと wave spectrum に基礎をおいたものとがあるが，ここでは前者の Sverdrup-Munk の予報理論に我々の結果を適用してみよう。[4] この理論では，風向・風速・吹走距離・連吹時間・減衰距離についてそれぞれ平均値を求めるのであるが，台風のように風の傾度が大きく，かつ台風自身がかなりの速度で移動している場合には上述の要素の平均値を求めることは困難で，又無意味とも考えられる。そこで便宜上，風速 20 m/s で風向が八丈島を指している風域を追跡して，それによって生ずる波を求めてみた。又，比較の為に 40 m/s の風域による波も計算してみた。例えば Tess 台風の場合に吹走距離の大きさは，20 m/s の風に対してはほぼ 500 S. M., 40 m/s の風に対してはほぼ 130 S. M. となった。それらの結果を第5図に示す。なお予報値を示す曲線は予報値の最大値を結ぶように引かれてある。

A 図は Tess 台風の波高を示すが，予報値は実測値の 1.5 倍も大きく，あまり良く合わない。しかも実測値は最大波高であり，予報値は significant wave height であるからその差は一層大きくなるはずである。しかしその最大の起時は，三者ともよく一致している。波高の変化も 20m/s の場合と 40m/s の場合は一致しているが，これは風速が大きいと吹走距離が小さくなるためで，台風内のどのような風域に着目して予報値を求めても，大体同じ程度の値が得られることを暗示している。B図は Tess 台風による週期の変化を示しているが，実測に較べて予報値は何れの場合も著しく小さい。

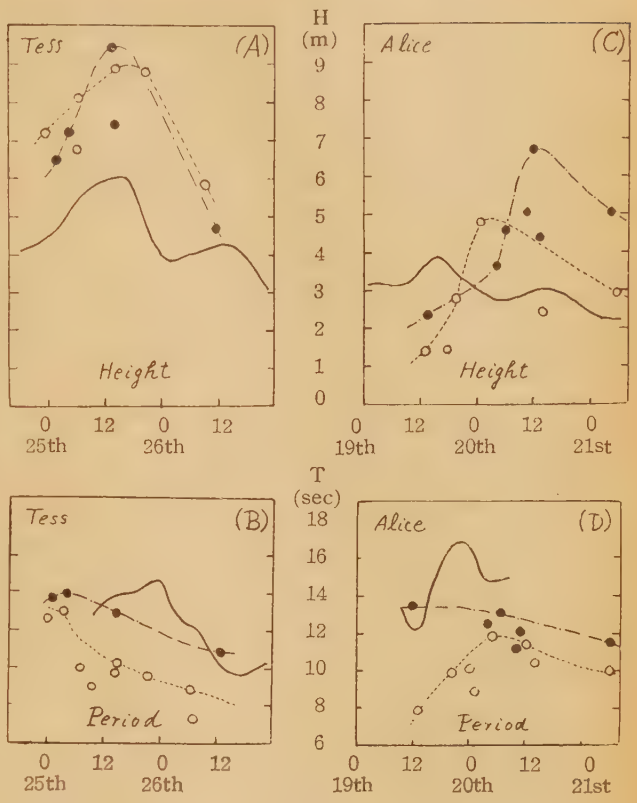

Fig. 5. The comparison between observed values and forecasted ones of wave height and period.
——— This line shows observed values taken by a wave recorder.
···○··· This line shows forecasted values caused by the wind whose velocity is twenty meters per second.
—·●—· This line shows forecasted values caused by the wind whose velocity is forty meters per second.

Alice 台風の場合の波高と週期についての比較はC図，D図にそれぞれ示されているが，波高は勿論，最大波高の起時も実測よりかなり遅れて起っている。週期も Tess 台風の場合と同様，実測より著しく小さい。Alice 台風のように島の東側を台風が北上する場合には八重根は島蔭になるので，波の予報にはそれを考察せねばならぬが，現段階ではまだ困難である。

Table 2.

台風	最大波高			最大週期		
	実測	20m/s	40m/s	実測	20m/s	40m/s
Tess	610	900	940	14.6	13.1	14.0
Alice	400	480	670	16.7	12.8	13.1

以上の結果をまとめて第2表に示す。予報値も実測値と同じく，Tess 台風の方が Alice 台風より波高が大きい。これは台風の規模と八丈島までの距離に基因している。

さて S. M. の理論において週期の予報値が実際に較べて系統的に小さいことは多くの人に指摘

な振動系を意味するかは不明である。実際問題からしても，波高の高い長週期の波は沿岸施設に対する浪害に対して重要な意味をもつものと考えられる。

6. 中間波の観測

Alice 台風の時，八重根港の沖合に漁船が数隻避難してきた。船と船との間隔から，うねりの波長と波速を求め得た。その値を第3表に示す。なお，水深がほぼ 30m であるから中間波 (elliptic trochoidal wave) の公式を用いて計算した結果も併せてのせておいた。観測の精度からして，オーダーは合っているといえよう。

Table 3.

週期	実測		中間波		
	波長	速度	波長	位相速度	群速度
14sec	200 m	50 km/h	214 m	55 km/h	45 km/h
17sec	250 m	—	271 m	—	—

7. 要 約

(1) 台風が八丈島の東側を通るか，西側を通るかによって，襲来する波の模様はかなり異なる。台風が真直ぐ北上する際の波浪予報上参考になる点として

a. 台風が北緯 20° の線まで北上してきた頃から八丈島の波は高まり始まる。

b. 台風が八丈島に最も接近した頃波高は最大になり，週期は数時間遅れて最大になる。

c. 台風が本州に上陸する場合には，波高も週期も急速に減少し，2日後にはその影響はなくなるが，東方洋上に去った場合には，4日後にもかなりの高さと週期をもった波が残っている。

d. 島の表側と裏側（波に対して島蔭）の波高比は 3：1 である。ただしこれは十数秒という長い波に対してであって，週期が小さいとこの比は大きくなる。

(2) 週期2分前後，波高 3m の長週期の波が観測されることがあるが，これは波と風による mass transport に基因する，一種の振動と考えられる。

(3) Sverdrup-Munk の予報値と実測値を比較した。予報値は実測値より，波高は高く，週期は低くなっている。台風のように，傾度が急激で，移動が速い場合には，S. M. の仮定がなり立たず，適用はかなり困難である。

終りに，熱心に観測を行われた八丈島測候所員の方々及び研究の便宜を与えられた藤井海洋課長に深く感謝の意を表する。なお，この研究費の一部は UNESCO 国内委員会に負うもので，ここに同会に対し感謝する次第である。

文 献

(1) 奥山熊一 (1947)：うねりと低気圧の関係について．研究速報，第28号．

(2) 樺沢実 (1949)：台風とうねりの関係について．研究時報，第1巻，第7号．

(3) M. Nakano, S. Unoki and Y. Kuga (1953)：On the Result of Wave Observations at Jogashima Island and its Application for Wave Forecasting. Papers. Meteor. Geophys. Vol. 4, No. 3～4.

(4) H. U. Sverdrup and W. H. Munk (1947) : Wind, Sea and Swell : Theory of Relations for Forecasting. U.S. Hydrogr. Off. Pub. 601. ; なお図表は水路要報第20号 (1950年) に所載のものを使用した.

(5) W. H. Munk and R. S. Arthur (1951) : Forecasting Ocean Waves. Compendium of Meteor.

(6) M.Nakano (1949) : On the Secondary Undulations of Tides Caused by Cyclonic Storms. (1st Paper). Oceanogr. Mag. Vol. 1, No. 1.

(7) W.H. Munk (1949) : Surf Beats. Trans. Amer. Geophy. Union, Vol. 30.

前線性豪雨の移動法則について

斎　藤　将　一*

On a Law of Frontal Heavy Rainfall Movement

S. Saito

551.577.37:551.509.54

In regard to the movement of frontal heavy-rainfall areas, Dr. Ōtani has presented that there are two kinds of frontal heavy-rainfall movements, the one moving normal to a front and the other parallel to it. In this paper, the above suggestion is examined by use of synoptic charts and it is concluded that the suggestion is correct and useful.

§ 1. はしがき

ある地方に豪雨が降りはじめたことは，特殊気象電報によって速報を受けることができる。そして，その豪雨がどんな進路で移動するかを予想することができれば，かなりの時間的余裕をもって大雨の注意報・警報を出すことができる。豪雨の移動の特性については，大谷博士の説(1)がある。すなわち，「豪雨の移動には前線に直角のものと平行のものがある。」この小論においてはこの説を種々の豪雨の移動から帰納して，法則としての価値あることを示す。

§ 2. 1951 年梅雨末期の豪雨の移動について

1951 年 7 月 7 日から 17 日の間，西日本に数回にわたり豪雨が発生したが，その時の豪雨移動と前線との関係をのべよう。

まず，豪雨の移動の大勢をつかむために，西日本の各地点毎に 3 時間の移動合計雨量を計算し，これを各時間毎にそれぞれ地図上に記入した雨量分布図をつくり，これにもとづいて 3 時間雨量の移動状況を調べた。つぎに，各地の 10 分間雨量変化図をつくり，この図示された各地の雨の降り方の特徴を照し合わせ，その上豪雨移動の大勢を参考にして，同一系統の降雨と目される各地のピークの時刻を読みとった。これを各降雨の系統毎に等時線を描いて検討し，この結果によってピークの時刻を決定した。第 1 表はその結果であるが，ピークが 1.5 mm より少ないものは移動が不規則であるので，これは省略してある。

第 1 表の結果から各降雨系の移動を示す等時線を描くと，第 1 ～ 4 図のようになる。第 1 図において a, b, c, d 系統の雨は 8 日から 9 日にかけて，西日本南海上から日本海へ北上した温暖前線に伴うものである。この前線の移動は第 5 図 a に示してある。これを見ると，はじめの三系統の雨は前線に平行な移動をしており，おわりの豪雨は前線に直角の方向に移動している。この両者の特

* 大阪管区気象台

海水の泡沫性の研究(第9報)—海水泡沫層内における泡粒の頻度分布について

阿　部　友　三　郎

中央気象台海洋報告　第3巻　4号（別冊）

昭和29年12月

海水泡沫性の研究（第9報）
海水泡沫層内における泡粒の頻度分布について

阿　部　友　三　郎
（気象研究所海洋研究室）

A Study on the Foaming of Sea Water (9th report)
—On the Distribution of the Size of Bubbles in Foam Layer of Sea water—

by
Tomosaburo Abe
(Oceanographic Laboratory, Meteorological Research Institute)

Abstract: From the standpoint of statistical mechanics, the author discussed the frequency distribution of the size of bubbles in foam layer of sea water and obtained the following result:

The theoretical values of the frequencies calculated by statistical methods agreed fairly well with those derived from experimental data; thus it appears that it is possible to deal with the phenomena relating to the foaming by means of statistical mechanics or mathematical probability.

§1. 緒　言

前報で筆者は，海水泡沫層の崩壊をエネルギー論的立場から考察して，分子又は原子間に起る化学反応の際考えられる活性化エネルギーの如きものを，この崩壊にも考え得ることを示し，これを化学反応論の類推で取扱つた。

今回も亦，泡沫層をエネルギー論的立場から扱つてみた。即ち，この泡沫層内の泡粒の大きさについての頻度分布を簡単な統計力学を用いて理論的に計算し，一方，実験的に求めたこの分布とを比較した所，両者はかなりよく一致することがわかつた。斯様な分布の問題は他の地球物理学上の分野にもしばしば起るものであり，多少の知見ともなれば幸と思い，次にその大略を報告する。

§2. 泡粒頻度分布の理論的考察

筆者が行つた実験の場合につき，泡粒が形成される過程を考えてみよう。

硬質硝子製振盪管（断面角型約 $4\times4\ cm^2$，長さ 15 cm）に予め $^3/_5$ 海水を封入したものを一定振幅（約 1.5 cm），一定周期（約毎秒 15 回）の振動を上下に与える。即ち振動の形でエネルギーを海水に与えるわけである。さて，この海水中には，もともと微視的な種々の不均一さ（例えば，ミクロに

見て，局所的密度の，温度の，塩分濃度の，又は溶存気体濃度等の不均一さ）が無数にあり，これ等が，海水中何処に特に多く又は少くということなく，一様に分布されていると考えられる。今，ここに外部から振動の形でエネルギーが与えられると，このエネルギーは適宜に分割されて，前記不均一の部分に集積され，ここが中心，所謂核となり，海水は割れる。するとそこへ空気，水蒸気等が入り込んで，所謂泡粒が形成される。又このエネルギーの分割の程度に応じ，大小様々の大きさの泡粒が生れるのであろうと考える。而して，更に振動が続けられると，今生れたばかりの泡粒の一部は破壊分割され，小さくなり又は周囲え溶け込んで消失する。他方，新しく生れ出るものもあり，泡粒同志互に合体して成長して行くものもある。振動の続くかぎり斯様な泡粒の新生，合体，分裂及び消滅等が引続き起り，丁度気体論における分子渾沌 molecularchaos の如き様相を呈する。併し，適当な時間を経過すると，生成される割合と破壊消失する割合とが等しくなり，ここで，泡粒の数は増加も，減少もしない平衡状態に達するものと考えられる。これ以後は時間的に不変の定常状態となる。実験上，泡粒数を示す一応の目安と考えられる泡沫層の高さは振盪数十秒でこの平衡に達している。この際，最初に生じた泡粒の有するエネルギーを e とする。

さて，今この定常状態にて海水系え単位時間に E なるエネルギーが与えられているとし，このため N 個（十分大）の泡粒が形成されていたとする。この E 或は ne が泡粒え分配され方を考えてみる。さて ne のエネルギーが，この N 個の泡粒に分配されて，泡粒は種々なる大きさのエネルギー，言い換れば，大きさの種々なる値を採る様になると考えるのである。従つてこの ne のエネルギーを N 個の泡粒に分配する方法の数を $M_N(n)$ とすれば，統計力学でよく知られている様に，

$$M_N(n)=\frac{(n+N-1)!}{n!(N-1)!} \quad \cdots\cdots(1)$$

である。この関係を用いて，ある特定の泡粒に xn なるエネルギーが分配される場合の probability $p(x)$ を求めてみることにする $(x\geqq 0)$。

この場合，ある特定の泡粒に xe なるエネルギーが分配されると，残余のエネルギー，即ち $(n-x)e$ が，残りの $(N-1)$ 個の泡粒に分配されるわけである。このときの可能な微視的状態の数は明らかに，

$$M_{N-1}(n-x) \quad \cdots\cdots(2)$$

である。

すべての分配方法の数は，$\sum_{x=0}^{n} M_{N-1}(n-x)$ であり，これは $M_N(n)$ に外ならぬ。

従つて，求める $p(x)$ は次の通りである。

$$p(x)=\frac{M_{N-1}(n-x)}{\sum_{x=0}^{n} M_{N-1}(n-x)}=\frac{M_{N-1}(n-x)}{M_N(n)} \quad \cdots\cdots(3)$$

計算の便宜上（3）式を更に簡単化してみる。

$$\text{即ち, } p(x)=\frac{\frac{(n-x+N-2)!}{(n-x)!(N-2)!}}{\frac{(n+N-1)!}{n!\,(N-1)!}}=\frac{(N-1)!\cdot n!\cdot(n+N-x-2)!}{(N-2)!\cdot(n-x)!\cdot(n+N-1)!}$$

$$=(N-1)\times\frac{n(n-1)(n-2)\cdots\cdots(n-x+1)(n+N-x-2)!}{(n+N-1)(n+N-2)\cdots\cdots(n+N-x-1)\cdot(n+N-x-2)!} \quad \cdots\cdots(4)$$

ここで，$N\gg1$，$x\varepsilon\ll E$，とすれば，(4) 式は，

$$p(x)\fallingdotseq\frac{N-1}{n+N}\left(\frac{n}{n+N}\right)^x\fallingdotseq\frac{N}{n+N}\left(\frac{n}{n+N}\right)^x$$

$$=\frac{1}{\frac{n}{N}+1}\cdot\left(\frac{\frac{n}{N}}{\frac{n}{N}+1}\right)^x\fallingdotseq\frac{1}{\bar{e}+1}\cdot\left(\frac{\bar{e}}{\bar{e}+1}\right)^x \quad \cdots\cdots(5)$$

但し，ここに ε は泡粒の有する平均エネルギーである。

§3. 泡粒頻度分布の実測値

次に，この頻度分布を実験的に求めるのであるが，勿論求める分布は $t=0$ の状態であり，且未だ所謂，泡沫層も出来ず，生成された泡粒が海水内に at random に分散されている状態を考えているのである。これを求めることは，実験上も，測定上もかなり困難であるので，一応次に示す第一近似の状態で満足することにした。即ち，これまで屢々利用した2秒毎の泡沫層の実測値を外挿して，$t=0$ の泡沫層の状態を求め，これをもつて，現在求めている海水中に分散されている泡粒初期の状態と見做した。勿論両層は同じく初期ではあるが，海水中に分散された泡粒と，一方海水上に所謂泡沫層を造つた泡粒とは potential の点では異る。即ち泡沫層内では泡粒は相互作用による potential を持つと考えなくてはならぬし，加えて，これが層下部の海水面に接する部分近くと，上部の気相に接する部分近くではこの相互作用も異り，簡単には求められない。これに関しては他日取扱いたい。尚，振

Table 1 Frequencies of Sizes of Bubbles Sea Water : 14.42‰Cl, 21°C

Range of dia.(mm) (Median dia.) / Time(sec)	0.0~0.2 (0.1)	0.2~0.4 (0.3)	0.4~0.6 (0.5)	0.6~0.8 (0.7)	0.8~1.0 (0.9)	1.0~1.2 (1.1)	1.2~1.4 (1.3)	
2	48.1	24.1	17.9	3.65	4.74	—	0.73	
4	25.1	27.1	30.0	14.1	2.00	1.20	0.85	
6	23.2	30.4	20.55	10.7	4.47	0.89	1.79	
8	21.2	26.9	11.5	9.6	7.69	11.5	3.84	Total
10	15.0	25.0	10.0	35.0	5.0	—	5.0	
Initial value (obtained by extrapolation)	49.0	28.0	20.0	2.2	1.5	—	—	100.7

盪停止直後の海水中に存在する泡粒の分布を何等かの方法で実験的に求めることが望ましい。

さて，14.42‰Cl の海水につき21℃で行つた実験値をみると，振盪停止後3sec時以内に存在する泡粒の大きさは median dia.で，主として0.1から0.9 mmまでのものがある(Table 1)。これを大きさ別に頻度の時間的変化をプロットすれば Fig. 1 の如くなる。次に大きさ別に，各時刻に存在する頻度を求めてみる。これまでの結果から，泡高は時間と exponential の関係にあることが求まつているので，先づ第一近似として，この頻度についても，時間に対して exponential の関係を仮定して，Table 1の値をプロットすると，Fig. 2 の如くなる(Pd を対数目盛に)。

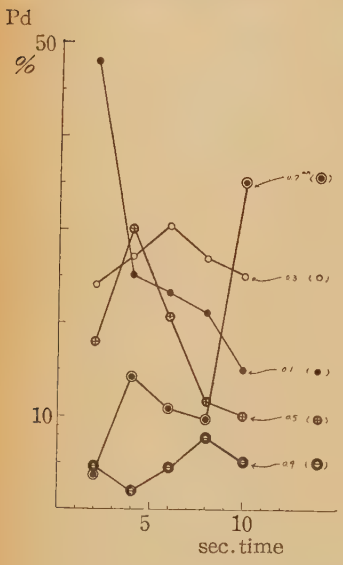

Fig. 1 Frequency distribution of the size of bubbles, Sea Water : 14.42‰Cl, 21℃
pd : frequency of bubble (dia. : d)

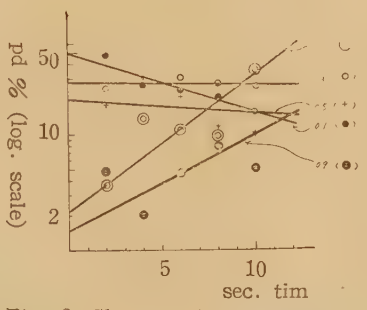

Fig. 2 Showing the determination of the Pod from experimental valures of pd.
where. Pd : frequency of bubble (dia. : d),
Pod : 〃 at initial,
β : decay const.
t : time,

全体を眺めると概ね log Pd は t に対し linear であると考えられる。唯0.9 mmの場合は，他の場合に比べてやゝ偏倚は大であるが，これも機械的に平均的な直線を引いておくことにする。以上の値より $t=0$ における泡粒の頻度 Pod を求めると Table 1 の最下欄の如く求まる。

§4. 泡粒の Mean surface energy.

非常に大きな粒子集団から，非常に多数 N 個の泡粒を任意に採り出した場合を考えてみる。この時，その泡粒の大きさとその存在する個数は Table 2 の n 欄の通りである。この泡粒は，その有するエネルギーを surface energy の形で蓄えていると仮定する。この場合泡粒はこれまでの実験結果から Fig. 3 の右上に示す如く近接する二枚の球面膜より成ると考えられ，この膜内に surface energy として蓄えられているわけである。又この泡粒集団の全泡粒の有するエネルギーの合計をもつてこの集団のエネルギーとする。従つて，この場合の全エネルギーを E とすれば，

$$E=2\sigma\pi\sum nd^2\cdot\mathrm{erg}=2\sigma\pi\times10.3N\times10^{-3}\mathrm{erg}\cdots\cdots(6)$$

ここに，σ は泡粒の単位面積に蓄えられた surface energy であり，d は泡粒の直径である。

さて周知の如く，表面張力を γ，その絶対温度を T とすれば，

Table 2

Range of dia. (mm.)	Median dia. (d)	Pod (%)	d^2	Number (n)	nd^2
0.0～0.2	0.1	49.0	1×10^{-2}	0.49N	0.49×10^{-2}N
0.2～0.4	0.3	28.0	9×10^{-2}	0.28N	2.52×10^{-2}N
0.4～0.6	0.5	20.0	25×10^{-2}	0.20N	5.00×10^{-2}N
0.6～0.8	0.7	2.2	49×10^{-2}	0.022N	1.08×10^{-2}N
0.8～1.0	0.9	1.5	81×10^{-2}	0.015N	1.22×10^{-2}N
	Total	100.7	—	100.7N	10.31×10^{-2}N
					$(=\sum nd^2)$

Where N : Total number of bubbles (large number)
Pod : Initial frequency value of bubbles (dia. : d)

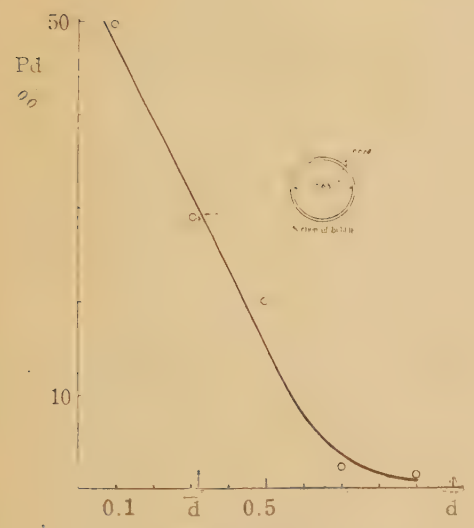

Fig. 3 Frequency distribution of size of bubble (experimental value)
Sea water : 14.42‰ Cl, 21°C

$$\sigma=\gamma-T\frac{d\gamma}{dT} \quad \cdots\cdots(7)$$

である。又海水の γ は Fleming, Revelle によれば，

$$\gamma=75.64-0.144\theta+0.0399\,\mathrm{Cl} \quad \cdots\cdots(8)$$

{θ は水温 °C} であるから，

$$\frac{d\gamma}{dT}=-0.144 \quad \cdots\cdots(9)$$

従つて，21°C　σ（即ち σ_{21}）は次の如く求まる。

$$\sigma_{21}=116\mathrm{erg}/\mathrm{cm}^3=1.16\mathrm{erg}/\mathrm{mm}^3 \quad (10)$$

故に，(6) 式より，

$$\bar{e}=\frac{E}{N}=0.206\sigma\pi\mathrm{erg}=0.75\mathrm{erg} \quad \cdots(6')$$

この仮想的泡粒の大きさ（d）を求めれば，

(6′) より　$\bar{d}^3=0.103\mathrm{mm}^3$ ……(11)

或は　$d=0.321\mathrm{mm}$ ……(11′)

§5. Pd につき理論値と実験値との比較

次に，前節の方法で求めた理論値と実験値とを比較してみる。両者の一致する程度をみるため，同一の図上にプロットする。そのため両者のエネルギーに比例する量（即ち，d^2 と x）を同一の単位で測るため，e の所，即ち $d^2=0.103\,\mathrm{mm}^2$ を考える。これは，実験値では $Pd=29.2\%$ であり，この Pd を示す x の値を（5）式から求めてみると，

$x=0.789$ (Table 3 参照), 而して, エネルギーの点では, $x=0.789$ と $\bar{d}^2=0.103$ とが互に対応するのであるから, x の値を d^2 軸上に重ね合せるためには, x の値を $\frac{0.103}{0.789}=0.1304$ 倍 (δ とおく) して, 求まる値を d^2 軸上にとればよいのである。斯様にして求めた Pd と d^2 の図が Fig. 4 である。

Table 3 Calculated values of frequency $p(x)$

x	$p(x)$	$\delta.x$	x	$p(x)$	$\delta\cdot x$
0.1	0.524	0.0130	0.8	0.289	0.104
0.2	0.481	0.0261	0.9	0.266	0.117
0.3	0.443	0.0391	1.0	0.244	0.130
0.4	0.406	0.0522	2.0	0.105	0.261
0.5	0.373	0.0652	3.0	0.045	0.392
0.6	0.343	0.0781	4.0	0.019	0.522
0.7	0.315	0.0913	5.0	0.0082	0.652
0.789	0.292		6.0	0.0035	0.782

where $p(x)=\frac{1}{\bar{e}+1}\left(\frac{\bar{e}}{\bar{e}+1}\right)^x=\frac{1}{0.75+1}\left(\frac{0.75}{0.75+1}\right)^x$
$\fallingdotseq 0.571\times 0.428^x$

所々多少不適当の個所はあるが, 全体の傾向としては, 理論値と実験値とはかなりよく一致することがわかる。即ち外部から振動等の形でエネルギーが海水系に与えられて, 海水が泡立つ現象を見ると, そのエネルギー授受の機構はかなりよく, 確率論的に解釈することができることを示している。ここで面白いことは, この泡沫層が崩壊して行く形式も確率論的に取扱い得たことである。そこで次のことが云え相である。現在扱つている泡沫現象は, その問題によつては, 確率論的, 換言すれば統計力学的に十分取扱い得るものと考えられる。

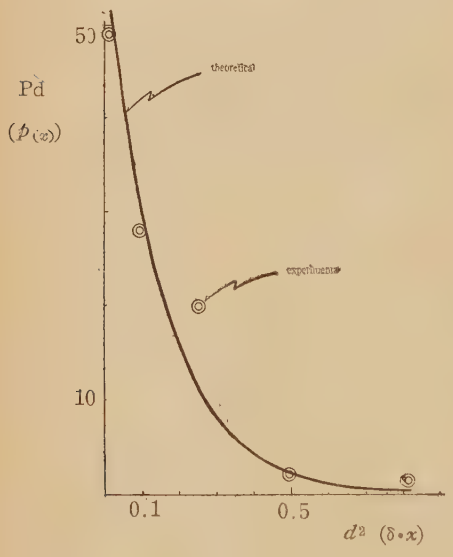

Fig. 4 Frequency distribution of theoretical and experimental values.

§6. 結 語

以上を要約すれば, 海水系が振盪等によつて泡立つ場合, 発生する泡粒の頻度分布につき統計力学的に取扱つてみた。その結果, 統計力学的に計算した理論値と, 実験値とはかなりよく一致する傾向にあることがわかつた。これまで実験的に求めた結果「泡沫層の高さの時間的変化が確率論的に取扱い得ること」とを考え併せると, 興味あることには, この種の泡沫現象は統計力学的に十分取扱い得るものと考えられる。

終りに臨み, 本研究に御興味を持たれ屢々有益なる御助言と御激励の言葉を賜つた海洋研究室長中野猿人先生, 当所地球化学研究室長三宅泰雄先生, 東京大学教授坪井忠二先生並に東京水産大学教授

宇田道隆先生に，厚く御礼申上げる。

尚計測用写真のわずらはしい仕事を御手伝い下さつた当所金沢五寿雄技官に深謝する。

参　考　文　献

阿部友三郎　中央気象台海洋報告　3巻1号5報　昭和28年
〃　〃　6報　〃
〃　日本海洋学会誌　9巻2号　昭和28年
〃　〃　10巻1号　〃　29年

R.H. Fowler, Statistical Mechanics, Cambridge Univ. Press. 1936.
H.U. Sverdrup and others, The Oceans, Prentice Hall Press. 1949.

Reprinted from the *Papers in Meteorology and Geophysics* Vol. V Nos. 3~4, 1955

A Study on the Foaming of Sea Water

—On the Mechanism of the Decay of Bubbles and Their Size Distribution in Foam Layer of Sea Water—

by

Tomosaburo Abe

Published by the Meteorological Research Institute,

Mabashi, Suginami, Tokyo, Japan

January 1955

551.463

A Study on the Foaming of Sea Water

—On the Mechanism of the Decay of Bubbles and Their Size Distribution in Foam Layer of Sea Water—

by

Tomosaburo Abe

Meteorological Research Institute

(Received December 15, 1954)

Abstract

In considering the process of the decay of foam layer of sea water, the author has introduced the same quantity "A" as the activation energy in chemical changes. Thus by using "A" he discussed the phenomenon. The quantity "A" increases with increasing concentration of sea water, up to a certain maximum, and then decreases with further increase of concentration. And also he discussed the frequency distribution of the size of bubbles in the foam layer by means of statistical methods. The theoretical values of the frequencies calculated by statistical methods agreed fairly well with those obtained by experiments; thus it appears that it is possible to deal with the phenomenon of foaming by means of statistical methods or mathematical probability.

1. Introduction

In observing surface conditions of the sea, Beaufort's scale is mainly used at present. Existence of white-chops produced by wind has an important effect on this scale. It is considered from our experimental results that the degrees of white-chops change with the chlorinity of sea water, and the temperature and stability of foam. The experimental relationships among these factors have already been reported by Y. MIYAKE and T. ABE, and recently the mechanism of the decay of foam layer of sea water in a glass ampule has been experimentally studied by the present author, and he reported also that the logarithm of the height of foam layer ($\log h$) decreases linearly with increasing time (t), i.e. $h=h_0e^{-kt}$, where h_0 represents the value of h at $t=0$, and k is the "decay constant".

In the present paper, a discussion will be made on the phenomenon of decay from the standpoint of energy. A discussion will also be made on the frequency distribution of the size of bubbles in the foam layer.

2. Activation energy

In has been experimentally obtained by the present author that the type of the decay of the bubbles in the foam layer is formally that of the so-called "1-st order chemical reaction," and it seems to be possible to treat this decay phenomenon by means of an analogy with chemical kinetics which has been fully discussed by many authors. Thus we may consider the so-called activation energy in the case of the decay of bubbles, too.

Now consider a certain gaseous reaction, and let its velocity constant be say, k', then the equation of Arrhenius is written as follows:

$$\frac{dI_n k'}{dT} = \frac{A'}{RT^2}, \tag{1}$$

where T is the absolute temperature, R the gas constant and A' the activation energy (i.e. the minimum disposable energy in a possibly effective reaction).

Integrating Equ. (1) with respect to T, assuming A' as independent of T as Arrhenius did, we have

$$\int dI_n k' = \frac{A'}{R} \int \frac{dT}{T^2},$$

or

$$I_n k' = I_n C - \frac{A'}{RT}, \tag{2}$$

or

$$k' = Ce^{-\frac{A'}{RT}},$$

where C is the characteristic constant of reaction.

Plotting $\log k'$ against $\frac{1}{T}$ for observations over a sufficient range of temperatures, it is found that Equ. (2) gives an adequate representation of the facts, that is, we can assume that there is a linear relation between $\log k'$ and $-\frac{1}{T}$.

Then, from Equ. (2), we have

$$A' = R \tan \alpha, \tag{3}$$

where α represents the gradient of the straight line.

We treated the experimental data on sea water in the same manner as mentioned above (Table 1, Fig. 1).

Fig. 1 shows the relation between the decay constant (k) and temperature (T) in the case of sea water, that is, $\log k$ for five cases of concentrations has been

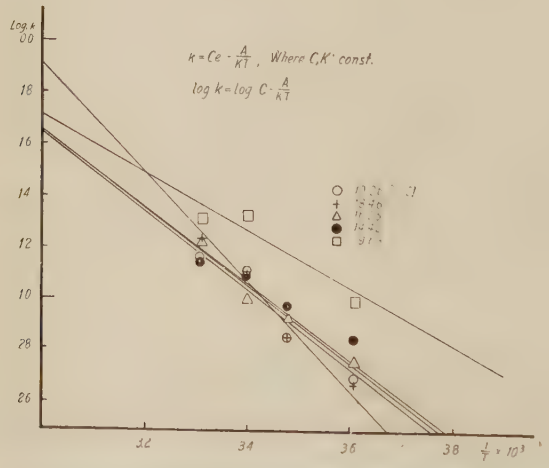

Fig. 1. Relation between the decay const. (k) and temp. (T) of sea water, where T is absolute temperature.

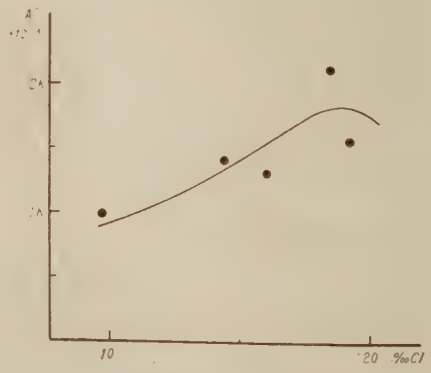

Fig. 2. Change of "A" with the Chlorinity of sea water.

plotted as functions of $\frac{1}{T}$, and they are mutually in linear relation approximately, and we obtained the values of "A" that correspond to A' in the gaseous reactions as mentioned above, where R corresponds to K.

The values of "A" increases with increasing *Cl* concentration up to a certain maximum value and decreases with further increase of the concentration (see Fig. 2). Since "A" is considered as the necessary minimum amount of energy which activates a bubble to decay, the larger the *Cl* concentration of sea water, the smaller the amount of bubbles which decay, but over a certain degree of concentration they again decay easily.

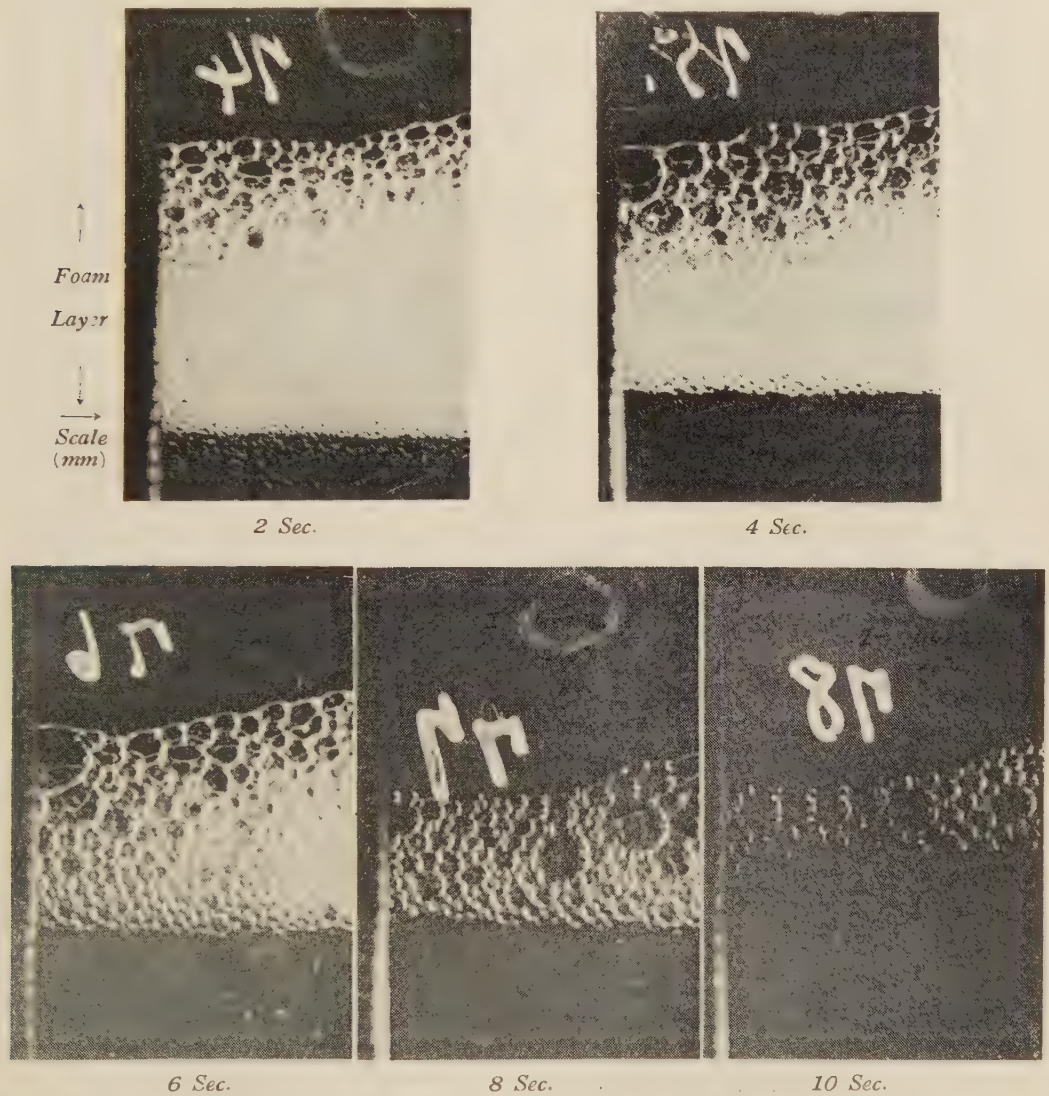

Fig 3. Changes in height of foam layer of sea water.
sea water: Cl. 14.42‰, Temp. 21°C

Table 1. Values of decay const. (k) and "A" of the various cases of sea water.

Concentration / Sea water temperature	Decay Const (k)					
	19.26‰Cl	18.46	16.04	14.42	12.82	9.63
29°C	0.143	0.171	0.166	0.137	0.145	0.200
21	0.124	0.128	0.099	0.131	0.109	0.214
14	0.071	0.071	0.084	0.094	—	—
5	0.071	0.047	0.058	0.049	—	0.097
"A"	146×10K	208×10K	150×10K	148×10K	—	100×10K

3. Theoretical treatments of the frequency distribution of the size of bubbles

The author examined the process of forming of bubbles in the foam layer in the case of his experiment.

The glass ample containing sea water was vibrated up and down by a vibrating apparatus with a constant frequency and amplitude, that is, energy was given to the system of sea water in the form of vibration. It is supposed that there are numerous micro heterogenous points in the system (heterogeneous points of local density, temperature, concentration of chlorinity and of concentration of dissolved gases etc.) and they are distributed uniformly and at random in the system. Then, when the energy is given to the system, it is divided up in various ways and the various divisions of energy accumulate properly into the heterogeneous points and innumerable cracks are born in the system. That is, various sizes of bubbles are born in sea water. Though these bubbles react against each other and then coagulations, decompositions and breakages sometimes occur, the rates of productions of bubbles become equal to those of disappearances, that is, the equilibrium of the state is reached. After this, the state of bubbles is statistically constant.

At the stationary state, the energy $E(=ne)$ is given to the system of sea water for a unit time (e is the energy of bubble which is produced in the initial stage), and there are N bubbles in it (N is a large number).

From a statistical point of view, he considered how to distribute the energy (ne) into each of the N bubbles in the system. The number of the ways of the distribution is distinctly $\frac{(n+N-1)!}{n!(N-1)!}$ (put $M_N(n)$ to it)

$$M_N(n)=\frac{(n+N-1)!}{n!(N-1)!}\,. \tag{4}$$

Using this equation, the probability $p(x)$, which energy xe is distributed to a certain bubble, is calculated ($x\geqq1$).
Thus

$$p(x)=\frac{M_{N-1}(n-x)}{\sum_{x=0}^{n} M_{N-1}(n-x)}=\frac{M_{N-1}(n-x)}{M_N(n)} \tag{5}$$

$$=\frac{(N-1)!\,n!(n+N-x-2)!}{(N-2)!\,(n-x)!\,(n+N-1)!}$$

$$=(N-1)\frac{n(n-1)\ldots(n-x+1)(n+N-x-2)!}{(n+N-1)(n+N-2)\ldots(n+N-x-1)(n+N-x-2)!}\,.$$

Now, in the special case ($N \gg 1$, $x_2 \gg E$),
the equetion (5) takes the following simplified form:

$$(6) \qquad p(x) \fallingdotseq \frac{N-1}{n+N}\left(\frac{n}{n+N}\right)^x \fallingdotseq \frac{1}{\frac{n}{N}-1}\left(\frac{\frac{n}{N}}{\frac{n}{N}+1}\right)^x = \frac{1}{\bar{e}+1}\left(\frac{\bar{e}}{\bar{e}+1}\right)^x,$$

where $\bar{e}$ is the mean energy of bubbles.

4. The observed values of the frequency distribution of bubbles

Though the author wishes to obtain the actual values of the frequencies of bubbles in the system of sea water at an initial stage, this is a very difficult work in experiment. And so he is satisfied, as the first approximation, with the values of those at the initial layer: those were obtained by extrapolation of the values of each size of bubbles, assuming that each bubble has decayed in exponential type with time [i.e. $p(x)=p_{0x}e^{-\beta t}$, where β is the decay const., p_{0x} the value of $p(x)$ at initial]. Of course the bubbles of which the foam layer is composed, have potential energy owing to the mutual interactions above and beyond the surface energy itself.

Now, the observed values of frequencies of the sizes of bubbles of sea water having 14.42‰ Cl at 20±1°C, are shown in Table 2 and Fig. 4.

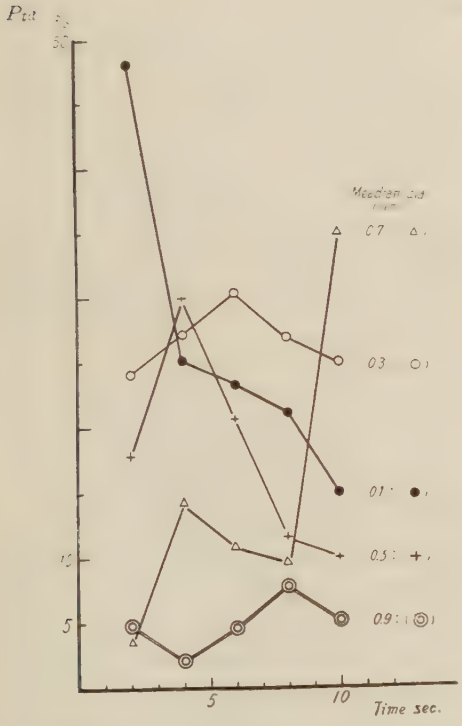

Fig. 4. Changes of the frequency with time, sea water: 14.42‰ Cl, 21°C

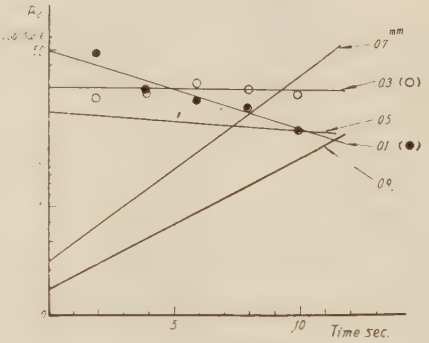

Fig. 5. Determination of the $P_{0\alpha}$, assuming the relation $P_{t\alpha}=P_{0\alpha}e^{-\beta t}$.
$P_{t\alpha}$: Frequency at $t=t$
$P_{0\alpha}$: Frequency at $t=0$
β : Decay const.
t : Time.

Table 2. Frequencies of Sizes of Bubbles, Sea Water: 14.42‰ Cl, 21°C.

Range of dia. (mm) (Median dia.) / Time (Sec.)	0.0～0.2 (0.1)	0.2～0.4 (0.3)	0.4～0.6 (0.5)	0.6～0.8 (0.7)	0.8～1.0 (0.9)	1.0～.12 (1.1)	1.2～1.4 (1.3)	
2	48.1%	24.1	17.9	3.65	4.74	—	0.73	
4	25.1	27.1	30.0	14.1	2.00	1.20	0.85	
6	23.2	30.4	20.55	10.7	4.47	0.89	1.79	
8	21.2	26.9	11.5	9.60	7.69	11.5	3.84	
10	15.0	25.0	10.0	35.0	5.00	—	5.00	
Initial value.								(Total)
Obtained by extrapolation	49.0	28.0	20.0	2.2	1.5	—	—	100.6

The value of the lowest column in the Table are those of P_{0d} obtained by extrapolation of the above values (showing in Fig. 5 the determination of the P_{0d} from the values of P_{td}, where P_{td} is value at time t).

5. Mean surface energy of bubble

The bubbles are supposed to be spheres surrounded by thin membranes and the energy of bubbles is preserved by those membranes in the form of surface energy (see Fig. 6).

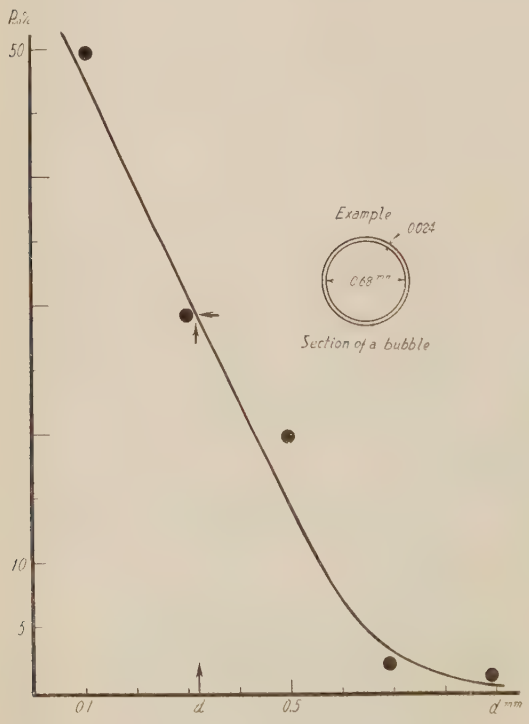

Fig. 6. Frequency distribution of sizes of bubbles, sea watre 14.42‰ Cl, 21°C, "Experimental value"

If the total number of bubbles be N (very large) and the total surface energy of the system is equal to E (see Table 3),

$$(7)\quad E=2\sigma\pi\sum nd^2 \text{ erg.}=2\sigma\pi \times 0.103N \text{ erg.}$$

where σ is the surface energy per unit area of a bubble.

As it is seen in the textbook of thermodynamics

$$(8)\quad \sigma=\gamma-T\frac{d\gamma}{dT},$$

where γ is the surface tension.

According to FLEMING and REVELLE,

$$(9)\quad \gamma_\theta=75.64-0.144\theta+0.0399\,\mathrm{Cl},$$

where γ_θ is the surface tension at 0°C, Cl the chlorinity of sea water.

Thus $\frac{d\gamma}{dT}=-0.144$,

$\therefore\ \sigma_{21}=1.16\text{erg/mm}^2$.

Then, if the mean surface energy of the bubble is $\bar{e}$, and its diameter $\bar{d}$,

$$(10)\quad \bar{e}=\frac{E}{N}=0.206\sigma\pi\text{erg}=0.75\text{erg},$$

Table 3. Caluculation of $\sum nd^2$.

Range of dia (mm)	Median dia (d)	P_{0d} (%)	d^2	Number (n)	nd^2
0.0~0.2	0.1	49.0	1×10^{-2}	$0.49N$	$0.49\times10^{-2}N$
0.2~0.4	0.3	28.0	9 〃	0.28 〃	2.52 〃
0.4~0.6	0.5	20.0	25 〃	0.20 〃	5.00 〃
0.6~0.8	0.7	2.2	49 〃	0.022 〃	1.08 〃
0.8~1.0	0.9	1.5	81 〃	0.015 〃	1.22 〃
	Total →	100.7		100.7 〃	10.31 ($\sum nd^2$) 〃

Where N : Number of bubbles (Large number)
P_{0d}: Initial frequency value of bubble (dia. d)

(11) $$\bar{d}=0.321\ \text{mm},$$

or

(12) $$\bar{d}^2=0.103\ \text{mm}^2.$$

Accordingly, from Equ. (6),

(6′) $$p(x)=\frac{1}{0.75+1}\left(\frac{0.75}{0.75+1}\right)^x=0.571\times0.428^x.$$

6. Comparison of the observed and the theoretical values of P_d

The quantities x and d^2 mentioned above are proportional to the energy which the bubble holds. The value of $\bar{d}^2$ at which mean surface energy $\bar{e}$, is 0.103 mm², and the frequency (P_d) of it is 29.2%. On the other hand, by the equation (6) the value of x at this frequency is obtained as follows (see Table 4):

$$x=0.789.$$

The ratio δ of the value of $\bar{d}^2$ to that of x which holds the same frequency P_d, is $\frac{0.103}{0.789}$ or 0.130.

Thus, the relation between the P_d and $\bar{d}^2$ or δ_x is shown in Fig. 7. It is seen that the theoretical values of the frequencies calculated by the statistical method agreed fairly well with those derived from experimental data.

It is interesting that we are able to discuss the process of decay of the foam layer of sea water by means of mathematical probability.

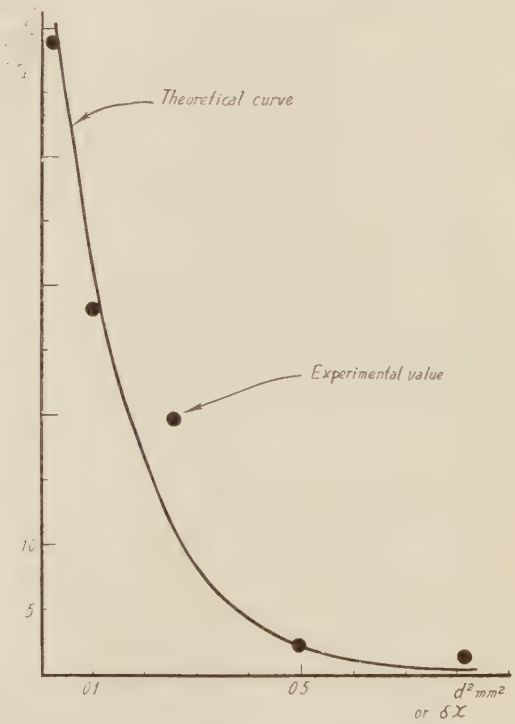

Fig. 7. Frequency distribution of theoretical and experimental values.

Table 4. Calculation of $p(x)$.

x	$p(x)$	δx	x	$p(x)$	δx
0.1	0.524	0.0130	0.8	0.289	0.1042
0.2	0.481	0.0261	0.9	0.266	0.1170
0.3	0.443	0.0391	1.0	0.244	0.1304
0.4	0.406	0.0522	2.0	0.105	0.261
0.5	0.373	0.0652	3.0	0.045	0.392
0.6	0.343	0.0781	4.0	0.019	0.522
0.7	0.315	0.0913	5.0	0.008	0.652
0.289	0.292	0.103	6.0	0.004	0.782

where $P(x)=0.571\times 0.428_x$, $\delta=\dfrac{0.103}{0.789}=0.130$

Acknowledgements—The author wishes here to express his sincere thanks to Dr. M. Nakano, Dr. Y. Miyake of this Institute, Prof. Dr. C. Tsubo: of Tokyo University and Prof. Dr. M. Uda of Tokyo University of Fisheries for their interest and encouragement throughout the study. He also wishes to thank to Mr. I. Kanazawa for his assistance in preparing the photographs used in this experiment.

References

[1] Miyake, Y. and Abe, T., 1948: A Study on the Foaming of Sea Water (I). Journ. Mar. Res. 7, p. 67.

[2] Abe, T., 1953: A Study on the Foaming of Sea Water and Inorganic Electrotyte Solutions (V). Oceanogr. Report. CMO. 3, p. 47. (in Japanese)

[3] Abe, T., 1953: A Study on the Foaming of Sea Water.—On the Mechanism of the Decay of Foam Layer of Sea Water. Records. Oceanogr. Works. Japan. N.S. 1, p. 18.

[4] Abe, T., 1954: A Study on the Foaming of Sea Water (VIII).—On the Mechanism of the Decay of Foam Layer of Sea Water. Journ. Oceanogr. Soc. Japan. 10, p. 15. (in Japanese)

[5] Abe, T., 1954: A Study on the Foaming of Sea Water (IX).—On the Distribution of the Size of Bubbles in Foam Layer of Sea Water. Oceanogr. Report. CMO. 3, p. 39. (in Japanese)

[6] Fowler, R.H., 1936: Statistical Mechanics, Cambridge Univ. Press.

[7] Hinshelwood, C.N., 1940: The Kinetics of Chemical Change, Oxford Univ. Press.

[8] Sverdrup, H.U. and others, 1949: The Oceans. Prentice-Hall. Press.

Reprinted from the *Papers in Meteorology and Geophysics* Vol. V Nos. 3~4, 1955

On the Structure of Ocean Currents (I)

—Test Manufacture of a New Current Meter
and Some Experiments on the Sea—

by

T. Nan'niti

Published by the Meteorological Research Institute,

Mabashi, Suginami, Tokyo, Japan

January 1955

551.460.18.3

On the Structure of Ocean Currents (I)

—Test Manufacture of a New Current Meter and Some Experiments on the Sea—

by

T. Nan'niti

Meteorological Research Institute

(Received December 20, 1954)

Abstract

Though the author had once made a new current meter using a phototube [1] and observed many interesting facts with it already [2] [3], it is very expensive to use it.

Now the author has made another and simpler current meter which will record current speed fluctuations more minutely but directions more roughly than the former. With it he observed ocean currents very well and discussed about them.

1. Introduction

In the previous papers [1] [2] [3], the author discussed somewhat the structure of ocean currents. To study the turbulence and structure of oceanic currents further, the author made a new type of current meter. Experiments on the sea have shown that minute current conditions can be observed very well and the current profiles can be seen easily by the instrument.

2. The new current meter

a) The principle of the method.

The current meter is composed of an underwater portion and a recorder on deck. These are connected by a three-fold rubber-covered cable of 50 meters long.

Current speeds are recorded on a paper tape in the recorder by the closing of the electric circuit in accordance with the frequency of rotation of the propeller.

A tape is rolled by an electric motor. Current directions are observed by a distribution of numbered and colored brass balls. The balls are dropped into a magnet box only when we want.

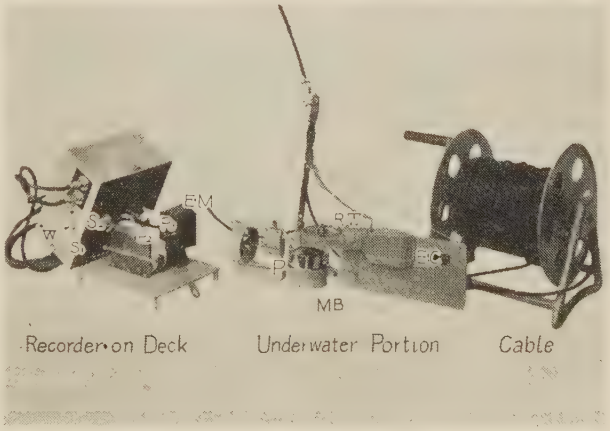

Fig. 1. The new current meter showing various components.

b) The details of the instrument.

The current meter is shown in Fig. 1. When water particles run 20 cm, the

propeller P revolves one cycle and the electric circuit is closed once as the schematic circuit diagram of Fig. 2 shows. Then the recording pen P_1 in the recorder on deck will depict one signal. So we can calculated the current speeds.

To measure current directions, we turn on the switch S_1 in the recorder. Then the other electric circuit is closed and a plastic rachet wheel RW in the underwater portion will be turned one pitch by the electro-magnetic force generated by the electric coil EC. The wheel RW has 48 holes in its margin, and in every hole there are differently numbered and colored balls. So one ball will drop into the magnet box MB as we turn on the switch S_1. The number of times the balls are dropped is indicated at a small window W and recorded by the pen P_3 on the tape also.

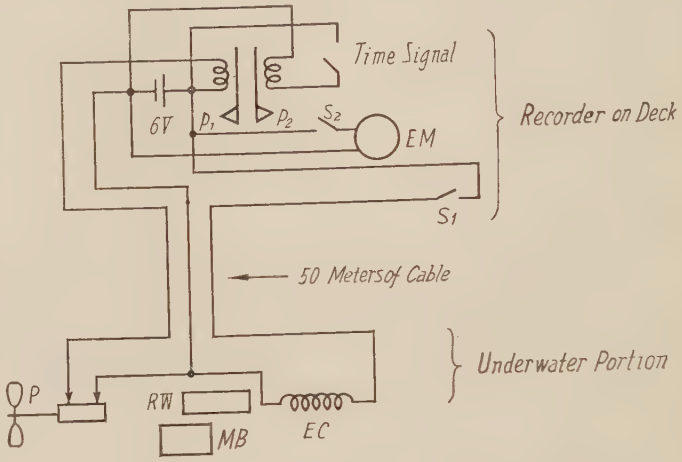

Fig. 2. Schematic circuit diagram of the instrument.

The tape is rolled with a speed of about 0.5 cm/sec by the electric motor EM when we turn on the switch S_2. The timing is marked on the chart at intervals of 30 sec. All the electric power required for the instrument is supplied by a battery of 6 volts. After one serial observation has been done we draw up the current meter, and we can find current directions by the distribution of balls.

3. Experimental results

The experiment was performed in Tokyo Bay on board the research ship "Ryôfû Maru" on August 16, 1954. The records are shown in Fig. 3. From the figure we can see periodic fluctuations of speed, its range being from 15 cm/sec to 50 cm/sec, with a period of about 2.5 sec in the layers from the surface to 3 m. The fluctuations must have been caused by the sea with a period of 2.5 sec, for the wind speed was 5.5 m/sec with the direction of the north at 22 h. Putting the wave length to be 10 m, the diminution of amplitude at 3 m layer is $e^{-2}=0.14$, at 5 m layer is $e^{-\pi}=0.04$ [4].

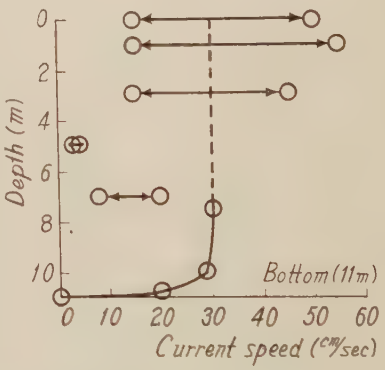

Fig. 4. Current profile from the record in Fig. 3.

There is a layer of minimum speed (3~4 cm/sec) at 5 m layer. The ship draws 4.5 m of water. And from 7.5 m to 10.9 m layer, 10 cm above the bottom, there is a steady constant speed (20~30 cm/sec).

So the current profile is shown in Fig. 4. The ship was at anchor and did not roll. So we suspect that there was a tidal current with the speed of 30 cm/sec and the disturbance caused by the sea was superposed on the tidal current. The

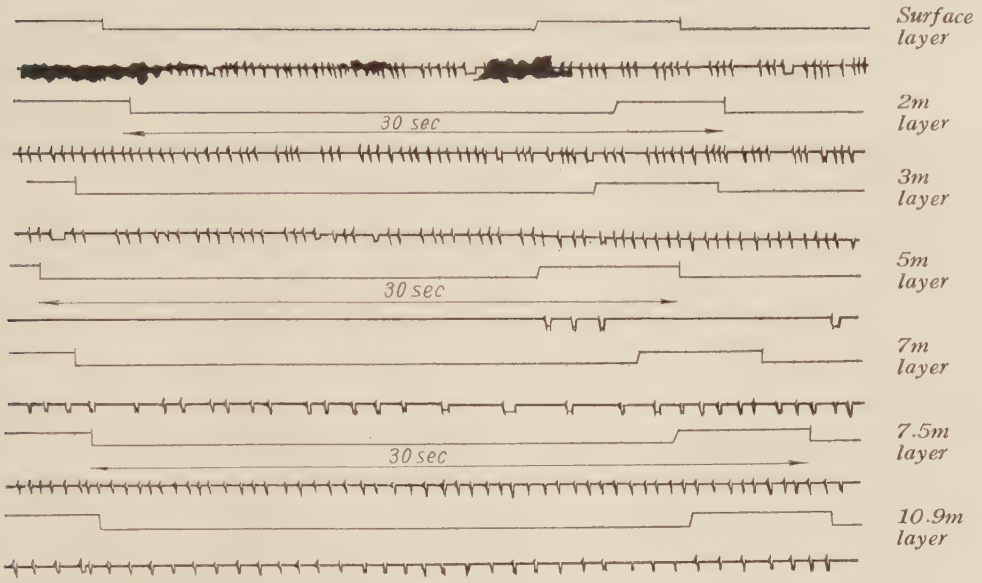

Fig. 3. A record of current obtained at Tokyo Bay. Note the periodic disturbance in shallower water.

current directions were not observed owing to our carelessness.

The next experiment was performed in an open sea (38°13′N, 142°58′E) at 20h 30 m on November 19, 1945. The record is shown in Fig. 5. It shows that from the surface to the 20 m layer, which is the lowest layer we observed, there are periodic fluctuations of speed (50~180 cm/sec) with periods of 7 to 8 sec.

Fig. 5. A record obtained at the open sea showing the periodic fluctuation caused by the drifing of the ship. When the current speed is very large, the time interval in which the electric circuit is being closed becomes so short that the electric current is switched off before the recording pen is sufficiently pulled by the electric coil, according the amplitude of the record becomes small.

The marine-meteorological data are as follows:

Wind ESE 16.3 m/sec. Sea ESE 5 (on Beaufort's)
Swell SSE 3 (on Beaufort's) period 8 sec, height 2¼ m.

The ship "Ryôfû Maru" (1200 tons) was drifting. The observed current speeds in each layer, from the top to the 20 m layer, fluctuate from 50 cm/sec to 180 cm/sec at periods of 7 to 8 sec, with the directions of 320° to 340°. The directions and periods of the current and wind are coincident with each other. So the obtained record must be the resultant of the drifting speed of the ship and the ocean current. Most of the resultant speed may be caused by the drifting of the current meter. So the drifting coefficient of the ship by the wind is about 1/16~3/16 [knot/m/sec].

The third experiment was done at 39°38'N, 143°32'E. The marine-meteorological data at 11 h on November 24 are as follows:

Wind S 11.5 m/sec, Sea S 3 (on Beaufort's)
Swell S 1 (on Beaufort's) period 9 sec, height 1.0 m.

The observed data by the current meter are as follows:

Depth (m)	Speed (cm/sec)	Direction	Period of fluctuations (sec)
5	80~100	191°	10
10	70~ 90	192°	10
20	75~100	226°	9.8
30	55~ 90	250°	9.5

But the periodic fluctuations can be slightly seen.

Assuming the drifting speed of the ship by the wind to be 12/16=0.75 knots to the north, then the ocean current ought to be as follows:

Depth (m)	Speed (cm/sec)	Ditection
5	127	188°
10	118	189°
20	120	213°
30	95	228°

The current speed slightly decreases downwards and the current direction changes from SSW to SW.

4. Conclusion

The author made a new current meter and he could observe ocean currents successfully.

It recorded periodic fluctuations of speed caused by the wave and the drifting of the research ship. It is a very useful instruments enabling us to observe currents easily and to find the actual underwater speed fluctuations and profile immediately.

Further observation will be done about periodic disturbances or irregular fluctuations of ocean currents by this instrument, and the result will be analyzed providing automatic means.

Acknowledgements—The author expresses his hearty thanks to Mr. M. Yasui and the members of the Oceanographical Section, Central Meteorological Observatory, for their help during the observation. His thanks are also due to Mr. M. Iwamiya, of Turumi Seiki Co., for the construction of the instrument.

The experiment was made by a grant in 1954 from the Special Committee on Marine Resources in the UNESCO Committee of Science Council of Japan.

References

[1] Nan'niti, T. 1953: A Current Meter Using a Phototube (I). Pap. Met. Geophys. 3, p. 286.
[2] Nan'niti, T. 1953: A Current Meter Using a Phototube (II). Pap. Met. Geophys. 4, p. 66.
[2] Nan'niti, T. 1954: A Current Meter Using a Phototube (III). Pap. Met. Geophys. 5, p. 54.
[4] Lamb, H. 1932: Hydrodynamics. Cambridge at the University Press, 6th Edition p. 365.

Errata to "A Current Meter Using a Phototube"

Volume	Page	Line	For	Read
3	294		Fig. 10	Fig. 11
	〃		Fig. 11	Fig. 12
5	57	13	has	had
	60	equation (11)	$\frac{(-1)^{m+1}}{2m-1}$	$\frac{(-1)^{m-1}}{2m-1}$
	〃	18	value	values
	〃	Fig. 8(a)	K=155	K=77.5
	〃	Fig. 8(b)	K= 77.5	K=155
	62	Fig. 12	(a) direction	(a) directions
	63	Fig. 13	10 cm	10 m
	〃	17	$u^{2\prime}\sim\overline{4.73}$	$\overline{u'^2}\sim4.73$
	〃	17~18	···K~269 c.g.s. So we Furthermore···9.3×10^3.	···K~269 c.g.s. Furthermore ·····9.3×10^3. So we

The Gothic numerals in the Column "Line" give ones from the bottom.

A Study on the Foaming of Sea Water.

——On the Mechanism of the Decay of Bubbles and their Size Distribution in Foam Layer of sea Water——

by

Tomosaburo Abe

(Oceanographic Laboratory, Meteorological Research Institute)

Reprinted from

RECORDS OF OCEANOGRAPHIC WORKS IN JAPAN,

Volume 2, No. 1, March 1955

Records of Oceanographic Works
in Japan, Vol. 2, No. 1,
March 1955

A Study on the Foaming of Sea Water.

——On the Mechanism of the Decay of Bubbles and their Size Distribution in Foam Layer of sea Water——

by
Tomosaburo Abe
(Oceanographic Laboratory, Meteorological Research Institute)

§ 1. Introduction

Existence of white-chops produced by wind has an important effect on Beaufort's scale. It is considered from our experimental results that the degrees of white-chops change with chlorinity of sea water, temperature and stability of foam. The experimental relationships among these factors have already been reported by Y. Miyake and T. Abe, and recently the mechanism of the decay of foam layer of sea water has been experimentally studied by the present author.

In the present paper, a discussion will be made on the phenomenon of decay from the standpoint of energy. A discussion will also be made on the frequency distribution of the size of bubbles in the foam layer.

§ 2. *Activation energy*

It has been experimentally obtained by the present author that the type of the decay of the bubbles in foam layer is formally that of the so-called "1-st order chemical reaction", and it seems to be possible to treat this decay phenomenon by means of an analogy with chemical kinetics which has been fully discussed by many authors. Thus we may consider the so-called activation energy in the case of the decay of bubbles, too.

Now consider a certain gaseous reaction, and let its velocity constant be K', say, then the equation of Arrhenius is written as follows;

$$\frac{dl_nK'}{dT}=\frac{A'}{RT^2} \quad \cdots\cdots(1)$$

where T is the absolute temperature, R the gas constant and A' the activation energy (i.e., the minimum disposable energy is a possibly effective reaction).

Integrating Eqn. (1) with respect to T, assuming A' as independent of T as Arrhenius did, we have

$$L_nK'=L_nC-\frac{A'}{RT} \quad \cdots\cdots(2)$$

where C is the characteristic constant of reaction. Plotting log K' against $\frac{1}{T}$

for observations over a sufficient range of temperatures, it is found that Eqn. (2) gives an adequate representation of the facts, that is, we can assume that there is a linear relation between log K' and $\frac{1}{T}$.

Then, from Eqn. (2) we have

$$A' = R \tan \alpha \quad \cdots\cdots (3)$$

Table 1

Concentration / Sea water temp.	Decay const. (k)					
	19.26‰ Cl.	18.46	16.04	14.42	12.82	9.63
29°C	0.143	0.170	0.166	0.137	0.145	0.200
21	0.124	0.128	0.099	0.131	0.109	0.214
14	0.071	0.071	0.084	0.094	–	–
5	0.071	0.047	0.058	0.049	–	0.097
"A"	146×10K	208×10K	150×10K	148×10K	–	100×10K

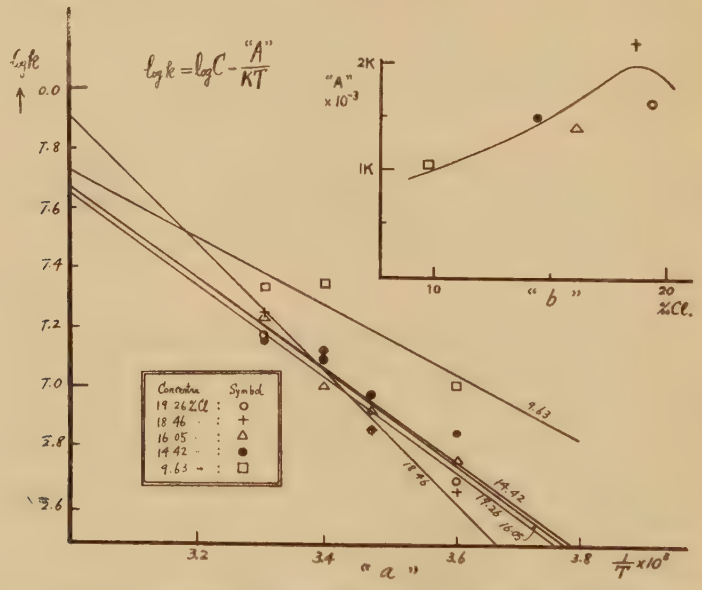

Fig. 1-a: Relation between the decay const. (k) and temp. (T) of sea water,
-b: Change of "A" with the Chlorinity of sea water

where α represents the gradient of the straight line.

We treated the experimental data on sea water in the same manner as mentioned above (Table 1, Fig. 1-a).

Fig. 1-a shows the relation between the decay constant (k) and temperature (T) in the case of sea water, that is, log k for five cases of concentrations have been plotted as functions of $\frac{1}{T}$, and they are mutually in linear relation approximately, and we obtained the values of "A" that correspond to A' in the

gaseous reactions as mentioned above, where R corresponds to K.

The values of "A" increases with increasing Cl concentration up to a certain maximum value and decreases with further increase of the concentration (see Fig. 1-b).

Since "A" is considered as necessary minimum amount of energy which activate a bubble to decay, the larger the Cl concentration of sea water, the smaller the amounts of bubbles which decay, but over a certain concentration they again decay easily.

§ 3. *Theoretical treatments of the frequency distribution of the size of bubbles.*

The author examines the process of forming of bubbles in foam layer in the case of his experiment.

The glass ampule containing sea water, was vibrated up and down by vibrating apparatus about constant frequency and amplitude, that is, energy was given to the system of sea water in a form of vibration. It is supposed that there are numerous micro heterogenious points in the system (i. e., heterogenious points of local density, temperature, concentration of chlorinity and of concentration of dessolved gases etc.) and they are distributed uniformly and at random in the system. Then, when the energy is given to the system, it is divided up in various ways and the various divisions of it accumulate properly into the heterogenious points and innumerable cracks are born in the system. That is, various sizes of bubbles are born in sea water. Though these bubbles react each other and then coagulations, decompositions and breakages sometimes occur, the rates of productions of bubbles become to be equal to that of disappearances, that is, the equilibrium of the state is reached. After this, the state of bubbles is statistically constant.

At the stationary state, the energy E (= ne) is given to the system of sea water for unit time (e is the energy of bubble which is produced in initial stage), and there are N bubbles in it (N is a large number).

From statistical point of view, he considered how to distribute the energy (ne) into the each of N bubbles in the system. The numbers of the ways of the distribution is distinctly $\frac{(n+N-1)!}{n!\,(N-1)!}$ (put $M_N(n)$ to it)

$$M_N(n) = \frac{(n+N-1)!}{n!\,(N-1)!} \quad \cdots\cdots(4)$$

Using this Fqn., the probability $P(x)$ which energy $x\,e$ is distributed to a certain bubble, is calculated ($x \geqq 0$).

Thus

$$P(x) = \frac{M_{N-1}(n-x)}{\sum_{x=0}^{n} M_{N-1}(n-x)} = \frac{M_{N-1}(n-x)}{M_N(n)} \quad \cdots\cdots(5)$$

Now, at the special case ($N \gg 1$, $xe \ll E$), the Eqn. (5) take the following simplified form:

$$P(x) \fallingdotseq \frac{N-1}{n+N}\left(\frac{n}{n+N}\right)^x \fallingdotseq \frac{1}{\bar{e}+1}\left(\frac{\bar{e}}{\bar{e}+1}\right)^x \quad \cdots\cdots(6)$$

where $\bar{e}$ is the mean energy of bubbles.

Though he wishes to obtain the actual values of frequencies of bubbles in the system of sea water at initial stage, this is a very difficult work in experiment. And so he satisfies, as the first approximation, with the values of those at the initial layer: those were obtained by extrapolation of the values of each size of bubbles, assuming that each bubble has decayed in exponential type.

Table 2, Frequencies of sizes of Bubbles. Sea water: 14.42‰Cl, 21°C

Range of dia. mm. (medion dia.) / Time sec.	0.~0.2 (0.1)	0.2~0.4 (0.3)	0.4~0.6 (0.5)	0.6~0.8 (0.7)	0.8~1.0 (0.9)	1.0~1.2 (1.1)	1.2~1.4 (1.3)	Total
2	48.1	24.1	17.9	3.65	4.74	–	0.73	
4	25.1	27.1	30.0	14.1	2.20	1.20	0.85	
6	23.2	30.4	20.5_5	10.7	4.47	0.89	1.79	
8	21.2	26.9	11.5	9.60	7.69	11.5	3.84	
10	15.0	25.0	10.0	35.0	5.00	–	5.0	
Initial value (obtained by extrapolation)	49.0	28.0	20.0	2.2	1.5	–	–	100.7

Now, the observed values of frequencies of sizes of bubbles of sea water having 14.42‰ Cl at 20 ± 1°C, are shown in Table 2. The values of the lowest column in the Table are those of P_{od} (i. e., initial frequency of bubble having dia. d) obtained by extrapolation of above values.

The bubbles are supposed to be spheres surrounded by thin membranes and energy of bubbles are preserved by those membranes in the form of surface energy (see Fig. 2).

Table 3

Range of dia. mm	median dia (d)	P_{od}	d^2	number (n)	nd^2
0~0.2	0.1	49.0	1×10^{-2}	0.49 N	0.49×10^{-2}N
0.2~0.4	0.3	28.0	9 〃	0.28 〃	2.52 〃
0.4~0.6	0.5	20.0	25 〃	0.20 〃	5.00 〃
0.6~0.8	0.7	2.2	49 〃	0.022 〃	1.08 〃
0.8~1.0	0.9	1.5	81 〃	0.015 〃	1.22 〃
	Total →	100.7		1.007 N	10.3 〃 ($=\Sigma nd^2$)

where N: Large number,
P_{od}: Initial frequency value of Bubble (dia. d).

If the total number of bubbles be N and the total surface energy of the system is equal to E (see Table 3),

$$E = 2\sigma\pi \Sigma nd^2 = 2\sigma\pi \times 0.103\, N\, erg \quad \cdots\cdots(7)$$

where σ is the surface energy per unit area of a bubble.

The calculated value of σ at 21°C is 1.16 erg/mm².

Then, if the mean surface energy of bubble is $\bar{e}$, and its diameter $\bar{d}$,

$$\bar{e} = \frac{E}{N} = 0.206\,\sigma\pi = 0.75\, erg \quad \cdots\cdots(8)$$

$$\bar{d} = 0.321\, mm \quad \cdots\cdots(9)$$

$$\text{or} \quad \bar{d}^2 = 0.103\, mm^2 \quad \cdots\cdots(9')$$

Accordingly, from Eqn. (6),

$$P(x) = \frac{1}{0.75+1}\left(\frac{0.75}{0.75+1}\right)^x = 0.571 \times 0.428^x \quad \cdots\cdots(6')$$

§ 4. *Comparison of the observed and theoretical values of* P_{od}

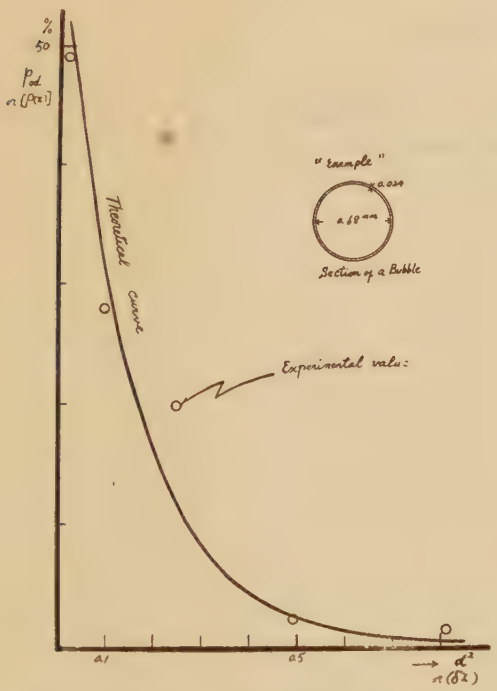

Fig. 2 Frequency Distribution of Theoretical and Experimental values

The quantities x and d^2 mentioned above, are that of proportional to the energy which bubble holds. The value of d^2 at which mean surface energy is $\bar{e}$, is 0.103 mm^2, and the frequency (P_{od}) of it is 29.2%. On the other hand, by the Eqn. (6′) the value of x at this frequency is obtained as follows, $x = 0.789$.

The ratio $\delta\#$ of value of d^2 and that of x which holds the same frequency P_{od}, is $\frac{0.103}{0.789}$ or 0.130.

Thus, the relation between the P_{od} and d^2 or x is shown in Fig. 2. It is seen that the theoretical values of the frequencies calculated by statistical method agreed fairly well with those derived from experimental data.

§ 5. *Summary and conclusion*

1. In considering the process of the decay of foam layer of sea water, the author has introduced the same quantity "A" as the activation energy in chemical changes. Thus by using "A" he discussed the phenomenon. The quantity "A" increases with increasing concentration of sea water up to a

certain maximum, and then decreases with further increase of concentration (§ 2).

2. Also he discussed the frequency distribution of the size of bubbles in the foam layer by means of statistical methods; The theoretical values of the frequencies calculated by statistical methods agreed fairly well with those obtained by experiments; Thus it appears that it is possible to deal with the phenomenon of foaming by means of statistical methods or mathematical probability (§ 4).

Acknowledgement—The author wishes to express his sincere thanks to Dr. M. Nakano, Dr. Y. Miyake of this Institute, Prof. Dr. C. Tsuboi of Tokyo University and Prof. Dr. M. Uda of Tokyo University of Fisheries for their interest and encouragement throughout the study and he also wishes to thank to Mr. I. Kanazawa for his assistance in preparing the photographs used in this experiment.

References

Miyake, Y. and Abe, T., 1948 : Journ. Mar. Res. 7, No. 2.
Abe, T., 1953 : Oceanogr. Rep. CMO 3, No. 1~2 (in Japanese)
Abe, T., 1953 : Records. Oceanogr. Works. Japan. N. S. 1, No. 2.
Abe, T., 1954 : Journ. Oceanogr. Soc. Japan. 10, No. 1, (in Japanese)
Abe, T., 1954 : Pap. Met. Geophys. 5. No. 3~4.

A Note on Forecasting Ocean Waves Caused by Typhoons

By

Sanae Unoki and Masito Nakano
(Meteorological Research Institute)

Reprinted from

RECORDS OF OCEANOGRAPHIC WORKS IN JAPAN,

Volume 2, No. 1, March 1955

Records of Oceanograghic Works
in Japan. Vol. 2. No. 1.
March 1955

A Note on Forecasting Ocean Waves Caused by Typhoons

By

Sanae Unoki and Masito Nakano
(Meteorological Research Institute)

§ 1. Introduction

The ocean waves which give the greatest damage to Japan are those caused by typhoons, and any quantitative discussion has scarcely been made hitherto on this problem. This seems to be due to the fact that there has been no precise wave observation hitherto and that it is difficult to apply the new theories of wave forecasting to these waves, owing to the fact that the typhoons move very rapidly and the variation of the direction and speed of wind in typhoon area is violent. Indeed the theory of ocean wave forecast has made a remarkable progress recently, but these theories rest on many assumptions, and in practising wave forecast, much empirical knowledge is required. In the present paper, a consideration is made concerning what kind of ocean waves is generated by typhoons and how about the method of forecasting of these waves, taking the case of waves at Hachijo Island (Fig. 3) as an example.

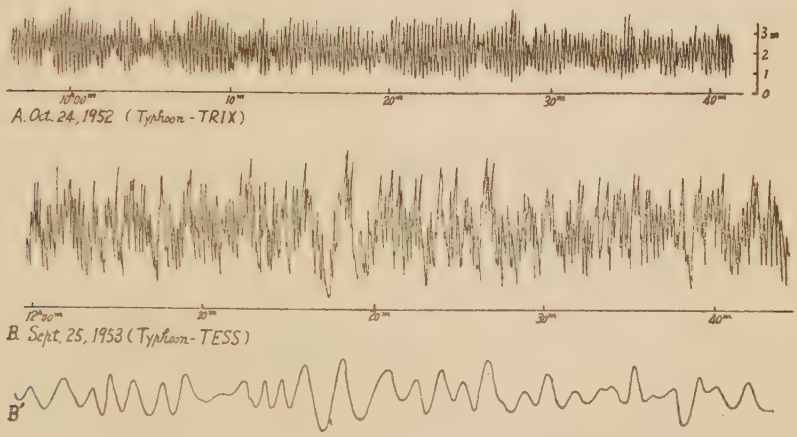

Fig. 1. Two examples of wave records in the case of typhoons. B′shows a peculiar long wave obtaied by smoothing record B.

The case may be conveniently divided into two cases as follows : Namely, (1) the case where a typhoon moves westward far to the south of Japan and passes through Formosa and the Philippines (Fig. 3), and (2) the case where a

typhoon comes up north and then leaves eastward describing a parabolic path approximately (Fig. 6). Indeed waves are, of course, higher in the latter case, but in the former case, too, conspicuous swells surge upon the Pacific coast of Japan and frequently give considerable damages. Moreover, the forerunner of swells which comes out from typhoon area has been known by Japanese people as "doyōnami", and has been utilized in weather forecast as a warning of the coming typhoon. Besides, an example of wave records and that of variation of waves for respective cases are shown in Figs. 1 and 2, respectively.

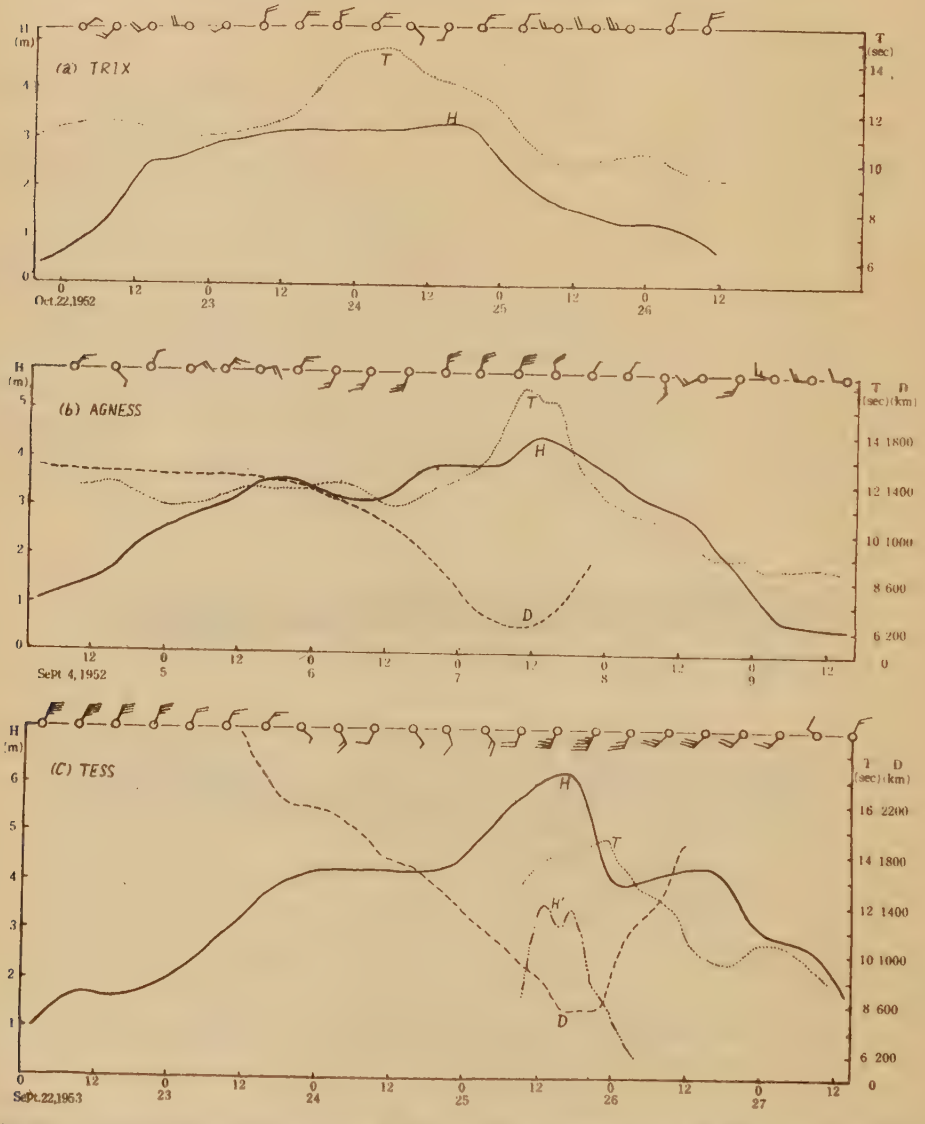

Fig. 2. Some examples of variation with time of wave-height and wave-period. The full line, H, represents the variation with time of wave-height, and the dotted line, T, that of wave-period ; the broken line, D, represents the distance from Hachijo Island to the center of typhoon.

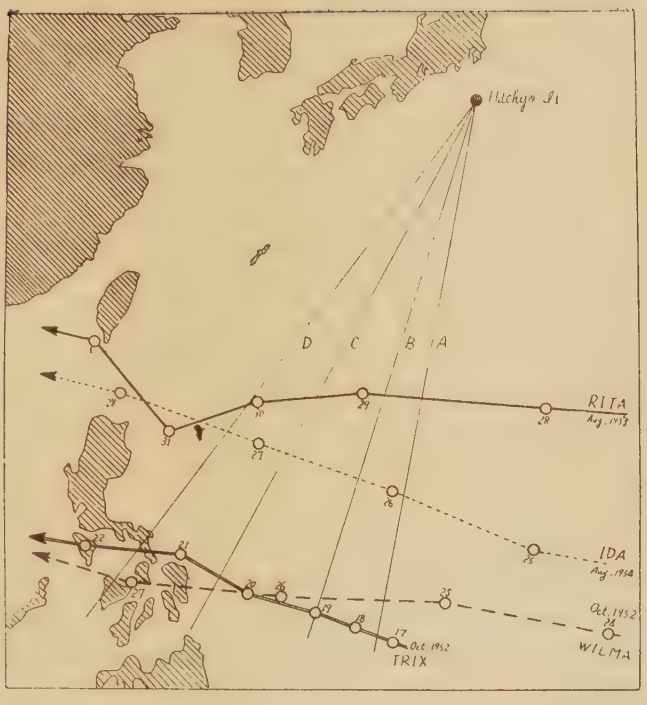

Fig. 3. The tracks of four typhoons which moved westward. Small white circles represent the position of the center of each typhoon at 09h of the date shown by the numeral beside it.

§ 2. The case where a typhoon moves westward far to the south of Japan

Four typhoons were investigated as examples belonging to this case. Fig. 3 shows their paths and Table 1 their elements, from which we can see the following facts :

(1) It is remarked that high waves with wave-height of 3~4m are occurring,

Table 1

Name of typhoon Date	TRIX Oct. 1952	WILMA Oct. 1952	RITA Aug. 1953	IDA Aug. 1954
Lowest central pressure (mb)	960	930	940	895
Distance of nearest approach (km)	2700	2600	1500	2000
Average speed of typhoon (km/hr)	14	35	29	31
Maximum wave-height (m)	3.3	2.5	2.8	4.2
Maximum wave-period (sec)	14.6	13.5	–	–
Duration of higher waves with wave-height over 2m (day)	2.5	2.0	2.5<	6<
Calculated wave-height (m)	3.0	1.5	2.4	3.4
Calculated wave-period (sec)	15.5	14.5	12.0	14.0
Travel time (hr)	78	84	55	64

though typhoons are apart as far as 2000~3000 km.

(2) Also the wave-period is as large as 13~15 sec, and is far larger in comparison with that of the waves caused by cyclones.

(3) The more intense the typhoon is (for example, the case of Typhoon IDA) and the nearer it approaches to the station (compare the Typhoons WILMA and RITA), the waves are naturally higher.

(4) In the case where a typhoon travels slowly, waves tend to become high. For instance, in the the case of Thphoon TRIX, the waves are very high, though the lowest central pressure is 960 mb and is fairy higher in comparison with other typhoons. This is due to the fact that the duration of wind in this case is vey long, as is made clear by drawing the "wind data diagram". According to T. Ōtani (1940), the height of swell seems to be different for different typhoons, even if the intensity of the typhoon is equal, and this may be explained by the above consideration.

(5) Duration of higher waves is very long, considering their wave-height. This may be a matter of course, if we consider the paths of these typhoons. Accordingly, in this case wave-height curve is rather flat, showing no conspicuous peak, as seen in Fig. 2 (A), which represents the wave-height curve for the case of Typhoon TRIX.

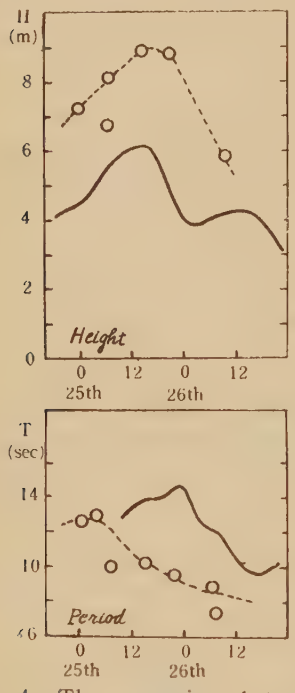

Fig. 4. The comparison between observed (full lines) and forecast values (broken lines) of wave-height and wave-period. (The case of Typhoon TESS)

Method of wave forecasting.

In the case of typhoons, the direction and speed of wind usually change violently from time to time as well as from place to place, and so it is very difficult to determine mean wind velocity, fetch and duration accurately from mere weather charts and compute waves, and accordingly the result is not good. For instance, Fig. 4 shows an example of the results of wave forecasting by means of Sverdrup-Munk's method, and from this figure it is seen that the calculated values are decidedly larger for the wave-height and decidedly smaller for the wave-period, in comparison with the observed ones. Hence the present authors constructed "wind data diagrams" (Darbyshire, 1952), and then applied Sverdrup-Munk's method of wave forecasting. In the following this method of treatment will be briefly described for the case of Thphoon TRIX.

Several straight lines were drawn radially at suitable intervals from the forecasting point (Hachijo Island), as shown by the straight lines A, B, C, D in Fig. 3, and radial component of wind velocity was computed for each point on each of these straight lines using successive weather charts, where the sign of the component was taken as positive or negative according as it is directed toward or away from the forecasting point. Thus, the "wind data diagram" as shown by Fig. 5 (upper) (diagram for C-line) is obtained for each straight line. From

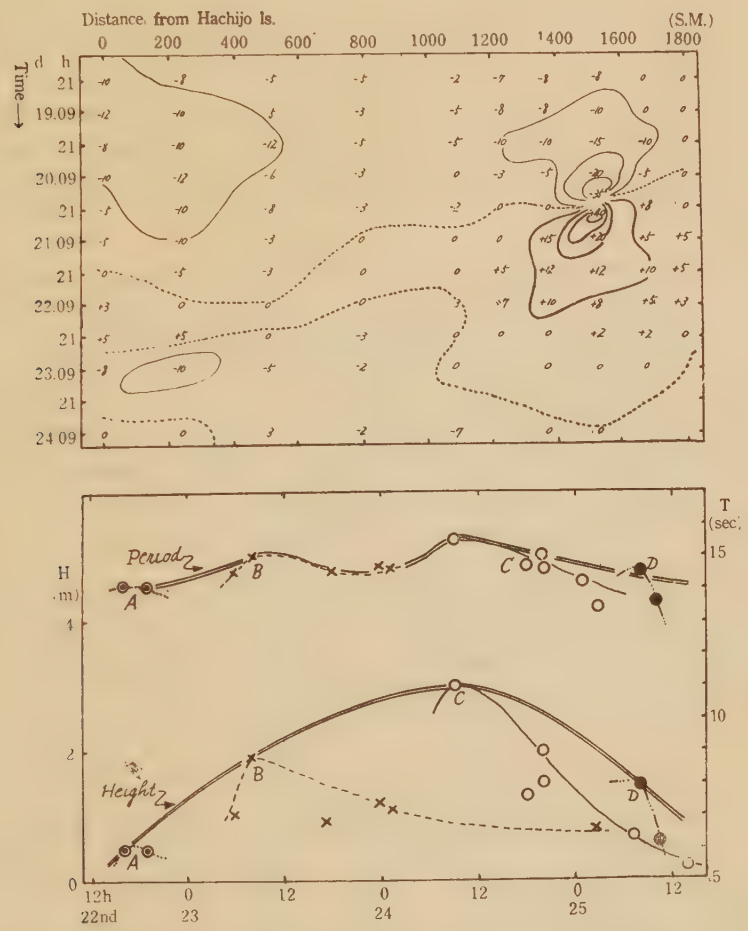

Fig. 5. The upper figure shows the wind data diagram for C-line in Fig. 3; the numerals denote the radial component of wind velocity in m/s. The lower figure shows the forecast values of wave-height and wave-period.

these diagrams the elements of wind can be determined with less arbitrariness. The waves generated along these straight lines and come to the forecasting point were calculated by Sverdrup-Munk's method, the result of which is shown in Fig. 5 (lower).

The height- and period- curves indicated by A, B, C, D are due to winds along straight lines A, B, C, D, respectively. The envelopes of these curves may be regarded as representing the theoretical height- and period-curves of the waves due to the typhoon in question, and if we compare these theoretical curves with actual ones shown in Fig. 2 (A), we can recognize the following facts ; namely, as regards the wave-height the theoretical and actual values agree in substance with each other in their absolute magnitude as well as their tendency of variation. And such is the case with the wave-period, except the parts with lower wave-height where the effect of local wind waves is large. For other typhoons likewise, the maximum values of the calculated wave-height and wave-period are given in Table 1, and if we compare these theoretical values with observed ones, it is seen that although the former is somewhat smaller than the latter for wave-height and contrary for wave-period, yet the two are in satisfactory agreement for practical purposes, provided that the "refraction effect" is taken into account.

Besides,Sverdrup-Munk's method has, indeed, its drawbacks, viewed in the light of wave spectrum etc., but since the result of calculation agrees with observation in such a degree as mentioned above, and its operation is also simple in comparison with other methods, it may be said to be a very effective method. Moreover, it is here added that recently K. Kajiura (Kajiura et al, 1954) have applied the method of wave forecasting by Pierson, Neumann and James (Pierson et al, 1953) to a typhoon, using wind data diagrams, and have obtained a result which is in good accord with observations.

§ 3. The case where a typhoon comes up north and then leaves eastward.

Nine typhoons as shown in Table 2 were investigated as examples belonging to this case. Fig. 6 shows the paths of these typhoos, and Fig. 7 an example of weather charts for the case of Typhoon TESS.

Tabie 2

Name of typhoon	POLLY	ROSE	AGNESS	CARMEN	DELLA	TESS	VIOLA	ALICE	GRACE
Date	Oct. 1952	Oct. 1952	Nov. 1952	Nov. 1952	Nov. 1952	Sept. 1953	Oct. 1953	Oct. 1953	Aug. 1954
Lowest central pressure (mb)	975	985	920	962	998	900	967	915	940
Distance of nearest approach (km)	−230	−350	−200	−470	+100	+300	−700	−600	+350
Maximum wave-height (m)	(3.5)	2.0	4.5	2.4	(2.5)	6.1	2.4	3.9	5.8
Maximum wave-period (sec)	15.0<	10.7	15.8	12.0	–	14.6	–	16.7	–
t_2 (day)	–	0.1	4.0	0.6	0.9	4.5	0.3	4.8	7.3
t_3 (day)	(1.5)	0.0	3.0	0.0	0.0	3.6	0.0	1.3	7.0

t_D-t_B (day)	–	–	3.3	1.3	1.5	3.7	1.3	1.5	7.4
t_H-t_D (hr)	+5~13	−9	+3	+2	+2	−1	+0~22	+1	−12
t_T-t_D (hr)	–	+12	+1	+7	–	+5	–	+6~10	–
t_C-t_D (day)	2.3	0.2	1.9	1.5	1.4	2.1	1.9	–	(1.0)

(Note)

t_B : Time when the waves began to grow.

t_C : Time when the waves have disappeared.

t_D : Time when the typhoon approaches nearest to the station.

t_H : Time when the maximum wave-height appeared.

t_T : Time when the maximum wave-period appeared.

t_2 : Duration of higher waves with wave-height over 2m.

t_3 : Duration of higher waves with wave-height over 3 m.

The + or − sign of the "distance of the nearest approach" of a typhoon corresponds to the case where a typhoon passes on the northern or southern side of Hachijo Island, respectively.

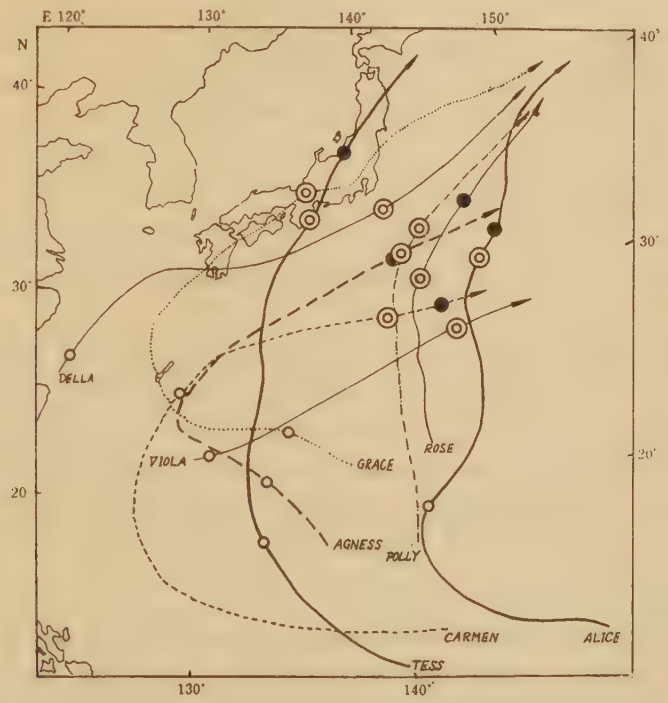

Fig. 6. The tracks of typhoons which come up north and then leave eastward.

(1) Beginning of growth of waves.

In Fig. 6, the points marked with ○ on the paths of the typhoons show the position of the centre of each typhoon at the time when waves begin to grow

at Hachijo Island, and from this figure we can recognize an interesting fact that waves begin to grow at Hachijo Island when a typhoon approaches within a certain distance (about 1500 km), almost regardless of the intensity and the path of the typhoon.

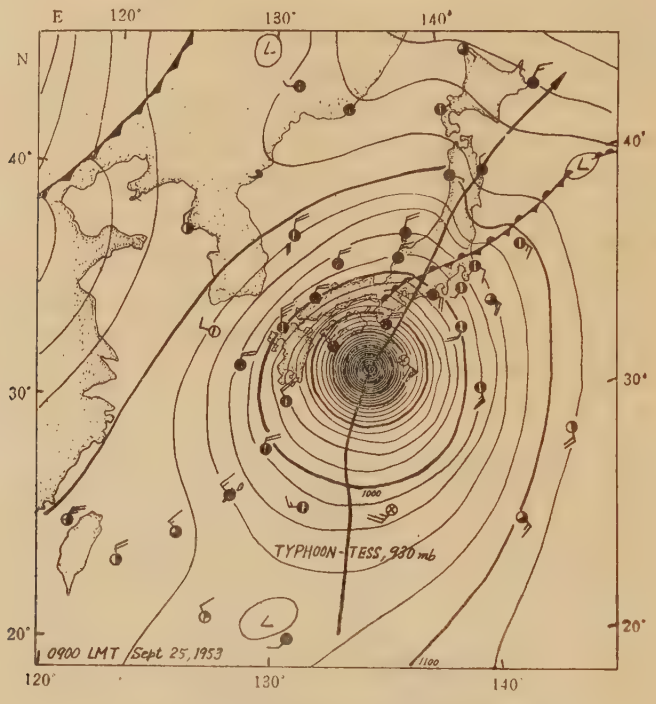

Fig. 7. An example of weather maps.

Referring to Table 2, the value of $t_D - t_B$ (the time interval from the time when waves begin to grow at Hachijo Island to the time when the typhoon approaches nearest to the station) changes from about 1 day to 7 days. This time interval is mainly affected by the speed and the path of the typhoon ; namely, it is generally large when the path of the typhoon fetches a large compass to the west of Hachijo Island.

(2) The maximum of wave-height.

In Fig. 6, the points marked with ◎ on the paths of the typhoons show the position of the centre of each typhoon at the time when the wave-height at Hachijo Island becomes maximum, and it is seen that the maximum wave-height occurs toward the time when the typhoon approaches nearest to this Island. (See the values of $t_H - t_D$ in Table 2)

Now, from Table 2 a diagram as shown in Fig. 8 (left-hand side) was constructed on the consideration that the maximum wave-height depends upon the intensity and the distance of the nearest approach of a typhoon. The compari-

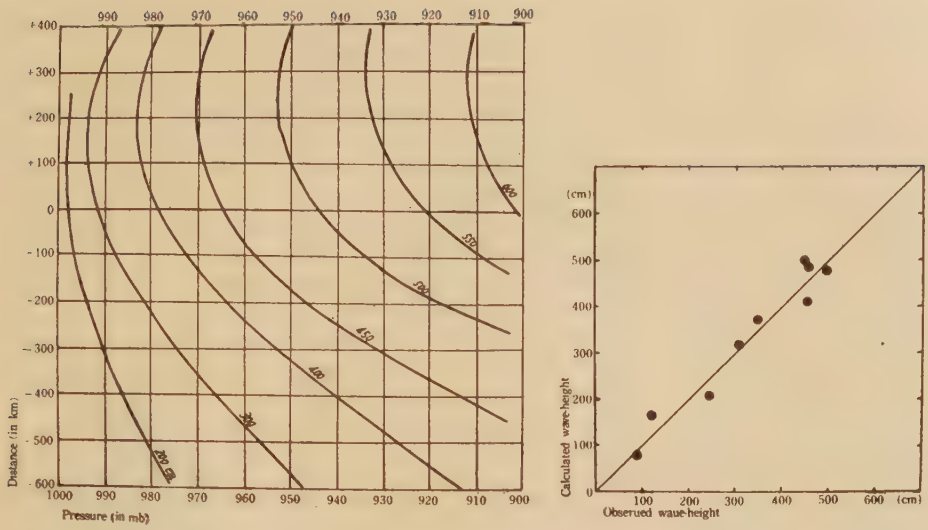

Fig. 8. Left: Relation among the wave-height, the lowest central pressure of a typhoon and the distance of nearest approach. Right : Comparison between observed and calculated wave-height.

son of the values read off from the curves in Fig. 8 (left-hand side) with those observed is shown in Fig. 8 (right-hand side), from which we can see that Fig. 8 (left hand side) gives a satisfactory result in practice. Although Fig. 8 (left-hand side) may require some amendment with further accumulation of observed data, yet this experimental diagram will be useful in wave forecast, at least for the first approximation. In this figure, it is remarked that waves tend to become higher in the case when a typhoon passes northwest of Hachijo Island than in the case when it passes southeast of it, and this can be easily understood if we consider that in the former case the island lies in the dangerous semi-circle of the typhoon and that the observing station is situated on the southwestern coast of the island.

(3) The maximum of wave-period.

In Fig. 6, the points markd with ● on the paths of the typhoons show the position of the centre of each typhoon at the time when the maximum wave-period occurred at Hachijo Island. Again, in Table 2, the quantity $t_T - t_D$ gives the time interval from the time of the nearest approach of a typhoon to Hachijo Island to the time of occurrence of the maximum wave-period. From these we can see that the maximum wave-period occurs several hours later than the time of the nearest approach of the typhoon.

In the case of strong typhoons, the wave-period frequently becomes over 15 sec. Moreover, according to Table 2, a tendency is seen such that the wave-period is larger in the case where a typhoon passes on the southern side of Hachijo Island than in the case where it passes on the northern side of it, and

this is natural if we consider that in the former case swells are predominant, while in the latter case "wind waves" are predominant.

Besides, in the case of Typhoon ALLCE, it was reported that swells with the period of 20~25 sec surged upon the coast of Ito, Shizuoka Prefecture, for about a day, one or two days after the typhoon left over ocean to the east of Japan, and destroyed a mole several dozen metres long. At that time the weather was clam in the vicinity of Ito, and waves were scarcely seen on the surface of the sea as far as several hundred metres off shore, except in the immediate neighbourhood of the coast where unusually high swell was surging, according to report. At any rate, it is to be remarked that such long swells sometimes appear in the case of typhoons. Fig. 9 shows an example of frequency distribution of the period of waves due to typhoons, and it is seen that the distribution is nearly of normal type and that there exist long swells with wave-period of 20 sec or more as mentioned above.

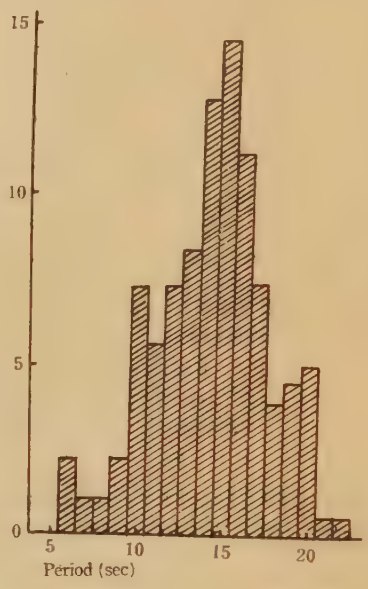

Fig. 9. The frequency distribution of wave-period at Yayene (Hachijo Is.) from 13h to 16h of 25th, Sept. 1953. (The case of Typhoon TESS)

(4) Subsidence of waves.

In Table 2, the quantity $t_C - t_D$ represents the time interval from the time when a typhoon approaches nearest to Hachijo Island to the time when waves have disappeared and it is seen that the waves usually subside after a day or so, in the case of a weak typhoon, or about two days and a half, in the case of a strong typhoon, from the time when the typhoon approaches nearest to the station, Again, if we compare $t_H - t_B$ (the time interval from the time when waves begin to grow to the time when the wave-height becomes maximum) with $t_C - t_H$ (the time interval from the time when the wave-height becomes maximum to the time when the waves have disappeared), we can see that, in the case where the typhoon passes on the northern side of Hachijo Island, the former is larger than the latter, while on the contrary, in the case where the typhoon passes on the southern side of Hachijo Island, the latter is rather larger. This will be due to the fact that in the case where the typhoon passes on the northern side of Hachijo Island, it frequently fetches a large compass westward, and mostly strikes the Japan Island, and so waves will not be newly generated.

(5) Duration of higher waves.

As for the duration of higher waves for different intensities and paths of

typhoons, we can form a probable estimate from the values of t_2 or t_3 in Table 2.

(6) Waves with long period near the coast.

In the case of Typhoon TESS, as seen in the wave record of Fig. 1 B and B′ waves with especially long period as long as 2～3 minutes appeared, in addition to ordinary waves. The variation of these wave-heights with time is shown by the curve H′ in Fig. 2 (C); the maximum wave-height of these long waves attained as much as 3.5 m. And it has already been shown that these waves are not a mere "surf beat" (Munk, 1949) but a kind of oscillation of water in the vicinity of the coast, produced by a water-drift due to southwesterly winds with speed over 30 knots blowing right against the coast of Yayene, together with mass transport due to high wave (Daidoji, Unoki and Kajiura, 1954). At any rate, it is not a negligible matter in practical wave forecast that waves with very long period and with wave-height over 3 m superpose themselves upon high "wind waves".

Acknowledgments

The authors wish to express their hearty thanks to Mr. S. Daidoji, director of the Hachijojima weather Station, and the members of that station who have heartily cooperated with the authors in making wave observations for a long time. Equal thanks are due to Mr. K. Kajiura of the Tokyo University and Mr. J. Sugiura of the Central Meteorological Observatory for their kind help and valuable informations. Further the authors are indebted to the Special Committee on Marine Resources, Japanese National Commission for UNESCO for financial aids.

References

(1) Daidoji, S., S. Unoki and K. Kajiura, 1954 : Waves at Hachijo Island caused by Typhoon TESS and ALICE in 1953 (in Japanese). Journ. Meteor. Res. Vol. 6, pp. 221-229.

(2) Darbyshire, J. 1952 : The generation of waves by wind. Proc. Roy. Soc. A. 215, pp.229-328.

(3) Kajiura, K., H. Miyoshi and K. Takano, 1954 : On the waves at Hachijo Island (unpublished).

(4) Munk, W. H., 1949 : Surf beats. Trans. Amer. Geophys. Uni. Vol 30, No. 6.

(5) Ōtani, T., 1940: "Bofū-u or Storms" (in Japanese). Iwanami Book Co.

(6) Pierson, W. J., G. Neumann and R. W. James, 1953: Practical methods for observing and forecasting ocean waves by means of wave spectra and statistics. Dept. of Met. Oceanogr., New York Univ. Tech. Rep. No. 1.

(7) Sverdrup, H. U., and W. H. Munk, 1947 : Wind, sea and swell ; theory of relations for forecasting.